(NASA-CR-168931) EIGENSPACE TECHNIQUES FOR ACTIVE FLUTTER SUPPRESSION Semiannual Progress Report, 1 Oct. 1981 - 31 Mar. 1982 (Minnesota Univ.) 116 p HC A06/MF A01 CSCL 01C G3/08

N82-24206

Unclas 09932

UNIVERSITY OF MINNESOTA

INSTITUTE OF TECHNOLOGY

DEPARTMENT OF AEROSPACE
ENGINEERING AND MECHANICS

MINNEAPOLIS, MINNESOTA 55455

Semi-Annual Progress Report
Oct 1, 1981 to March 31, 1982
NASA Research Grant NAG-1-217

EIGENSPACE TECHNIQUES FOR ACTIVE FLUTTER SUPPRESSION

W. L. Garrard
Department of Aerospace Engineering & Mechanics
University of Minnesota
Minneapolis, MN 55455

Semi-Annual Progress Report

Oct 1, 1981 to March 31, 1982

NASA Research Grant NAG-1-217

EIGENSPACE TECHNIQUES FOR ACTIVE FLUTTER SUPPRESSION

W. L. Garrard

Department of Aerospace Engineering & Mechanics

University of Minnesota

Minneapolis, MN 55455

I. Introduction

The first six months of the contract were spent in developing the mathematical models to be used in the control system design. A major task that was completed was the development of a computer program which takes aerodynamic and structural data supplied by NASA for the ARW-2 aircraft and converts these data into state space models suitable for use in modern control synthesis procedures. This program has the ability to generate reduced order models by eliminating selected modes. Reduced order models of inboard and outboard control surface actuator dynamics and a second order vertical wind gust model was developed. In addition, an analysis of the rigid body motion of the ARW-2 was conducted, and it was shown that the deletion of the aerodynamic lag states in the rigid body modes resulted in more accurate values for the eigenvalues associated with the plunge and pitch modes than were obtainable if the lag states were retained.

The remainder of the report consists of a summary of results in each of the areas outlined above. The details are given in Working Papers contained in the Appendix.

II. Actuator/Control Surface Models (Working Papers 1 & 5)

A. Elevator . (Working Paper 1) The elevator transfer function to be used is a simple first-order lag

$$u_e / u_{e_c} = \frac{20}{s + 20}$$

The allowable control surface activity levels of Mach 0.86 and 15000 ft. are $+7^\circ$ and -12° deflection and $\pm 80^\circ$/s for a 12 ft/s vertical gust. The bandwidth of the elevator is much less than the lowest flexural frequency (118 rad/sec), and the gain of the elevator at this frequency is 0.167 (-15.54 Db); therefore, it appears that the elevator will not be effective for flutter suppression.

B. Inboard Aileron . (Working Paper 1). An eleventh-order model with third-order numerator dynamics was given for the inboard aileron. The first, fourth, and sixth flexure modes appear to be the most important in modeling flutter. (See Section on Results.) The frequency of the sixth mode is 218 rad/s. In this range of frequencies, a fourth-order approximation of the actual inboard aileron transfer function exhibits a maximum error of 0.25 Db in gain and -9° in phase angle. It is proposed to use the fourth order approximation given as

$$u_i / u_{i_c} = 1.614 \times 10^{11} / (s^2 + 671s + 2.28 \times 10^5)(s^2 + 322s + 7.71 \times 10^5)$$

The activity for the inboard aileron is limited to 20° down and 10° up deflection and 130°/s deflection rate for at 12 ft/s gust at the flutter condition.

C. <u>Outboard</u> <u>Aileron</u> . (Working Paper 5) The modified transfer function for the outboard aileron is given in Working Paper 5. (Note the discussion on the Outboard Aileron given in Working Paper 1 is based on an earlier model of the aileron and should be ignored.) The exact transfer function is seventh order with second order numerator dynamics. A third-order approximation gives the same response characteristics as the exact model up to frequencies of 300 rad/s. This third order model is

$$u_o / u_{o_c} = 1.774 \times 10^7 / (s+180)(s^2+251s+(314)^2)$$

The outboard aileron has a maximum deflection of ±15° and deflection rate of 740°/sec for a 12 ft/s rms gust at the flutter condition.

III. <u>Wind Gust Model</u> (Working Paper 2) A second-order vertical wind gust model given below is to be used

$$w(s) / \eta(s) = \left(1+\sqrt{3}\, L/V\, s\right) / \left((L/V)s+1\right)^2$$

where

w = vertical gust velocity

L = characteristic length (2500 ft)

V = the forward velocity

η = white noise input with intensity, $(L/V)\sigma^2$

σ = rms gust velocity

At the flutter condition of Mach 0.86 and 15000 feet, σ =12 ft/s. At the gust test condition of Mach 0.7 and 15000 feet σ = 59 ft/sec. The control system should reduce bending moments 30 to 40% at all stations at the gust test condition.

IV. State Space Model (Working Paper 3)

Modern control design techniques require that the system be modeled in state space form as

$$\dot{Z} = AZ + BU_c + \Gamma\eta$$

where

Z = state vector

U_c = control vector

η = white noise input

The equations of motion for the flexible aircraft are given in the form

$$\left[Ms^2 + Cs + K\right]X + q\left[A_0 + A_1\left(\frac{cs}{2V}\right) + A_2\left(\frac{cs}{2V}\right)^2 + \sum_{m=1}^{n} \frac{D_m s}{s + \frac{2V}{c}\bar{k}_m}\right]\begin{bmatrix} X \\ U \\ W \end{bmatrix}$$

where

X = the rigid body (plunge and pitch) and elastic mode deflections

U = control surface deflections

W = vertical wind gust velocity

(See next Section and Working Paper 4 for details of this model.)

Incorporating the tranfer functions for the control surfaces and the vertical wing gust with the aircraft model results in a state vector, Z, consisting of (1) rigid body deflection and rates, (2) flexural displacements and rates, (3) elevator angular deflection, (4) inboard aileron angular deflection, deflection rate, and acceleration, (5) outboard aileron angular deflection and deflection rate, (6) wind gust velocity and an associated variable (see Working Paper 2), and (7) lag states associated with the unsteady aerodynamics. The control vector, U_c, consists of the commanded inputs to the elevator, the inboard aileron, and the outboard aileron. The white noise input is the forcing term for the wind gust model.

Since there are 10 flexural degrees of freedom, two rigid body degrees of freedom, a lag state for each degree of freedom and each reduced frequency included in the unsteady aerodynamic model, a first order elevator model, fourth and third order aileron models, and a second order gust model, the dimensionality of the state vector is 46 even if only one lag state is assumed. Thus it is necessary to computerize the manipulations required to construct the state space model. Such a program has been written and is running on the University of Minnesota Computer System. This program allows rigid body and flexure modes to be delected in order to generate a lower order model if required. Results obtained from use of this model are described later.

V. Unsteady Aerodynamic Model (Working Paper 4)

The flexible aircraft is modeled as

$$\left[M s^2 + C s + K \right] X + q \, Q(s) \begin{bmatrix} X \\ u \\ w \end{bmatrix} = 0$$

where

M = generalized mass matrix

C = generalized structural damping matrix

K = generalized stiffness matrix

q = dynamic pressure

Q = matrix of aerodynamic coefficients

w, X, U are defined in Section 4.

The matrix of aerodynamic influence coefficients, Q $(s = j \frac{2V}{c} k)$, was provided by NASA for a range of reduced frequencies. The aerodynamic influence coefficient matrix was approximated by

$$Q_A(s) = A_0 + A_1 \left(\frac{cs}{2V} \right) + A_2 \left(\frac{cs}{2V} \right)^2 + \sum_{m=1}^{n} \frac{D_m(s)}{s + \frac{2V}{c} \bar{K}_m}$$

The error matrix E(s) is defined as

$$E(s) = Q(s) - Q_A(s)$$

Determination of matrices A_o, A_1, A_2, and D_m which give the best least squares fit to the data is a relatively straightforward problem (see Working Paper 4).

The first column of the matrix A_o must be set equal to the first column of $Q(0)$ (which is zero) in order to reflect the fact that aerodynamic forces due to the plunge displacement are zero. The remaining matrices can be determined to give the best least squares fit to the data once the $\bar{k}_m$'s are specified. The selection of $\bar{k}_m$'s which result in a "best" fit is not so straightforward. (See Dowell, E. H. "A Simple Method for Converting Frequency Domain Aerodynamics to the Time Domain" NASA Tech. Memorandum 81844, Oct 1980.) An approach to the selection of the $\bar{k}_m$'s was developed as part of this study and appears to yield good results with minimal computational effort. This approach depends upon the fact that the spectral norm of a matrix equals its maximum singular value. Thus the maximum singular value of E(s), defined as $\sigma(E)$ equals E(s) and is a measure of the size of the error in the approximation of Q(s). The procedure is to (1) arbitrarily select values for the $\bar{k}_m$'s, (2) let the first column of A_o equal the first column of Q(0) (which is zero), (3) determine the remaining values of A_o, A_1, A_2, and D_m, m=1, ...n which give the best least squares fit to the data, (4) calculate the maximum singular value of the error matrix E(s), (5) vary the $\bar{k}_m$'s and repeat the process until this singular value achieves a minimum. Since only a few values of $\bar{k}_m$ are commonly used, a relatively simple search procedure can be used to determine the optimum values for the $\bar{k}_m$'s.

VI. Results

A. Rigid Body Modes (Working Paper 4)

The procedure described above was used to generate a mathematical model of the ARW-2 at the flutter condition of Mach 0.86 and 15000 feet. A single aerodynamic lag state was used. The value of $\bar{k}_1$ was varied until the maximum singular value of the error matrix was minimized for a reduced frequency of zero. The minimization was accomplished at zero frequency because it was felt that the approximation should be best at low frequencies since rigid body modes were to be studied. The resulting value of $\bar{k}_1$ was 0.13 which is very close to the reduced flutter frequency of 0.15. The elements of the Q matrix supplied by NASA were plotted in polar form and were compared with polar plots of the elements of the Q_A matrix resulting from the approximate model. As can be seen in Working Paper 4, these plots are almost identical, indicating that the approximation is extremely good.

All flexure modes were neglected, and the eigenvalues associated with the plunge and pitch modes were calculated as follows:

plunge $6.1146,\ 1.828 \times 10^{-7}$

pitch $-5.1767 + j\ 7.5543$

If the lag terms were neglected when the eigenvalues were calculated, the plunge and pitch eigenvalues were

plunge $3.391 \times 10^{-2},\ 7.588 \times 10^{-7}$

pitch $-1.1188 \pm j\ 3.5572$

These are not too different from the values given by Boeing of

plunge $-0.0092 \pm j\ .0437$

pitch $-1.4274 \pm j\ 2.422$

It appears that inclusion of the aerodynamic lag terms degrades the accuracy of the calculation of the rigid body eigenvalues and that elimination of the lag states associated with the rigid body modes improves the accuracy of the model. It is difficult at present to explain why this is so. The aerodynamic lag terms represent unsteady aerodynamic effect and since use of quasi-steady aerodynamics usually allows the accurate prediction of rigid body eigenvalues, it is not surprising that the eigenvalues calculated by neglecting the lag terms are near those given by Boeing. What is surprising is that the inclusion of the lag terms has such an effect on the eigenvalues. The time constants associated with the unsteady aerodynamics are less than .01 sec while the time constant associated with the short period mode is of the order of 0.5 sec and that of the plunge mode is approximately 125 sec.

B. Flexure Modes

An examination of the 10 flexure modes indicated that modes 2 and 5 were primarily fuselage bending modes, and mode 7 was exclusively a tail mode. Therefore, these three modes were not considered further in the analysis . Mode 1 was the first wing bending mode, mode 2 was the second wing bending mode, and mode 6 was the first wing torsion mode. These modes were obviously important and were retained. Modes 3 and 8 included wing tip bending and it was felt that these modes should also be analyzed further. Mode 9 was primarily wing bending and mode 10 was primarily wing torsion, and these modes were also retained. Thus seven flexure modes, the 1st, 3rd, 4th, 6th, 8th, 9th, and 10th, were used in the flutter analysis. A single lag term with reduced frequency of 0.13 was used. The loci of the eigenvalues of those modes as velocity is varied are shown in Fig 1. The data from which Fig. 1 is constructed is given in Table 1. It can be seen that the 1st mode flutters at a speed of approximately 9500 in/s at a frequency of approximately 120 rad/s. The results are based on aerodynamic data for a Mach number of 0.86; therefore, the values of the eigenvalues at low velocities are suspect, however, 9500 in/s corresponds to a Mach number of 0.75 which is reasonably close to 0.86. Fig 1 presents results which are very similar to those given by NASA; therefore, it is felt that the mathematical modeling has been done correctly. It should be noted that modes 3 and 8 are very insensitive to velocity, indicating that they are primarily vibrational modes not affected by aerodynamics. Modes 9 and 10 do however very considerably with velocity.

Eigenvalues were calculated using models in which various modes were deleted. (See Table 2.) It can be seen that even though the 1st mode flutters, a three mode model which contains the 1st, 4th, and 6th modes is required to accurately predict flutter. This is not surprising since classical flutter requires both a bending and a torsion mode. Both the 1st and 4th modes are bending and the 6th is torsion. It is interesting to note that at Mach 0.6, the 4th mode flutters. Deletion of the 3rd and 8th modes has almost no affect on the eigenvalues of the other modes, and the 9th and 10th modes have very little affect on the lower modes.

VII. Conclusions and Future Plans

It is felt that we now have a valid model of the aircraft to be used in our flutter control studies. Since the elevator has such a low bandwidth compared with the flutter frequencies, flutter control will be accomplished using the inboard and outboard ailerons. A model consisting of the 1st, 4th, and 6th modes will be used for control system design and a model containing the 1st, 4th, 6th, 9th, and 10th modes will be used for evaluation. A single aerodynamic lag state is proposed to be used in both the design and evaluation models. Currently a program to perform eigenspace design is being written as is a program to interface the aircraft model with an existing evaluation program for determining rms responses to stochastic wind gusts.

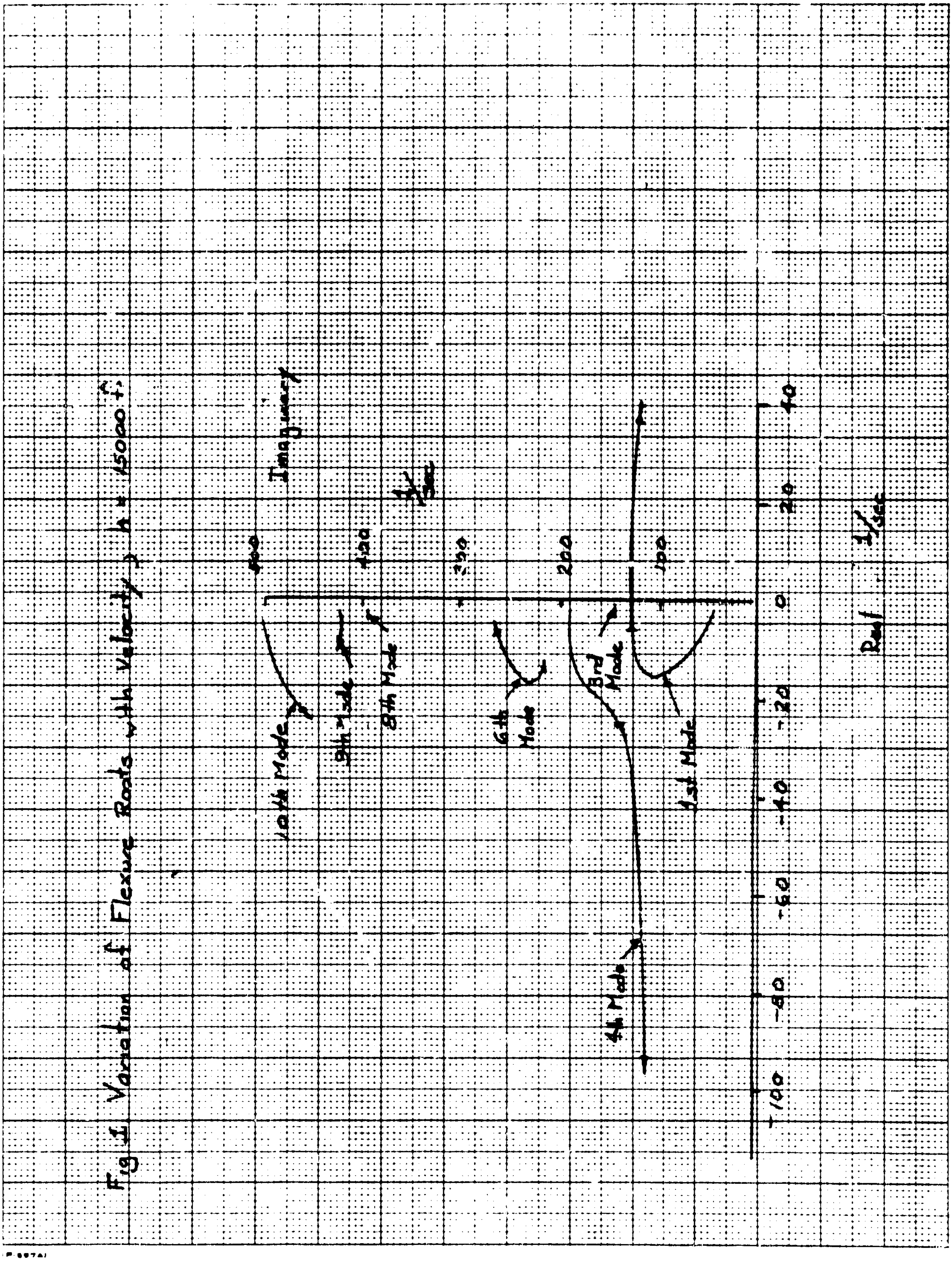

Fig 1 Variation of Flexure Roots with Velocity, h = 15000 ft

Table 1. Variation of Eigenvalues with Velocity at 15000 Feet

Dyn. Pressure (Psi)	Velocity (in/s)	Mode No.	Eigenvalue
0.0036	1000	10	-4.6 ± j 499.3
		9	-2.8 ± j 421.5
		8	-2.3 ± j 395.8
		6	-4.1 ± j 267.3
		4	-2.3 ± j 191.3
		3	-0.7 ± j 136.7
		1	-1.6 ± j 50.7
0.144	2000	10	-6.7 ± j 498.2
		9	-3.6 ± j 421.6
		8	-2.5 ± j 395.8
		6	-6.8 ± j 264.9
		4	-3.7 ± j 191.2
		3	-0.7 ± j 136.7
		1	-3.0 ± j 51.6
0.325	3000	10	-8.9 ± j 496.4
		9	-4.3 ± j 421.7
		8	-2.8 ± j 395.9
		6	-9.5 ± j 260.9
		4	-5.1 ± j 191.1
		3	-0.7 ± j 136.7
		1	-4.5 ± j 53.3
0.577	4000	10	-11.0 ± j 493.8
		9	- 5.1 ± j 421.9
		8	- 3.1 ± j 396.0
		6	-12.0 ± j 255.4
		4	- 6.6 ± j 190.3
		3	- 0.8 ± j 136.7
		1	- 6.0 ± j 55.9
0.902	5000	10	-13.1 ± j 490.5
		9	- 5.9 ± j 422.2
		8	- 3.3 ± j 396.2
		6	-14.3 ± j 248.2
		4	- 8.4 ± j 190.0
		3	- 0.8 ± j 136.7
		1	- 7.7 ± j 59.4
1.3	6000	10	-15.1 ± j 486.3
		9	- 6.7 ± j 422.5
		8	- 3.5 ± j 396.4
		6	-16.12± j 239.7
		4	-10.7 ± j 188.0
		3	- 0.8 ± j 136.8
		1	- 9.5 ± j 64.4

Table 1. Variation of Eigenvalues with Velocity at 15000 Feet

1.77	7000	10	$-17.16 \pm j\ 481.3$
		9	$-7.5 \pm j\ 422.9$
		8	$-3.7 \pm j\ 396.5$
		6	$-16.9 \pm j\ 230.5$
		4	$-13.9 \pm j\ 183.2$
		3	$-0.8 \pm j\ 136.8$
		1	$-11.7 \pm j\ 71.6$
2.31	8000	10	$-19.1 \pm j\ 475.5$
		9	$-8.4 \pm j\ 423.3$
		8	$-3.9 \pm j\ 396.8$
		6	$-16.4 \pm j\ 223.0$
		4	$-18.3 \pm j\ 171.5$
		3	$-0.9 \pm j\ 136.9$
		1	$-14.2 \pm j\ 82.9$
2.92	9000	10	$-21.2 \pm j\ 468.9$
		9	$-9.2 \pm j\ 423.8$
		8	$-4.0 \pm j\ 397.0$
		6	$-15.7 \pm j\ 218.8$
		4	$-24.0 \pm j\ 140.1$
		3	$-0.6 \pm j\ 137.4$
		1	$-16.3 \pm j\ 108.6$
3.61	10000	10	$-23.0 \pm j\ 461.2$
		9	$-10.1 \pm j\ 424.4$
		8	$-4.1 \pm j\ 397.2$
		6	$-16.0 \pm j\ 217.6$
		4	$-68.9 \pm j\ 117.9$
		3	$-0.5 \pm j\ 136.6$
		1	$+21.2 \pm j\ 121.9$
4.37	11000	10	$-24.8 \pm j\ 452.5$
		9	$-11.0 \pm j\ 425.0$
		8	$-4.1 \pm j\ 397.4$
		6	$-16.9 \pm j\ 218.3$
		4	$-97.1 \pm j\ 108.4$
		3	$-0.7 \pm j\ 136.6$
		1	$+41.6 \pm j\ 118.1$

Table 2. Eigenvalues for Combinations of Flexure Modes

Mode No.		Eigenvalue
	1 Mode Model	
1		-13.6 ± j 78.6
	2 Mode Model	
4		-14.7 ± j 180.2
1		-15.0 ± j 86.6
	2 Mode Model	
6		+14.9 ± j 134.2
1		-65.0 ± j 121.7
	3 Mode Model	
4		-14.7 ± j 180.2
3		- 0.9 ± j 136.8
1		-15.0 ± j 36.5
	3 Mode Model	
6		-15.7 ± j 216.1
4		-94.3 ± j 106.4
1		+39.9 ± j 118.0
	4 Mode Model	
6		-15.7 ± j 216.1
4		-94.2 ± j 106.6
3		- 0.7 ± j 136.6
1		+39.7 ± j 118.0
	5 Mode Model	
8		- 4.9 ± j 397.2
6		-15.7 ± j 216.1
4		-94.1 ± j 106.7
3		- 0.7 ± j 136.6
1		+39.6 ± j 118.7
	5 Mode Model	
10		-24.3 ± j 453.6
9		-10.2 ± j 425.0
6		-16.6 ± j 218.3
4		-94.2 ± j 108.7
1		+39.8 ± j 118.2
	6 Mode Model	
9		-10.9 ± j 424.9
8		- 4.2 ± j 397.4
6		-15.7 ± j 216.1
4		-93.7 ± j 107.2
3		- 0.7 ± j 136.6
1		+39.3 ± j 118.2
	7 Mode Model	
10		-24.8 ± j 452.5
9		-11.0 ± j 425.0
8		- 4.1 ± j 397.4
6		-16.9 ± j 218.3
4		-97.1 ± j 108.4
3		- 0.7 ± j 136.6
1		+41.6 ± j 118.1

Appendix

Working Papers 1 - 5

Working Paper No. 1
Actuator Models for
Flutter Control Study

W.L. Garrard
Dept. of Aerospace Engineering and Mechanics
University of Minnesota
Minneapolis, MN

Introduction

The DAST-2 vehicle has three independent control surfaces available for flutter and pitch control. These are an elevator, an inborad actuator, and an outboard actuator. This paper gives the transfer functions for these actuators and suggests some lower order model approximations for the ailerons.

Elevator

The elevator transfer function is a simple first order lag

$$u_e / u_{e_c} = \frac{20}{s+20} \qquad (1)$$

Bode plots for this transfer function are given in Figs. 1 and 2. The allowable rms control surface activity levels are +7° and -12° deflection and $\pm$80°/sec for a 12 ft/s vertical gust at the flutter condition of Mach 0.86 and 15000 ft. altitude.

Inboard Aileron

The transfer function for the inboard aileron is

$$u_i / u_{i_c} = 7.239 \times 10^{24} (s+610)(s^2 + 2800s + 3.126 \times 10^6) \Big/ (s+455.5)$$
$$(s^2 + 671s + 2.28 \times 10^5)(s^2 + 322s + 7.7078 \times 10^5)$$
$$(s^2 + 288.3s + 8.227 \times 10^5)(s^2 + 2843.9s + 3.183 \times 10^6)$$
$$(s^2 + 665.3s + 7.171 \times 10^7)$$

or in factored form

$$u_i/u_{v_c} = 7.239\times10^{24}(s+610)(s+1400\pm j\,1079.8)\Big/(s+455.5)(s+335.5\pm j\,339.8)$$
$$(s+161\pm j\,825.8)(s+144\pm j\,895.5)(s+1424.5\pm j\,1074.2)$$
$$(s+332.7\pm j\,8461.6)$$

ORIGINAL PAGE IS
OF POOR QUALITY

Bode plots for this transfer function are shown in Figs. 3 and 4. The terms $s^2 + 2800s + 3.126 \times 10^6$ in the numerator and $s^2 + 2848.9s + 3.183 \times 10^6$ can effectively be canceled. The two high frequency factors in the denominator $(s + 1424.5 \pm j\,1074.2)$ and $(s + 332.7 \pm j\,8461.6)$ have little effect on the dynamic response over the frequency range of interest in the control problem of 1 to 500 rad/s. Also the s + 610 term in the numerator comes fairly close to canceling the s + 455.5 term in the denominator and if there are no numerator dynamics the state space representation is simplified somewhat. All of these assumptions result in a sixth order model

$$u_i/u_{v_c} = 1.3705\times10^{11}\Big/(s+335.5\pm j\,339.8)(s+161\pm j\,825.8)(s+144\pm j\,895.5)$$

The Bode plots over the frequency range from 10 to 1000 rad/s are given in Figs. 5 and 6. It can be seen that the frequency response for the exact transfer function and the sixth order approximation are very close over this range of frequencies. The comparison is presented in detail in Table 1. The flutter frequency is about 150 rad/s and the correspondence between the sixth order and exact transfer function is very good near this frequency. At very high frequencies the exact transfer function has a phase shift of -180° and a slope of 40 DB/Decade greater than the sixth order approximation.

A fourth order approximation can be generated by eliminating the dynamics associated with the factor $s + 144 \pm j895.5$. This is somewhat difficult to justify as we retain the factor $s + 161 \pm j825.8$ which is about the same frequency. The resulting fourth order transfer function is

$$u_i/u_{v_c} = 1.614\times10^{11}\Big/(s+335.5\pm j\,339.8)(s+161\pm j\,825.8)$$

Bode plots for this transfer function are given in Figs. 7 and 8. The fourth-order model gives a reasonably good approximation of the exact transfer function up to about 300 rad/sec but deteriorates rapidly at higher frequencies. The numerical details of the comparison are given in Table 1.

The final approximation considered is second order and is given as

$$u_i/u_{ic} = 2280/(s + 335.5 \pm j\,339.8)$$

As can be seen from Figs. 9 and 10 and from Table 1, the accuracy of this model deteriorates fairly rapidly for frequencies above about 175 rad/s.

The activity for the inboard aileron is limited to -10° and +20° deflection and to 180°/sec deflection rate for a 12 ft/s vertical gust at the flutter condition.

<u>Outboard Aileron</u>

The transfer function for the outboard aileron is

$$u_o/u_{o_c} = 3.5398 \times 10^{24}/(s^2 + 1043.7s + 3.785 \times 10^5)(s^2 + 477.2s + 4.098 \times 10^5)$$
$$(s^2 + 1484.2s + 4.234 \times 10^6)(s^2 + 1147.4s + 5.39 \times 10^6)$$

or in factored form

$$u_o/u_{o_c} = 3.5398 \times 10^{24}/(s + 521.9 \pm j\,325.8)(s + 238.6 \pm j\,594)(s + 742.1 \pm j\,1919)$$
$$(s + 573.7 \pm j\,2249.6)$$

Bode plots for this transfer function are given in Figs. 11 and 12 for frequencies from 0.1 to 1000 rad/s and in Figs. 13 and 14 for frequencies from 10 to 1000 rad/s. If we consider only frequencies of the same order as the structural frequencies, a fourth order model results. This is given by

$$u_o/u_{o_c} = 1.551 \times 10^{11}/(s + 521.9 \pm j\,325.8)(s + 238.6 \pm j\,594)$$

Bode plots for this transfer function are given in Figs. 15 and 16. It can be seen that this gives a very good approximation of the exact transfer function over the frequency range of interest although at very high frequencies the exact model will exhibit a phase shift of -360° and a slope of -80 DB/Decade greater than the fourth order model.

A second order model given as

$$u_o/u_{o_c} = \frac{3755}{(s^2 + 521.9s + 325.8)}$$

was also examined and Bode plots for this model are shown in Figs. 17 and 18. The approximation resulting from use of this model is considerably worse than given by the fourth order model.

The outboard aileron has a rms deflection limit of $\pm 15°$ and a deflection rate limit of 710°/sec for a 12 ft/sec vertical gust at the flutter flight condition.

Conclusions and Recommendations

Initial controller designs will incorporate rigid body and first, fourth, and sixth elastic modes. Since the sixth mode has a frequency of 225 rad/s at the flutter condition, it is felt that the fourth order approximation of the inboard actuator whould be adequate even though the sixth order gives a considerably better approximation of the actuator dynamics for frequencies greater than 350 rad/sec. The fourth order model of the outboard actuator gives a very good approximation of the exact transfer function over the frequency range of interest.

Table 1: Comparison of Exact Transfer Function for Inboard Aileron and Various Lower Order Approximations

	Freq (rad/s)	Gain (Db)	Phase (deg)	Δ Gain (Db)	Δ Phase (Deg)
Exact	100	0	-27	--	--
	178	0.5	-45	--	--
	316	0.75	-81	--	--
	562	2.0	-162	--	--
	1000	0	-396	--	--
	830	6.6 (peak)	--	--	--
2nd Order Approx.	100	0	-18	0	-9
	178	0	-27	.5	-18
	316	-.075	-54	1.5	-27
	562	-4.5	-108	6.5	-54
	1000	-13.0	-135	13.0	-261
4th Order Approx.	100	0	-18	0	-9
	178	0.25	-36	0.25	-9
	316	0.5	-62	0.25	-19
	562	-0.5	-135	2.5	-27
	1000	-7.5	-270	7.5	-126
	298	0.5 (peak)	--	6.1	--
6th Order Approx.	100	0.25	-23	-.25	-6
	178	0.5	-40	0	-5
	316	1.25	-72	-.5	-9
	562	3.0	-145	-2.0	-23
	1000	4.5	-300	-4.5	-36
	830	8.3 (peak)	--	-1.7	--

Table 2: Comparison of Exact Transfer Function for Outboard Aileron and Various Lower Order Approximations

	Freq (rad/s)	Gain (Db)	Phase (Deg)	ΔGain (Db)	ΔFreq (Deg)
Exact	100	0	-27	--	--
	178	0.25	-45	--	--
	316	0.5	-90	--	--
	562	0.25	-180	--	--
	1000	-12.5	-306	--	--
	433	0.9 (peak)	--	--	--
2nd Order Approx.	100	0.0	-18	0	-9
	178	-0.5	-27	0.75	-18
	316	-1.0	-45	1.5	-45
	562	-4.0	-81	4.25	-99
	1000	-10.0	-108	-2.5	-198
4th Order Approx.	100	0	-23	0	-6
	178	0	-38	0.25	-7
	316	0.5	-72	0	-8
	562	-1.0	-162	1.25	-18
	1000	-15.0	-252	-2.5	-54
	376	0.4 (peak)	--	0.5	--

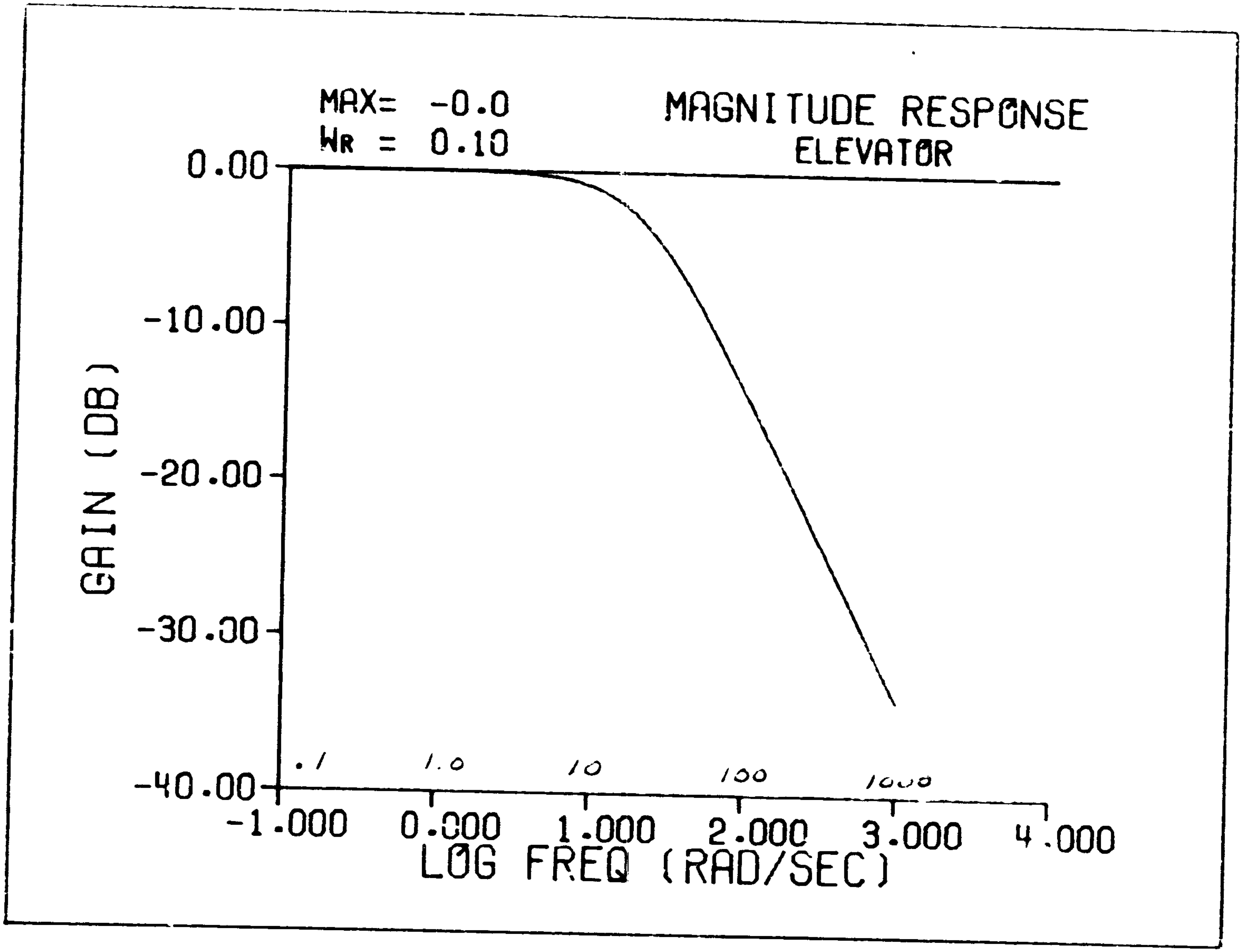
MAX= -0.0
WR = 0.10
MAGNITUDE RESPONSE
ELEVATOR
0.00
-10.00
-20.00
-30.00
-40.00
GAIN (DB)
.1
1.0
10
100
1000
-1.000
0.000
1.000
2.000
3.000
4.000
LOG FREQ (RAD/SEC)

Fig :

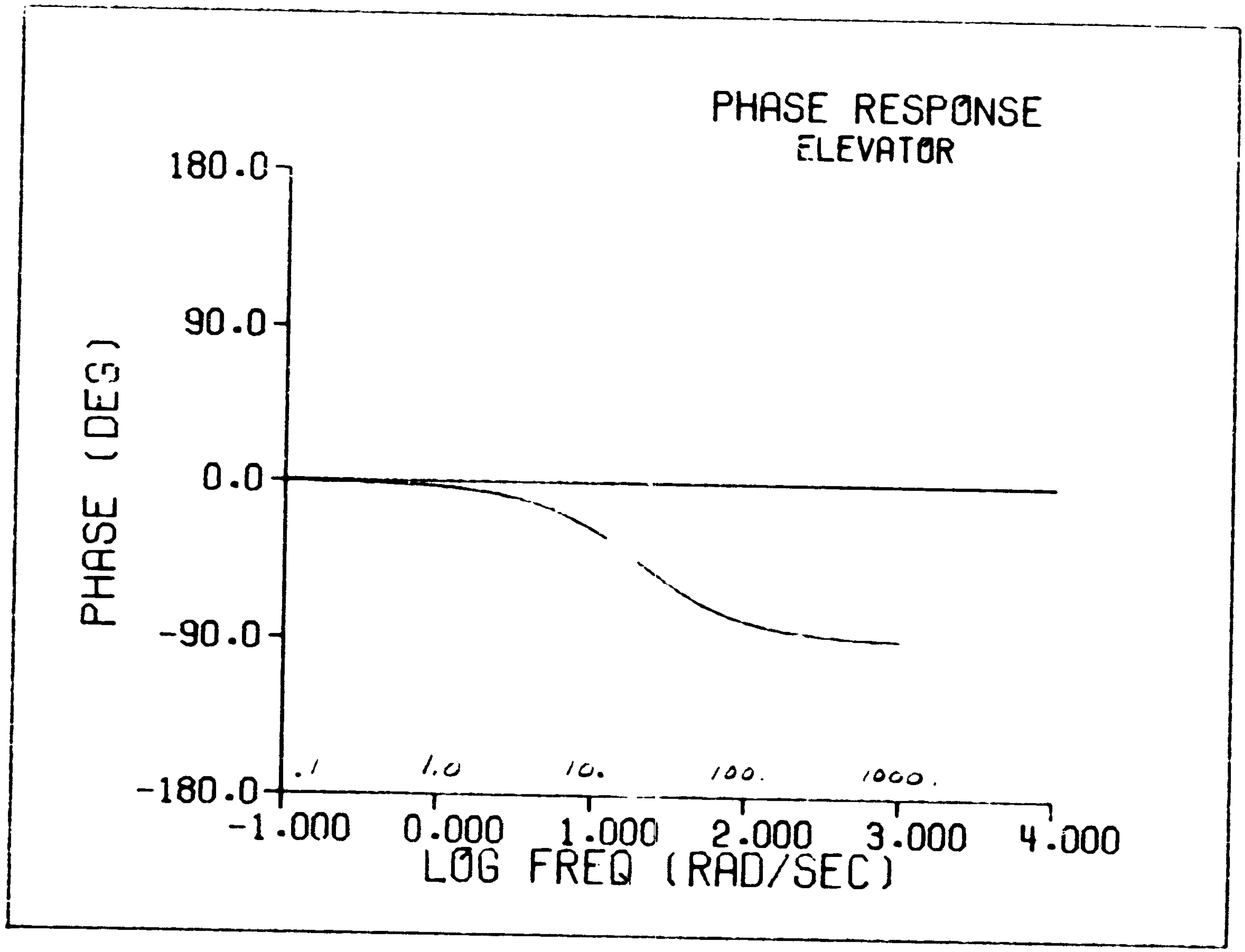
PHASE RESPONSE
ELEVATOR
180.0
90.0
0.0
-90.0
-180.0
PHASE (DEG)
.1
1.0
10.
100.
1000.
-1.000
0.000
1.000
2.000
3.000
4.000
LOG FREQ (RAD/SEC)

Fig 2

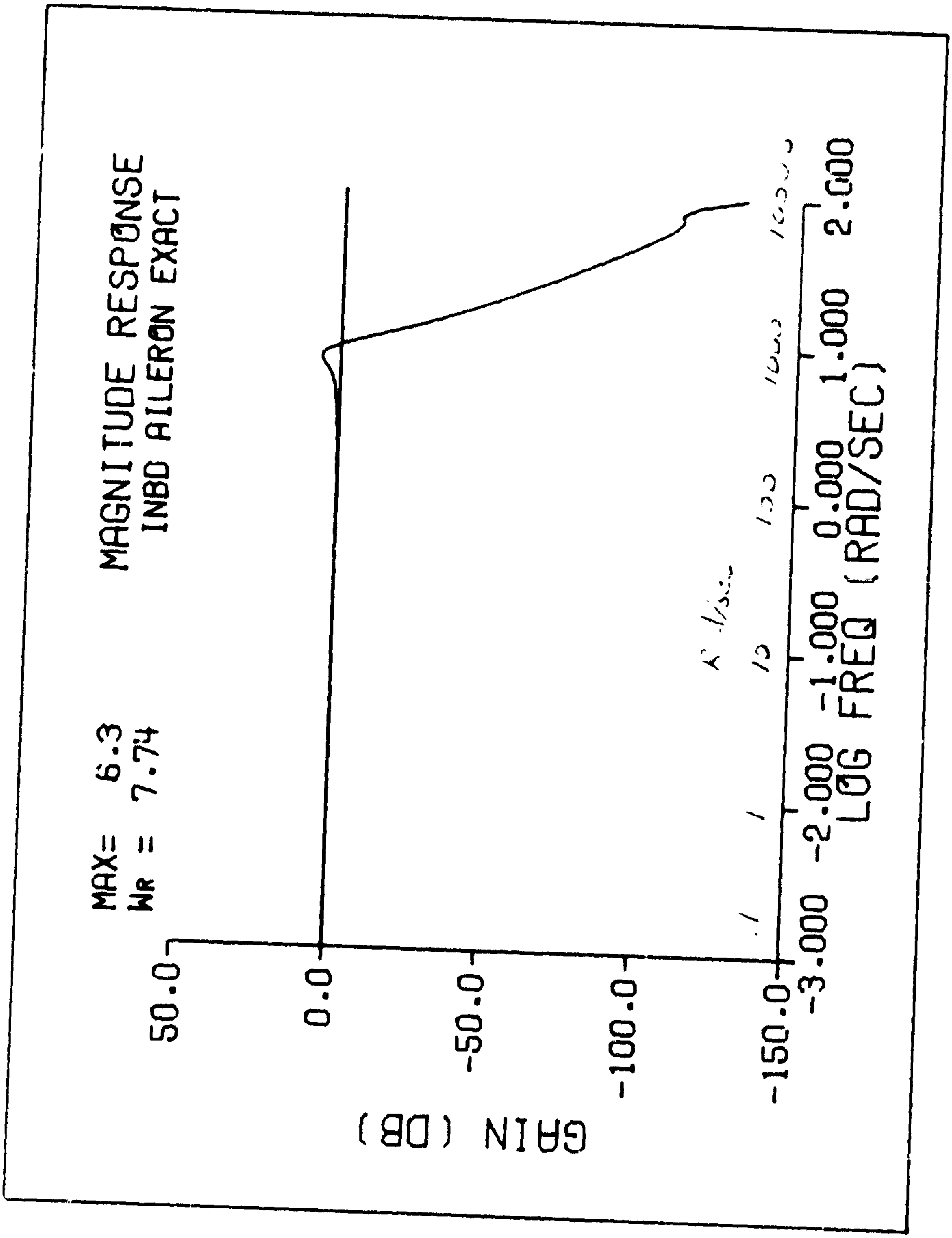
MAGNITUDE RESPONSE
INBD AILERON EXACT
MAX= 6.3
WR = 7.74
GAIN (DB)
50.0
0.0
-50.0
-100.0
-150.0
-3.000
-2.000
-1.000
0.000
1.000
2.000
LOG FREQ (RAD/SEC)

Fig 3

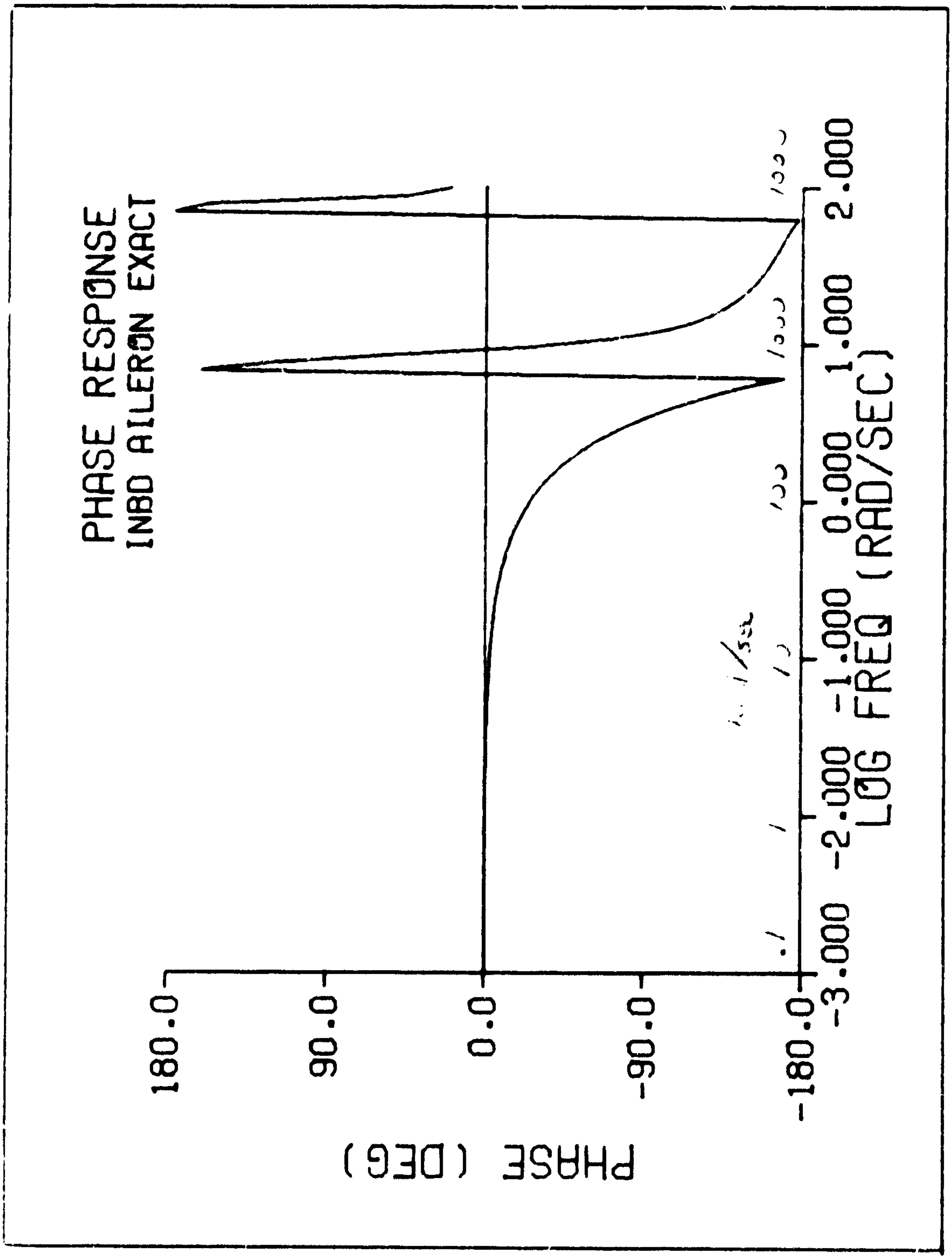
PHASE RESPONSE
INBD AILERON EXACT
PHASE (DEG)
180.0
90.0
0.0
-90.0
-180.0
-3.000
-2.000
-1.000
0.000
1.000
2.000
LOG FREQ (RAD/SEC)

Fig 4

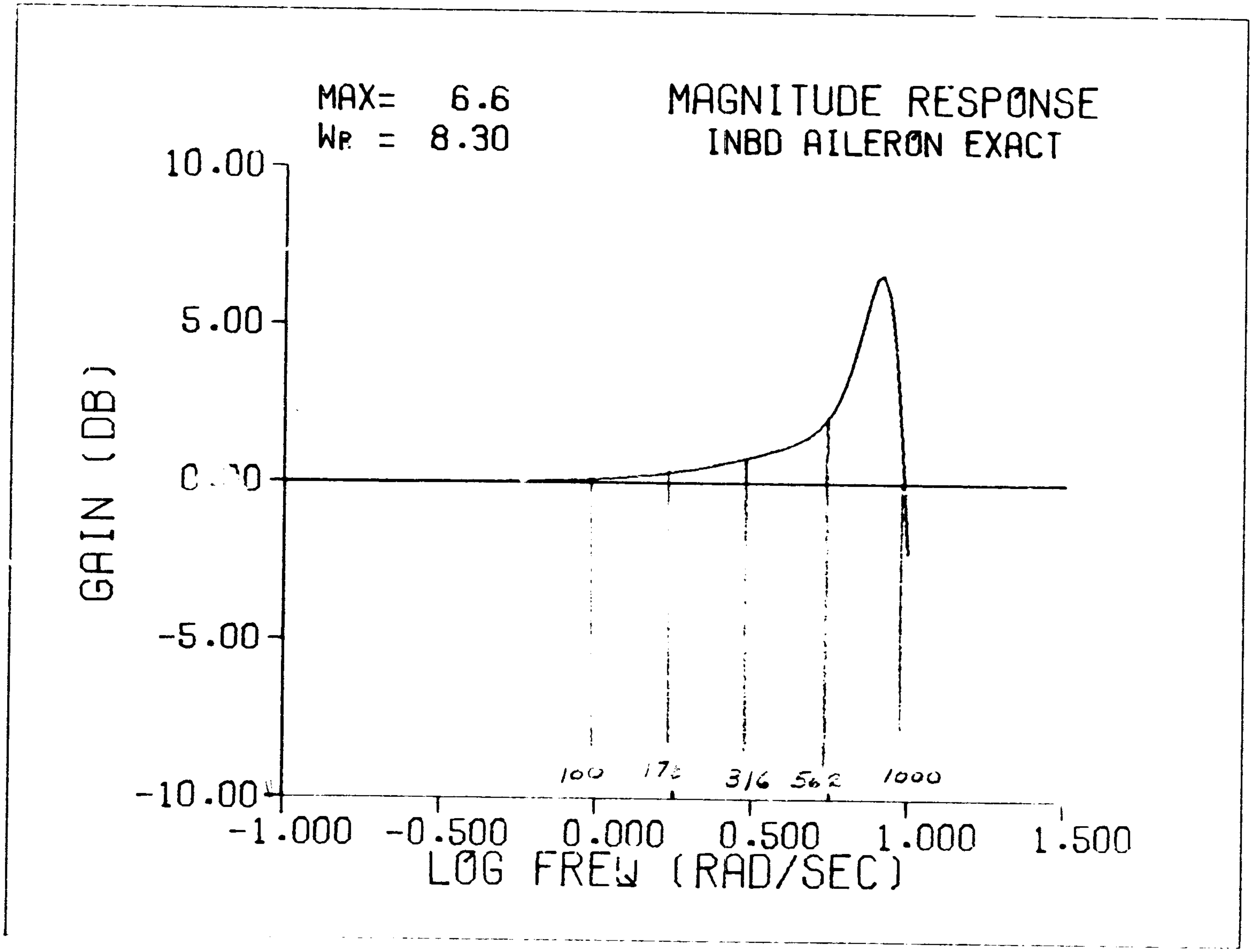
MAX= 6.6
WR = 8.30
MAGNITUDE RESPONSE
INBD AILERON EXACT
GAIN (DB)
10.00
5.00
-5.00
-10.00
100
178
316
562
1000
-1.000
-0.500
0.000
0.500
1.000
1.500
LOG FREQ (RAD/SEC)

Fig 5

ORIGINAL PAGE IS
OF POOR QUALITY

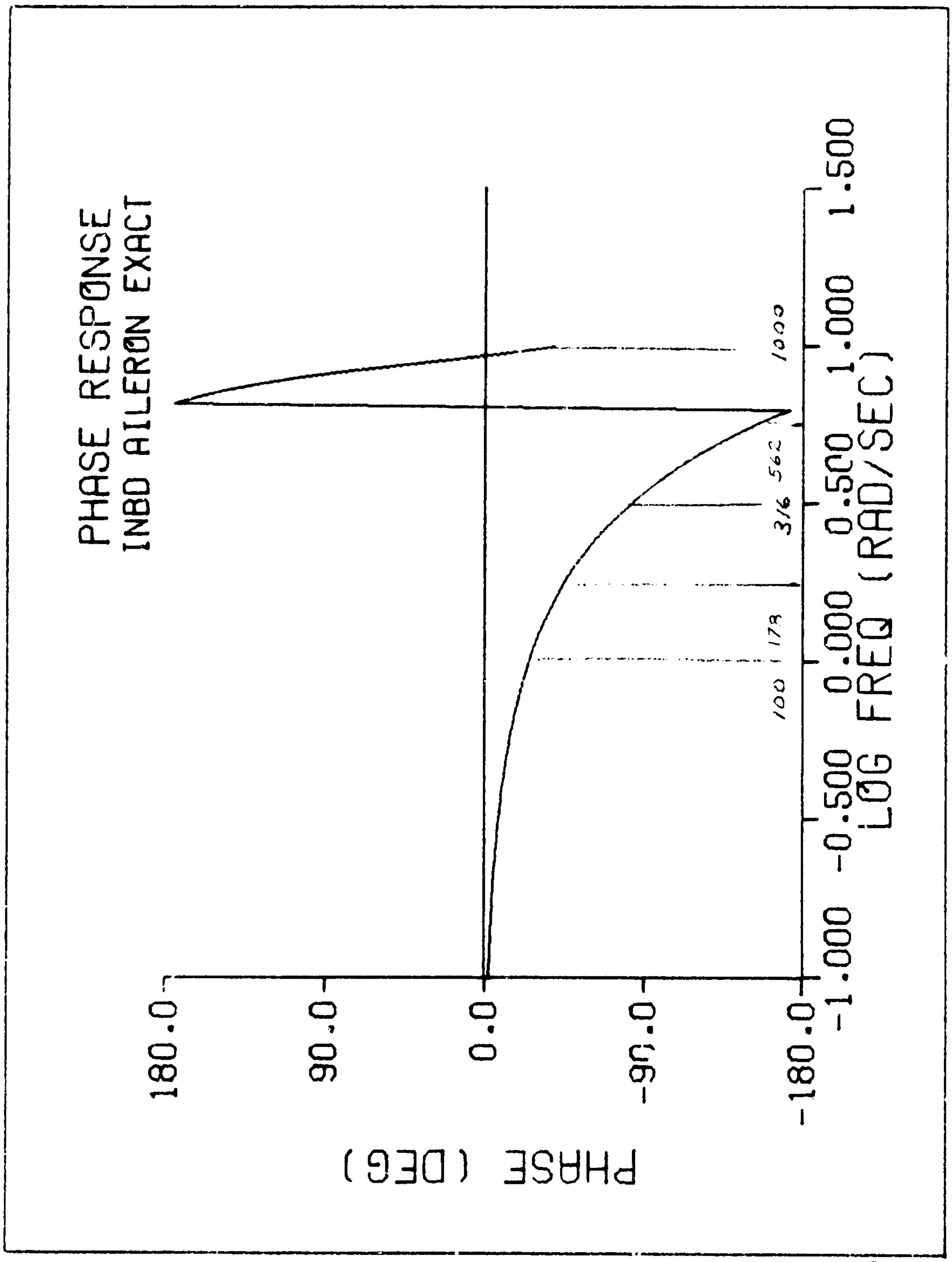

Fig 6

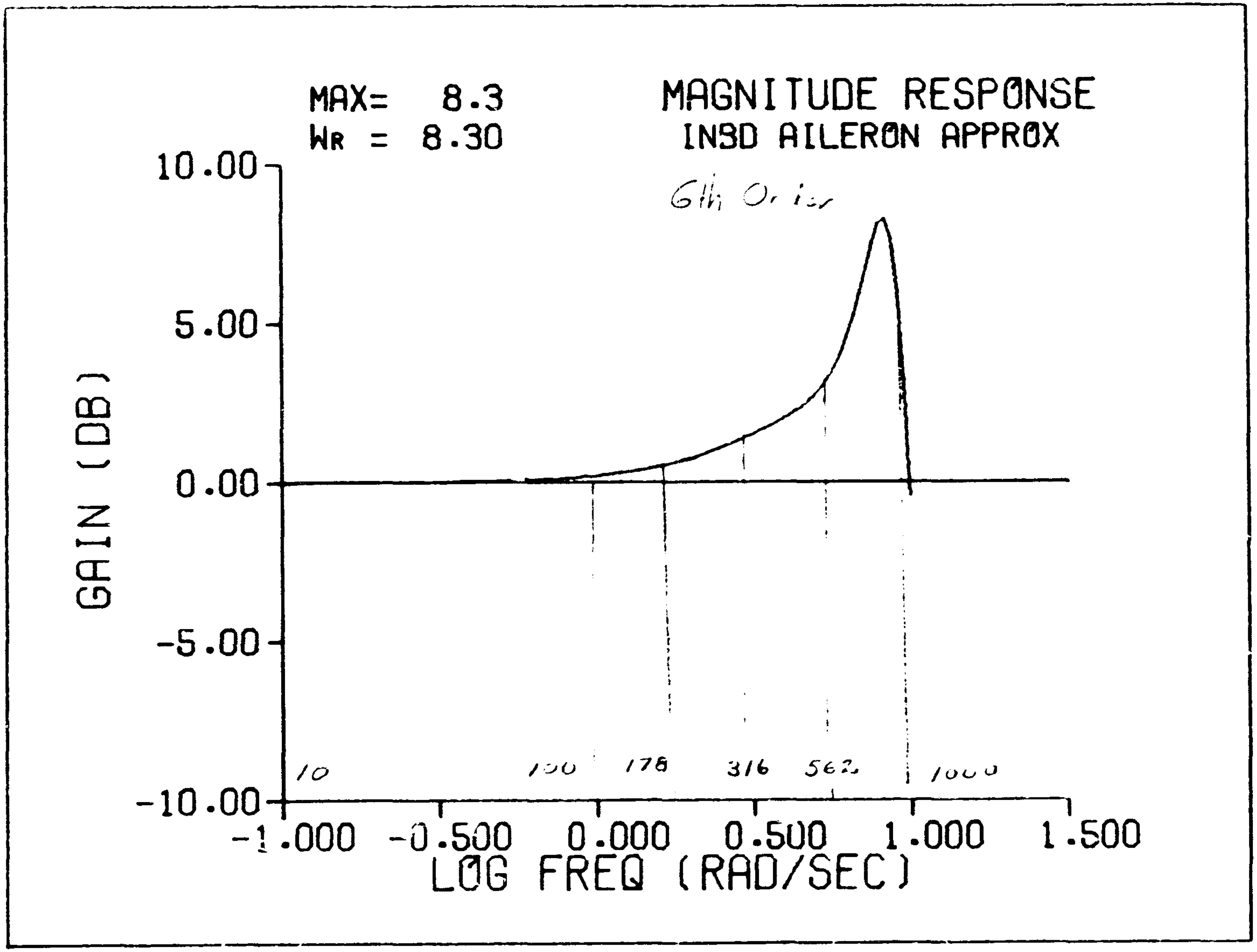
MAX= 8.3
WR = 8.30
MAGNITUDE RESPONSE
INBD AILERON APPROX
6th Order
GAIN (DB)
10.00
5.00
0.00
-5.00
-10.00
10
178
316
562
-1.000
-0.500
0.000
0.500
1.000
1.500
LOG FREQ (RAD/SEC)

Fig 7

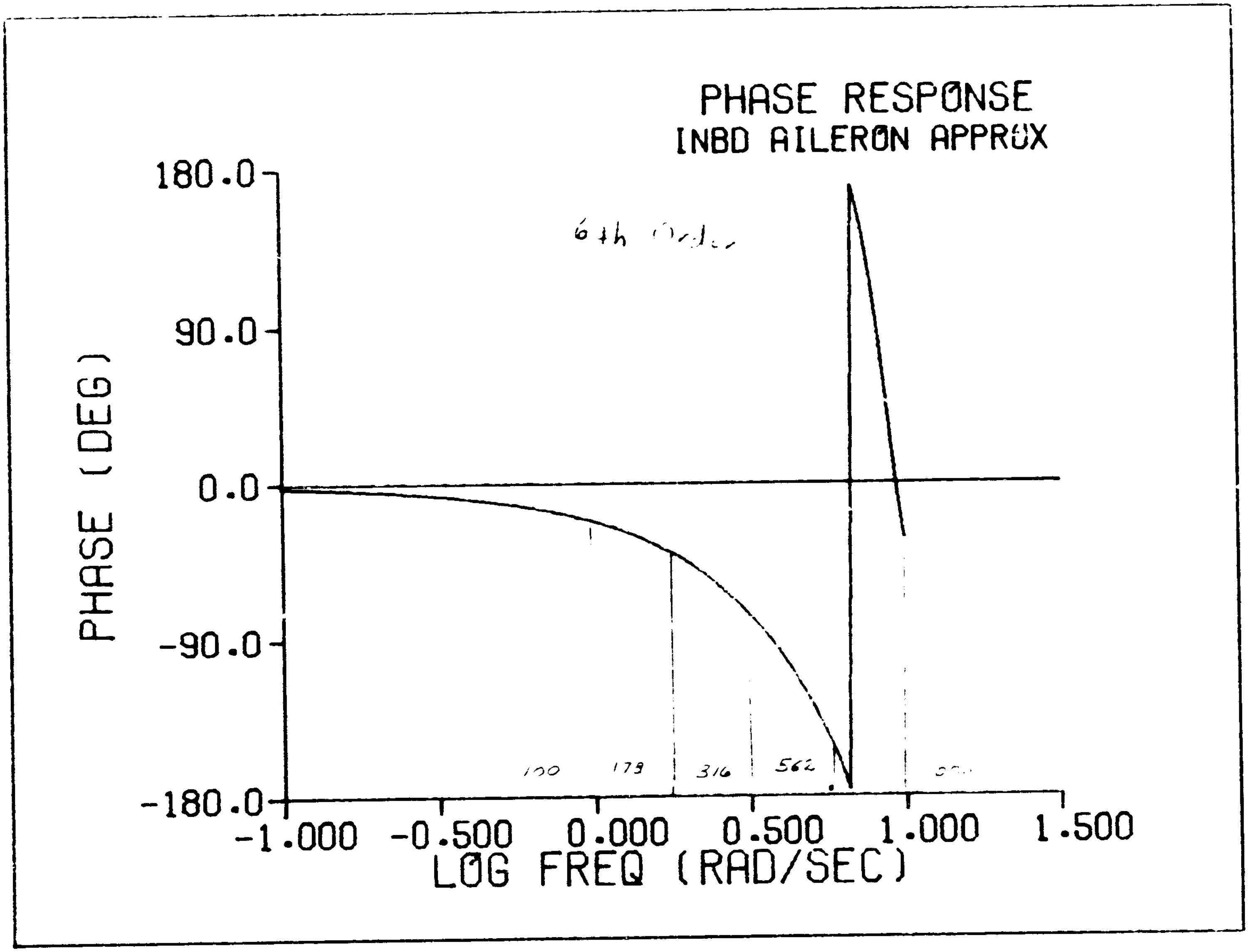

PHASE RESPONSE
INBD AILERON APPROX
6th Order
PHASE (DEG)
180.0
90.0
0.0
-90.0
-180.0
-1.000
-0.500
0.000
0.500
1.000
1.500
LOG FREQ (RAD/SEC)
100
178
316
562

Fig 8

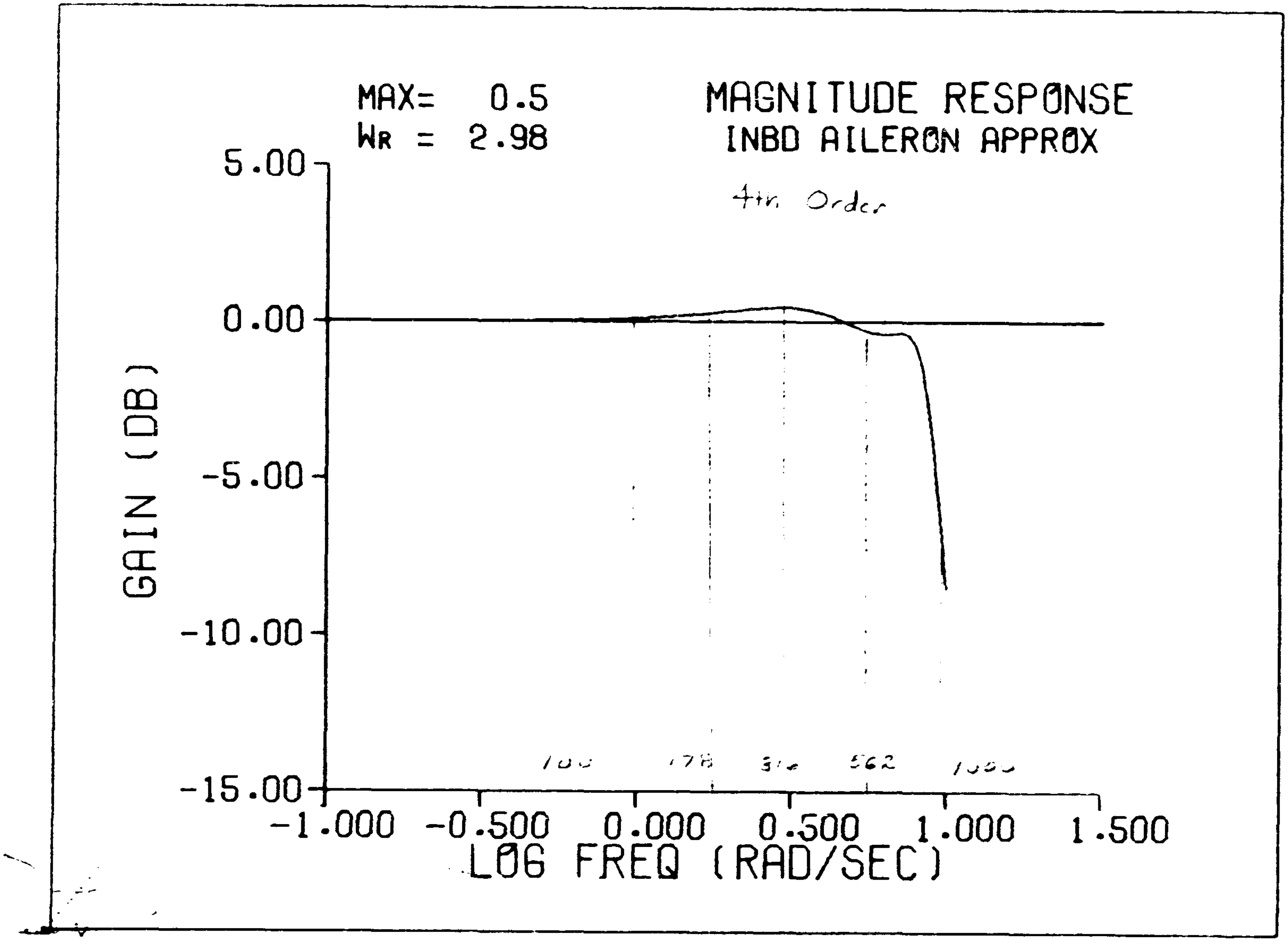
MAX= 0.5
WR = 2.98
MAGNITUDE RESPONSE
INBD AILERON APPROX
4th Order
5.00
0.00
-5.00
-10.00
-15.00
GAIN (DB)
178
562
-1.000
-0.500
0.000
0.500
1.000
1.500
LOG FREQ (RAD/SEC)

Fig 9

ORIGINAL PAGE IS
OF POOR QUALITY

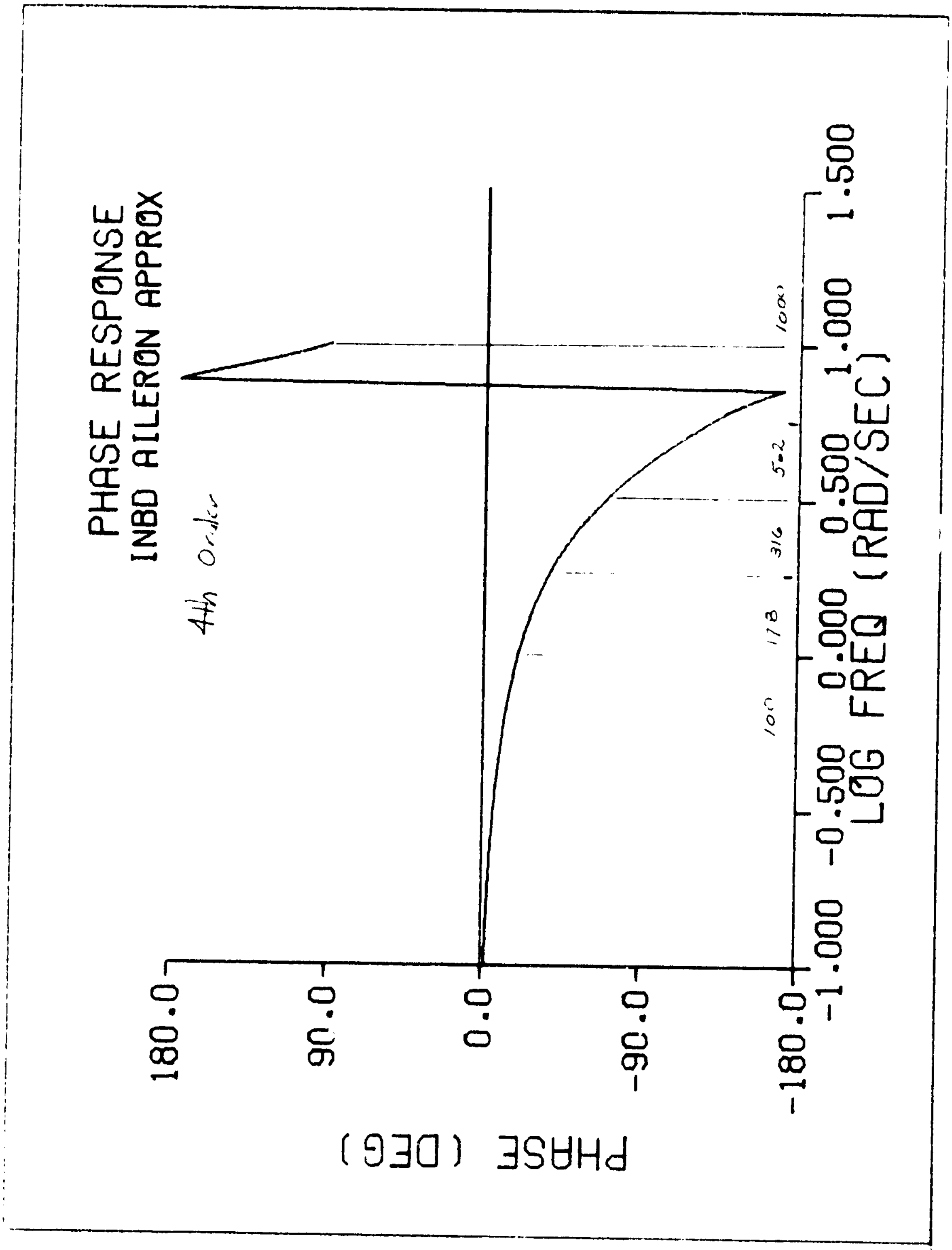

Fig 10

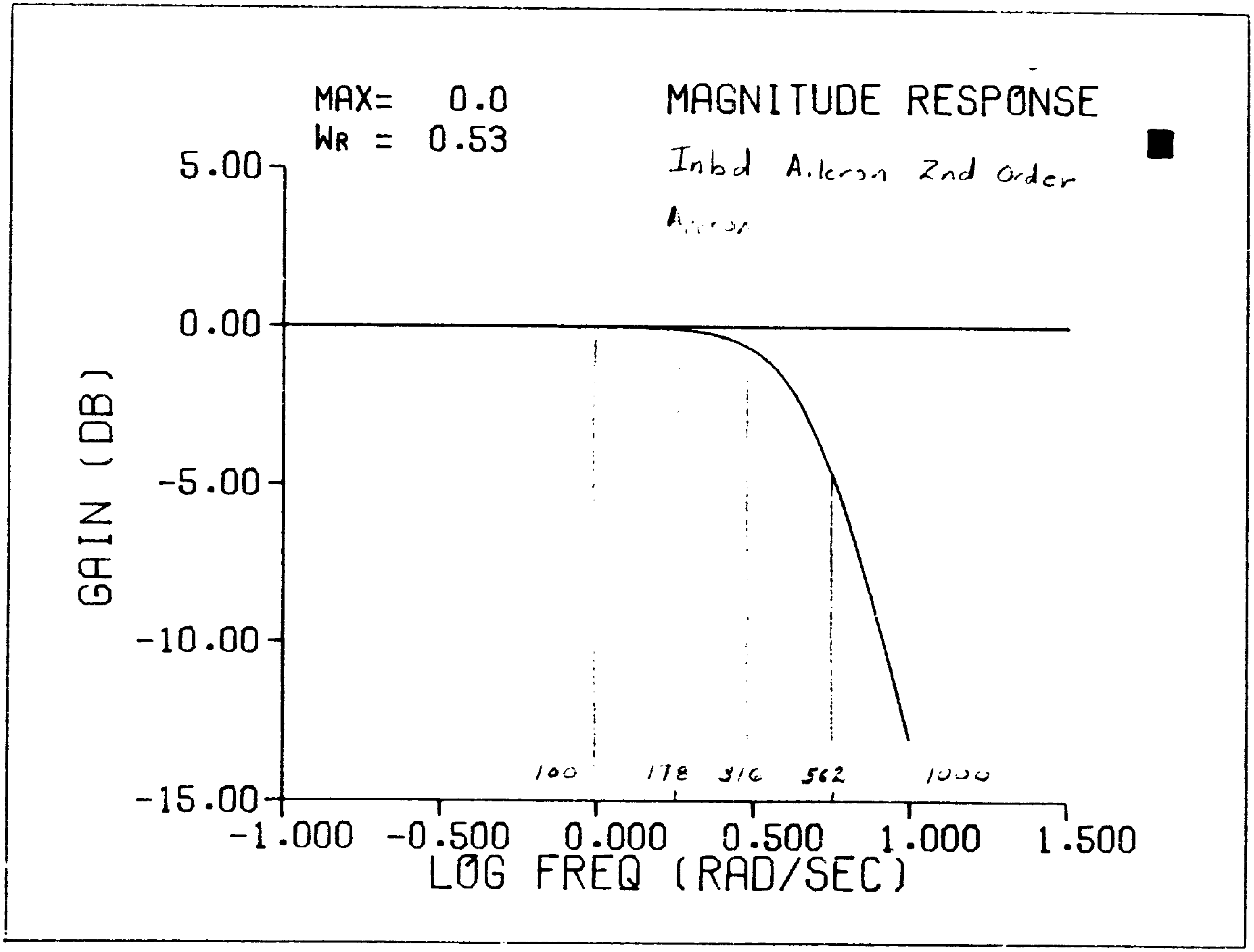
MAX= 0.0
WR = 0.53
MAGNITUDE RESPONSE
Inbd Aileron 2nd Order
Approx
GAIN (DB)
5.00
0.00
-5.00
-10.00
-15.00
100
178
316
562
1000
-1.000
-0.500
0.000
0.500
1.000
1.500
LOG FREQ (RAD/SEC)

Fig 11

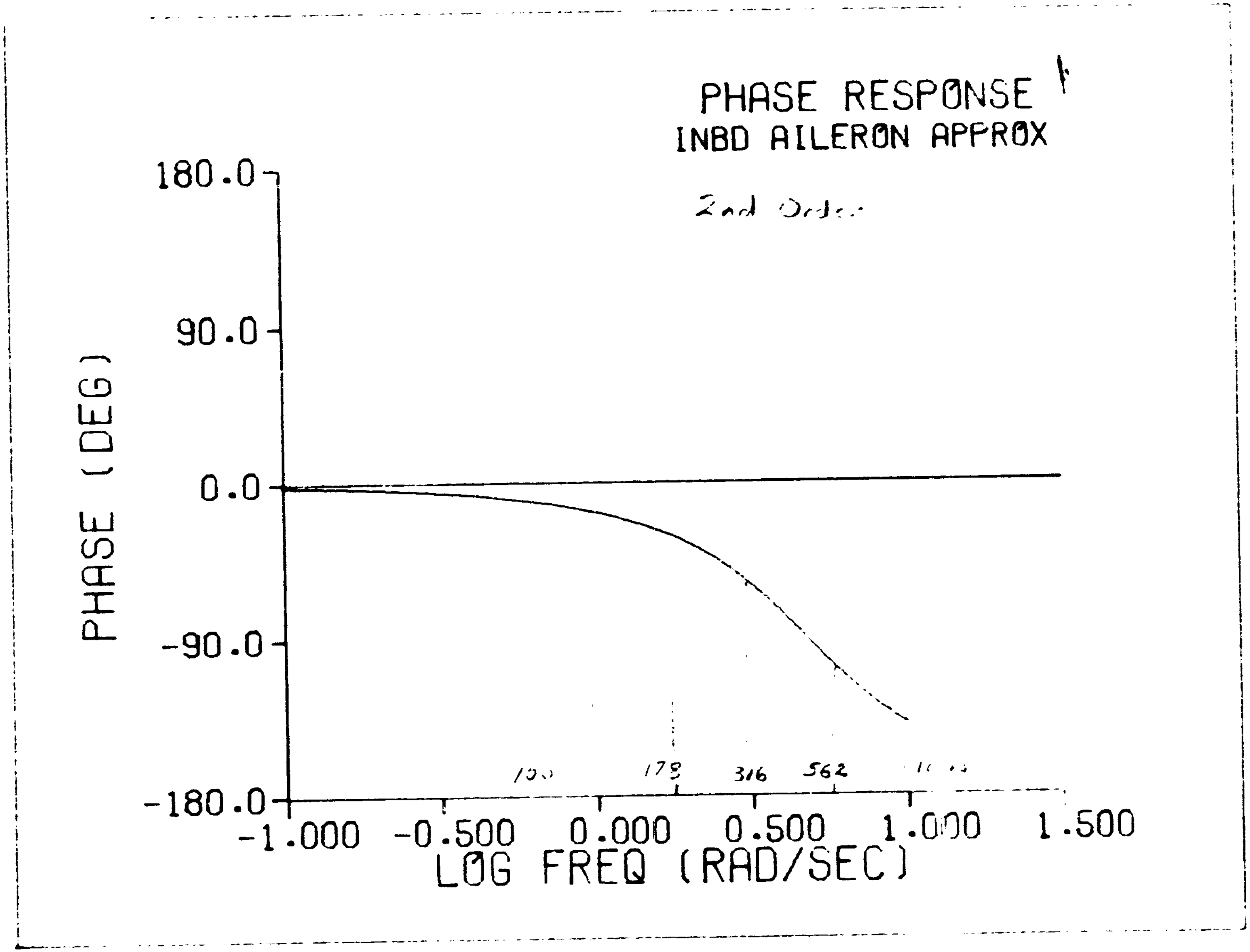
PHASE RESPONSE
INBD AILERON APPROX
2nd Order
180.0
90.0
0.0
-90.0
-180.0
PHASE (DEG)
178
316
562
-1.000
-0.500
0.000
0.500
1.000
1.500
LOG FREQ (RAD/SEC)

Fig 12

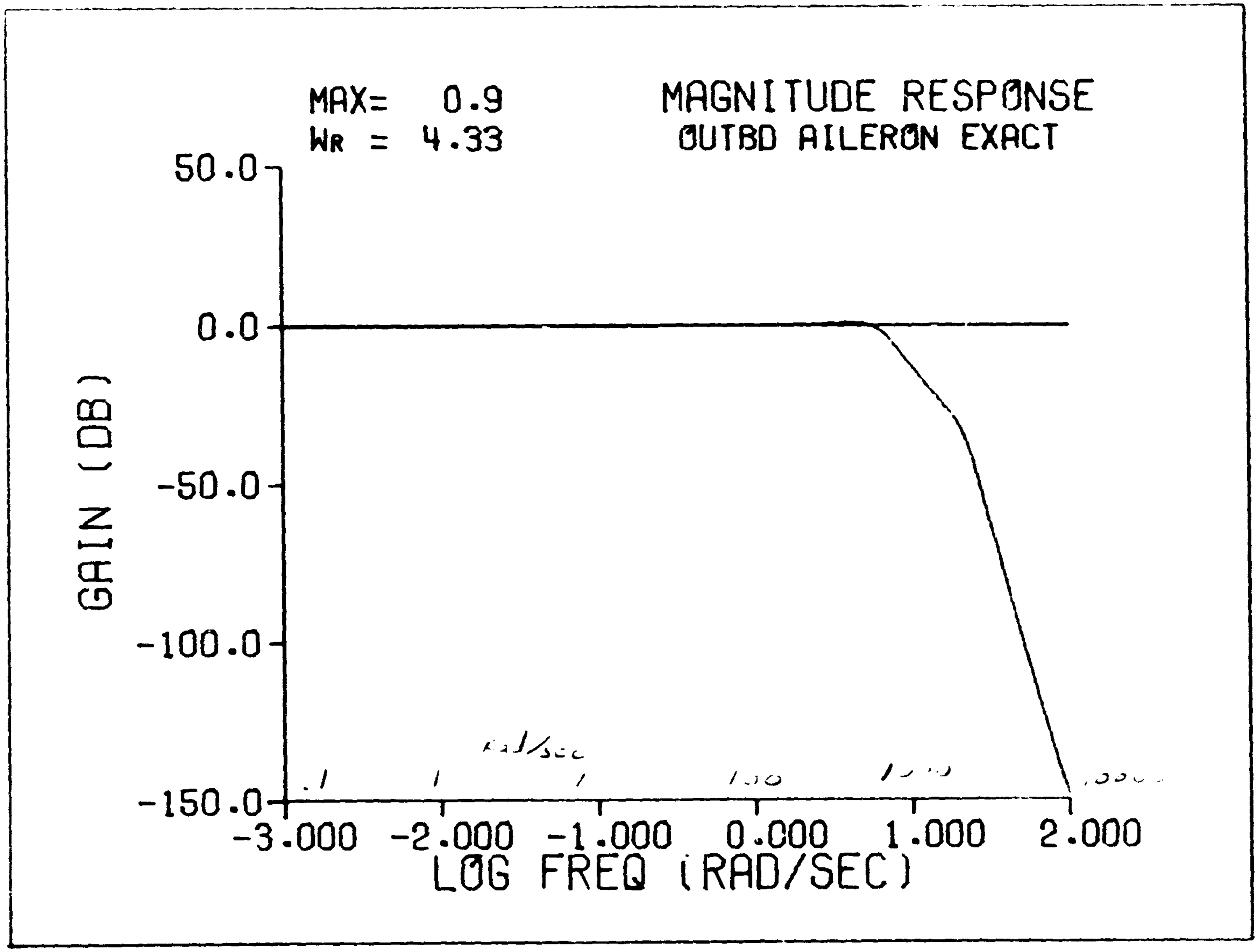
MAX= 0.9
WR = 4.33
MAGNITUDE RESPONSE
OUTBD AILERON EXACT
GAIN (DB)
50.0
0.0
-50.0
-100.0
-150.0
-3.000
-2.000
-1.000
0.000
1.000
2.000
LOG FREQ (RAD/SEC)

Fig 13

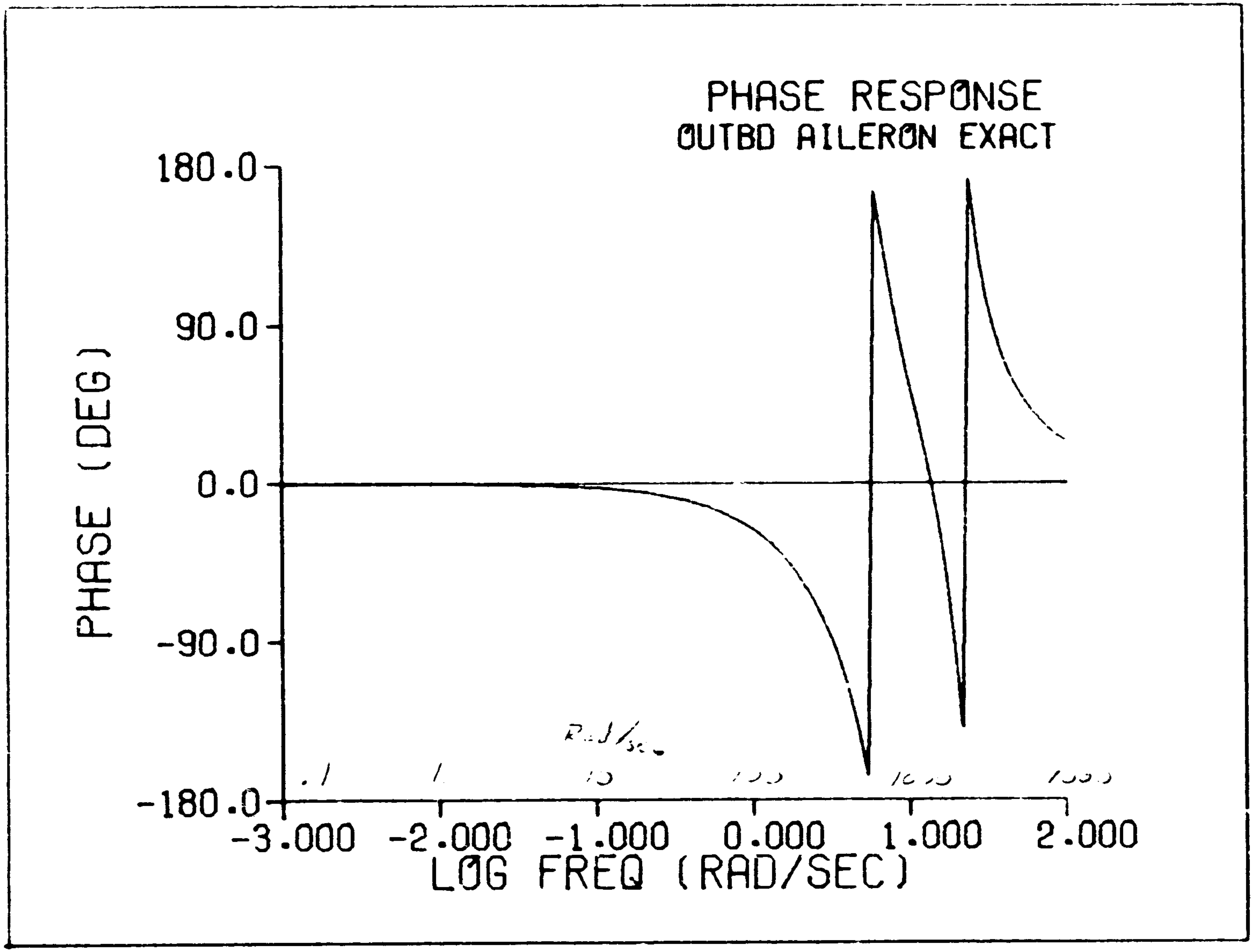
PHASE RESPONSE
OUTBD AILERON EXACT
PHASE (DEG)
180.0
90.0
0.0
-90.0
-180.0
Rad/sec
.1
1
10
100
1000
-3.000
-2.000
-1.000
0.000
1.000
2.000
LOG FREQ (RAD/SEC)

Fig 14

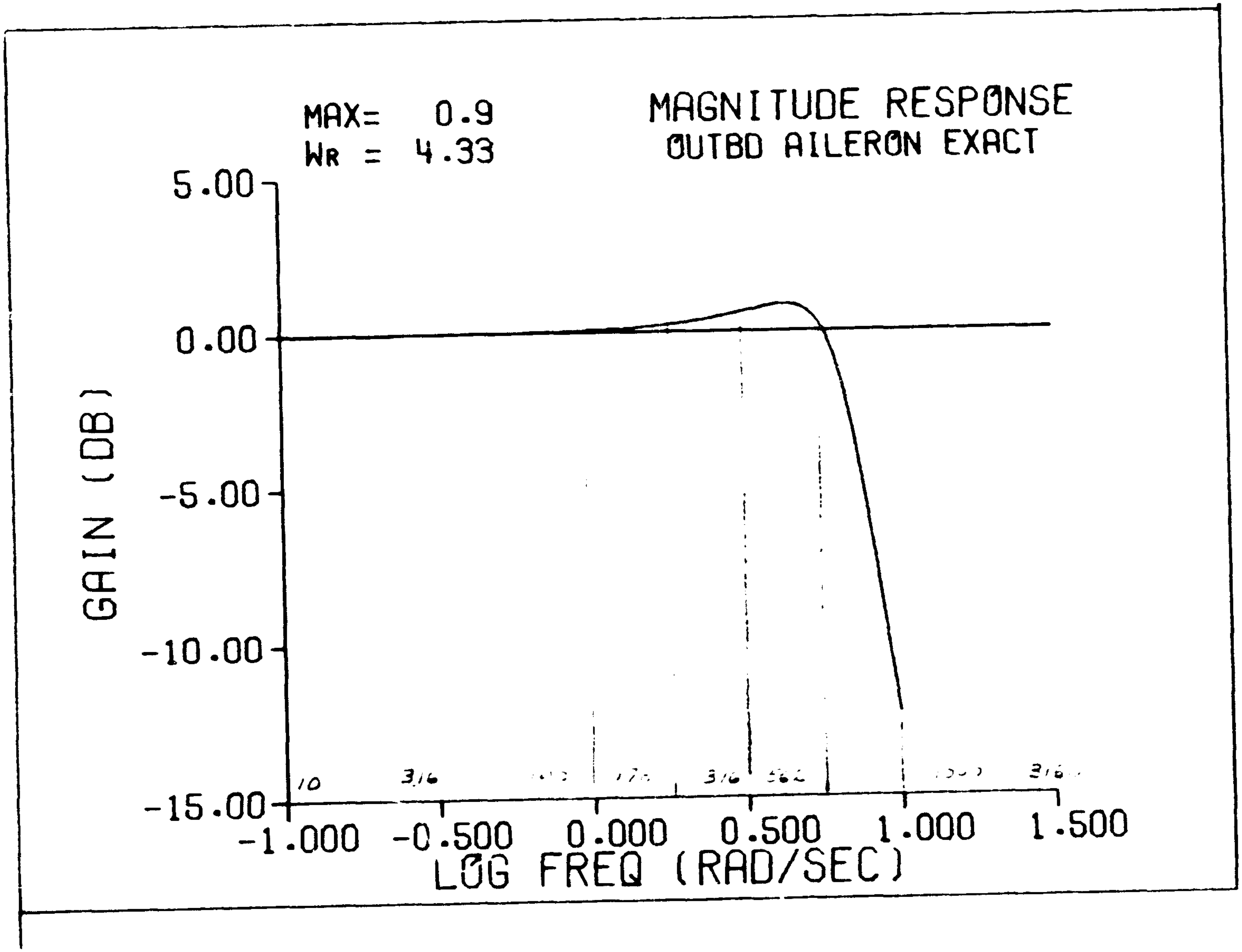

MAX= 0.9
WR = 4.33
MAGNITUDE RESPONSE
OUTBD AILERON EXACT
5.00
0.00
-5.00
-10.00
-15.00
GAIN (DB)
-1.000
-0.500
0.000
0.500
1.000
1.500
LOG FREQ (RAD/SEC)

Fig 15

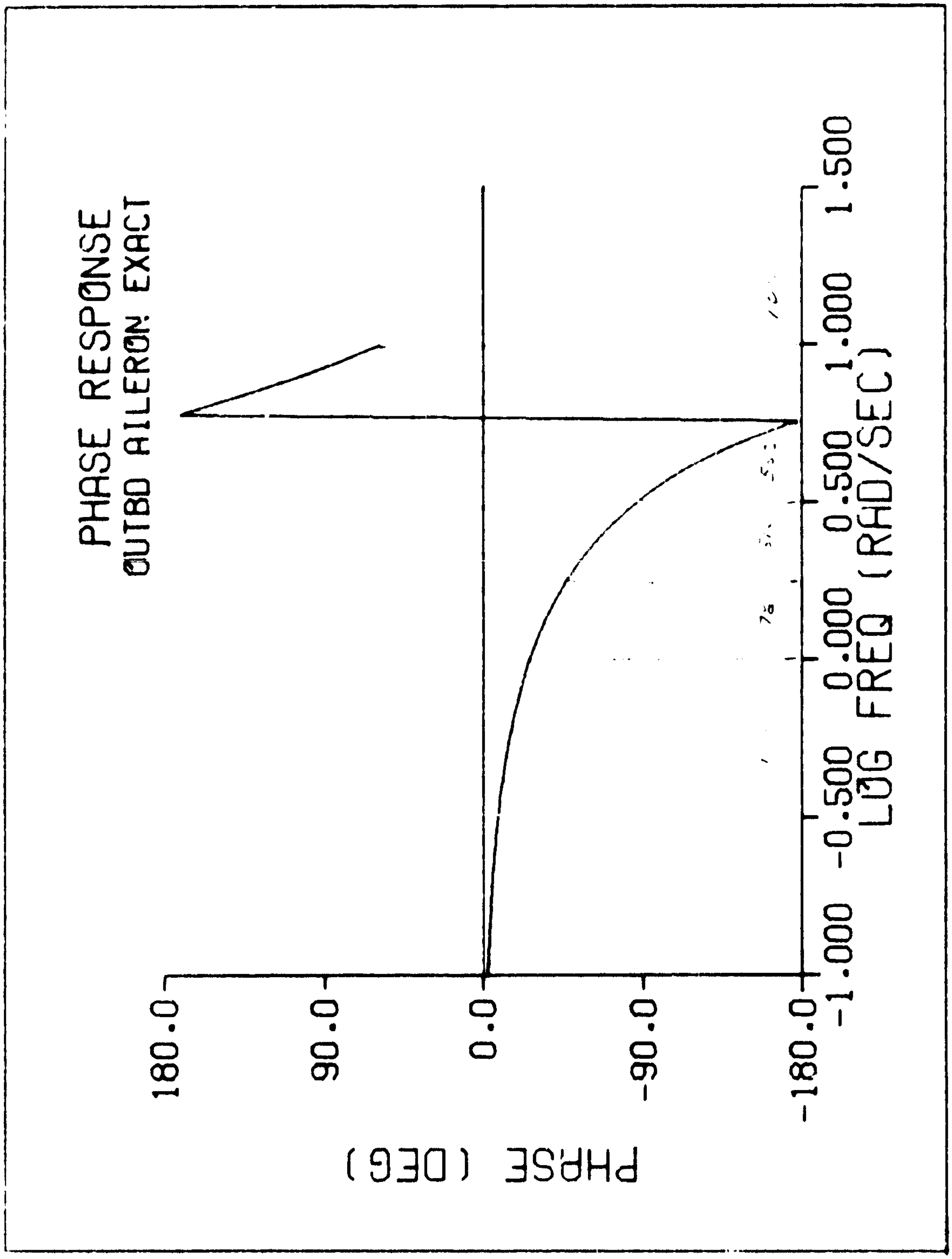
PHASE RESPONSE
OUTBD AILERON EXACT
PHASE (DEG)
180.0
90.0
0.0
-90.0
-180.0
-1.000
-0.500
0.000
0.500
1.000
1.500
LOG FREQ (RAD/SEC)

Fig 16

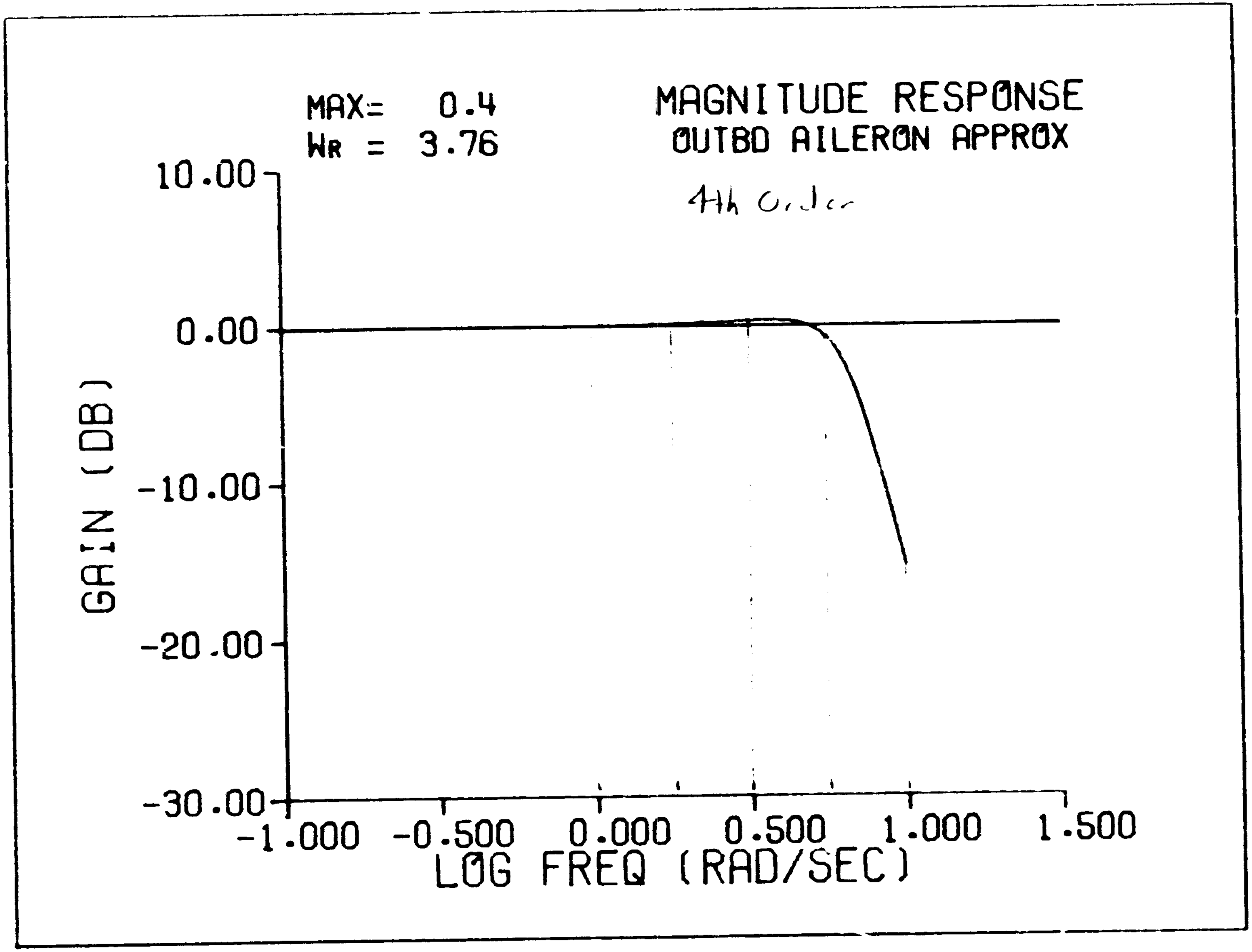
MAX= 0.4
WR = 3.76
MAGNITUDE RESPONSE
OUTBD AILERON APPROX
4th Order
10.00
0.00
-10.00
-20.00
-30.00
GAIN (DB)
-1.000
-0.500
0.000
0.500
1.000
1.500
LOG FREQ (RAD/SEC)

Fig 17

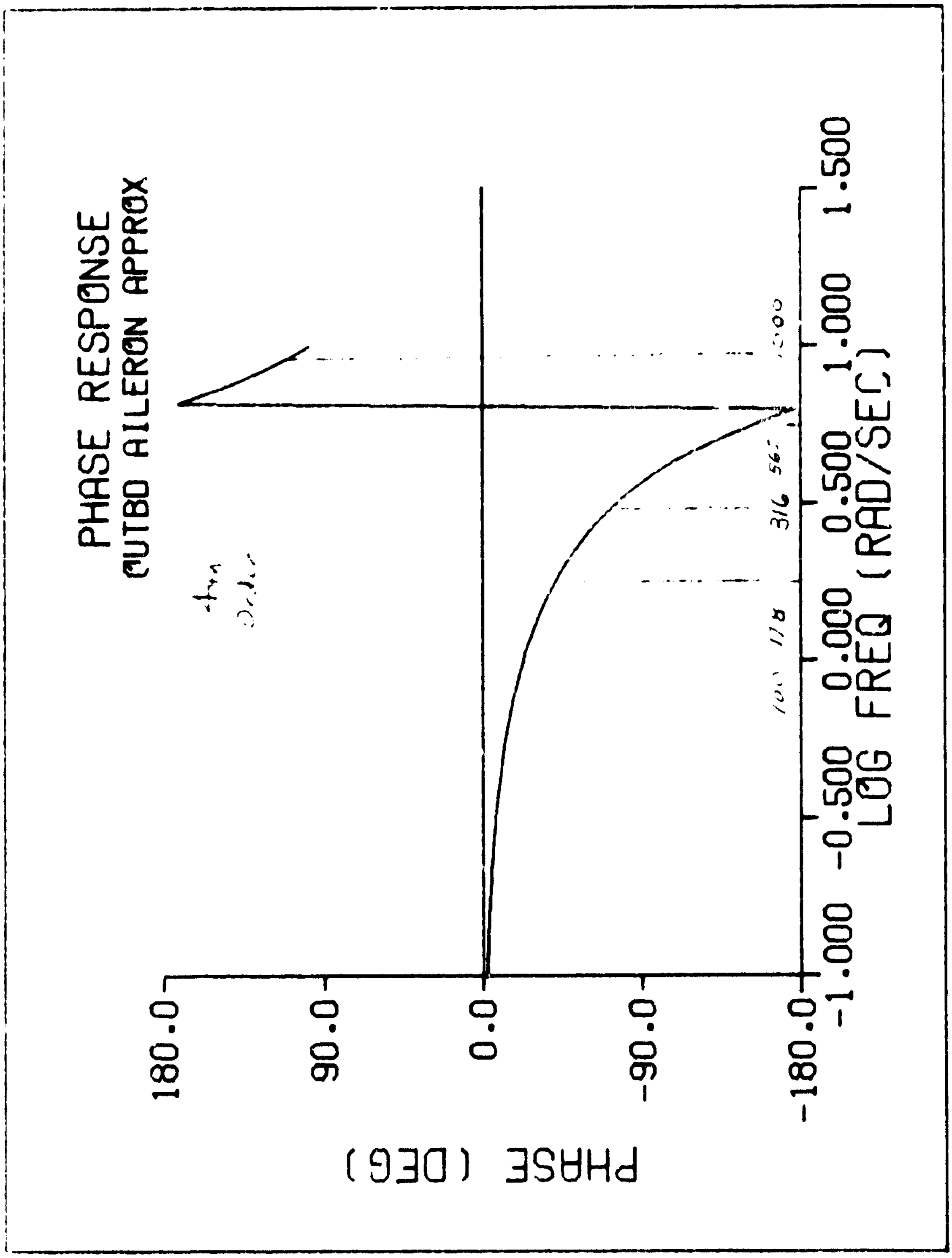
PHASE RESPONSE
OUTBD AILERON APPROX
PHASE (DEG)
180.0
90.0
0.0
-90.0
-180.0
LOG FREQ (RAD/SEC)
-1.000
-0.500
0.000
0.500
1.000
1.500

Fig 18

ORIGINAL PAGE IS
OF POOR QUALITY

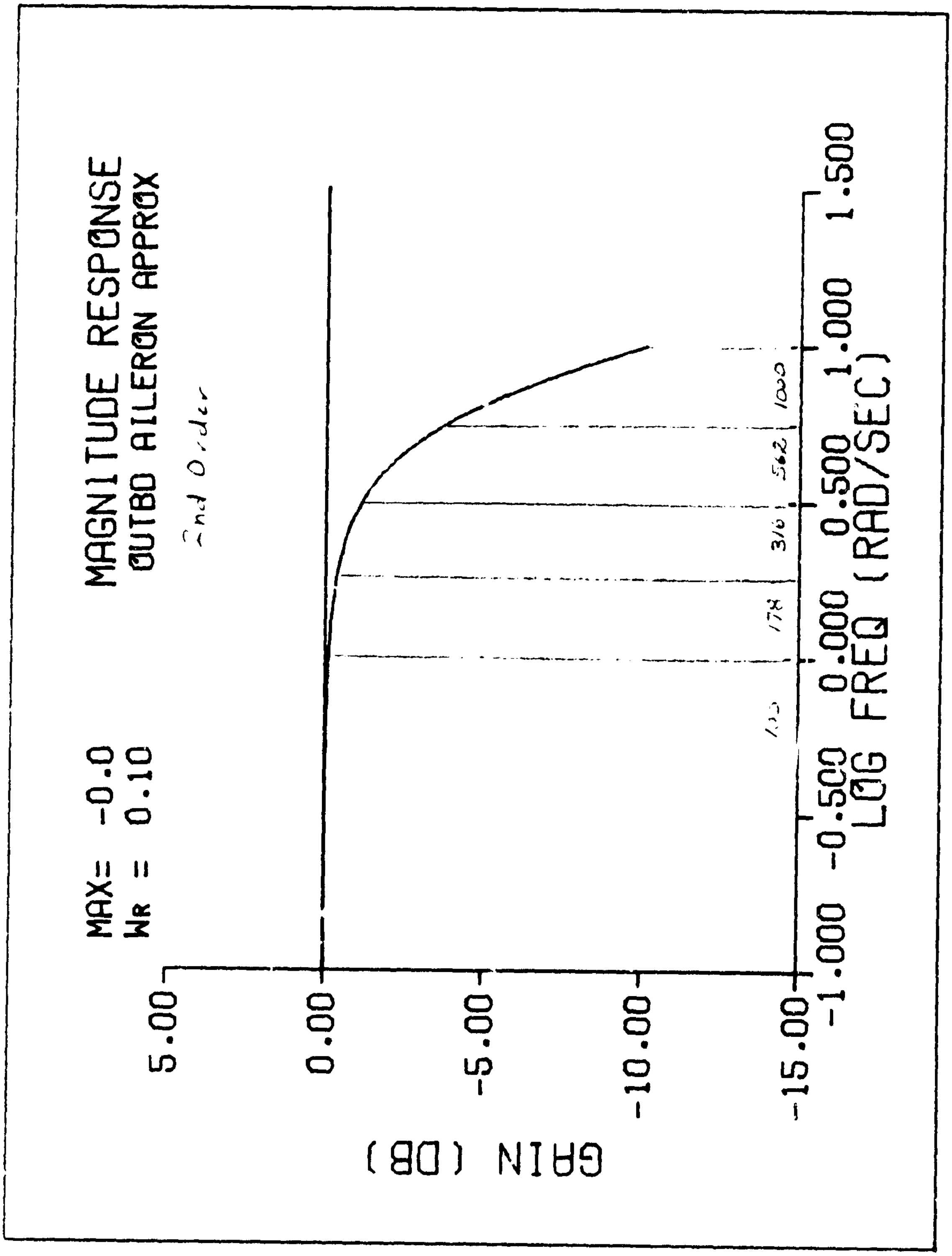

Fig 19

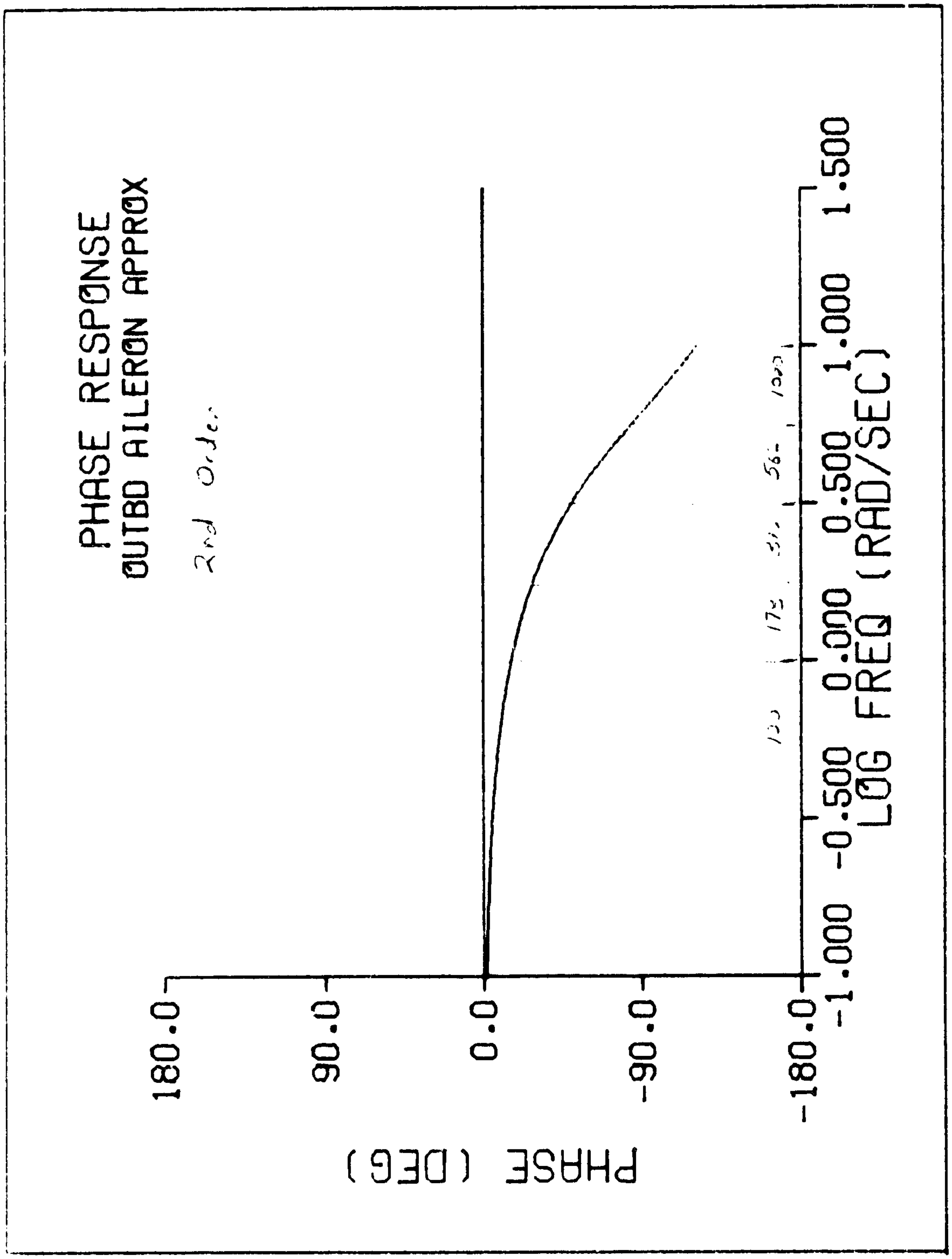
PHASE RESPONSE
OUTBD AILERON APPROX
PHASE (DEG)
180.0
90.0
0.0
-90.0
-180.0
-1.000
-0.500
0.000
0.500
1.000
1.500
LOG FREQ (RAD/SEC)

Fig 20

Working Paper No. 2

Gust Model for Flutter Control Study

W.L. Garrard
Dept. of Aerospace Engineering and Mechanics
University of Minnesota
Minneapolis, MN

Introduction

A second order vertical wind gust model is described. The vertical gust is to have a 12 ft/sec rms value at the flutter condition of Mach 0.86 and 15000 feet and a 59 ft/sec rms value for the gust test condition of Mach 0.7 and 15000 ft. A 30 to 40 percent reduction in bending moment at all stations is desired at this condition compared with the uncontrolled aircraft.

Gust Transfer Function

The transfer function for a second order gust model is given as

$$\frac{\delta(s)}{\eta(s)} = \frac{\left(1 + \sqrt{3}\,\frac{\ell}{v}\,s\right)}{\left(\left(\frac{\ell}{v}\right)s + 1\right)^2} = G(s)$$

where δ = the vertical gust velocity

ℓ = the characteristic length (2500 ft in this case)

v = the forward velocity

η = a white noise input

If we assume s_η is the spectral density of the white noise the expected value of δ^2 is given as

$$E[\delta^2] = \int_{-\infty}^{\infty} G(j\omega)\,G(-j\omega)\,s_\eta\,d\omega$$

If s_η is constant, this integral can be evaluated from standard tables [1] as

$$E[\delta^2] = 2 s_\eta \pi \left(\frac{v}{\ell}\right)$$

Now we want $E[\delta^2]$ to equal σ^2, the specified rms value of the gust; therefore,

$$s_\eta = \frac{\sigma^2}{2\pi}\left(\frac{\ell}{v}\right)$$

Now

$$s_\eta = \frac{1}{2\pi}\int_{-\infty}^{\infty} R_\eta(\tau)\, e^{-j\omega\tau}\, d\tau$$

where $R_\eta(\tau)$ is the autocorrelation function of η and since η is white noise

$$R_\eta(\tau) = \Lambda\, \delta(\tau)$$

where δ is the Dirac delta function. Then

$$s_\eta = \frac{\Lambda}{2\pi} = \frac{\sigma^2}{2\pi}\left(\frac{\ell}{v}\right)$$

therefore the intensity of the white noise is

$$\Lambda = \left(\frac{\ell}{v}\right)\sigma^2$$

At flutter, Mach = 0.86, h = 15000 ft, v = 908.8 ft/s, ℓ/v = 2.75

$$\delta(s)/\eta(s) = (1 + 4.76s)/(2.75s + 1)^2$$

and

Λ = 396.00

At the gust test condition, v = 739.7 ft/s, ℓ/v = 3.38

$$\delta(s)/\eta(s) = (1 + 5.85s)/(3.38s + 1)^2$$

and

Λ = 11765.78

Both transfer functions represent critically damped systems. The natural frequency at the flutter condition is

$$\omega_n = 0.363 \text{ rad/sec} \quad \text{(flutter condition)}$$

and at the gust test condition is

$$\omega_n = 0.296 \text{ rad/sec} \quad \text{(gust test condition)}$$

Bode plots for the flutter condition are shown in Figs. 1 and 2 and for the gust test condition in Figs. 3 and 4.

State Space Representation

Since the gust models contain numerator dynamics a little extra work is required to put them in state variable form. We can accomplish this by using the block diagram shown in Fig. 5. The transfer function is

$$\frac{\delta(s)}{\eta(s)} = \left(\frac{h_2}{h_1 \frac{2V}{\ell} + 1} \right) \left(\left(\frac{h_1}{h_1 \frac{2V}{\ell}} \right) s + 1 \right) \Big/ \left(s^2 + \frac{2V}{\ell} s + \left(\frac{V}{\ell} \right)^2 \right)$$

By inspection

$$h_1 = -.703\ \ell/V$$

and

$$h_2 = -.406 \left(V/\ell \right)^2$$

Now from the block diagram we have the equations of motion in state space form as

$$\dot{\delta} = z + 0.285 \left(V/\ell \right) \eta$$

$$\dot{z} = -2\left(\frac{V}{\ell}\right) z - \left(V/\ell\right)^2 \delta - 0.406 \left(V/\ell\right)^2 \eta$$

For M = 0.86 and 15000 feet

$$\dot{\delta} = z + 0.104\,\eta$$

$$\dot{z} = -0.727\,z - 0.132\,\delta - 0.0563\,\eta$$

and for M = 0.7 and 15000 feet

$$\dot{\delta} = z + 0.084\eta$$

$$\dot{z} = -0.529z - 0.0875\delta - 0.0355\eta$$

Reference

1. Crandall, S.H. and Mark, W.D., "Random Vibration", Academic Press, 1963, page 72.

ORIGINAL PAGE IS
OF POOR QUALITY

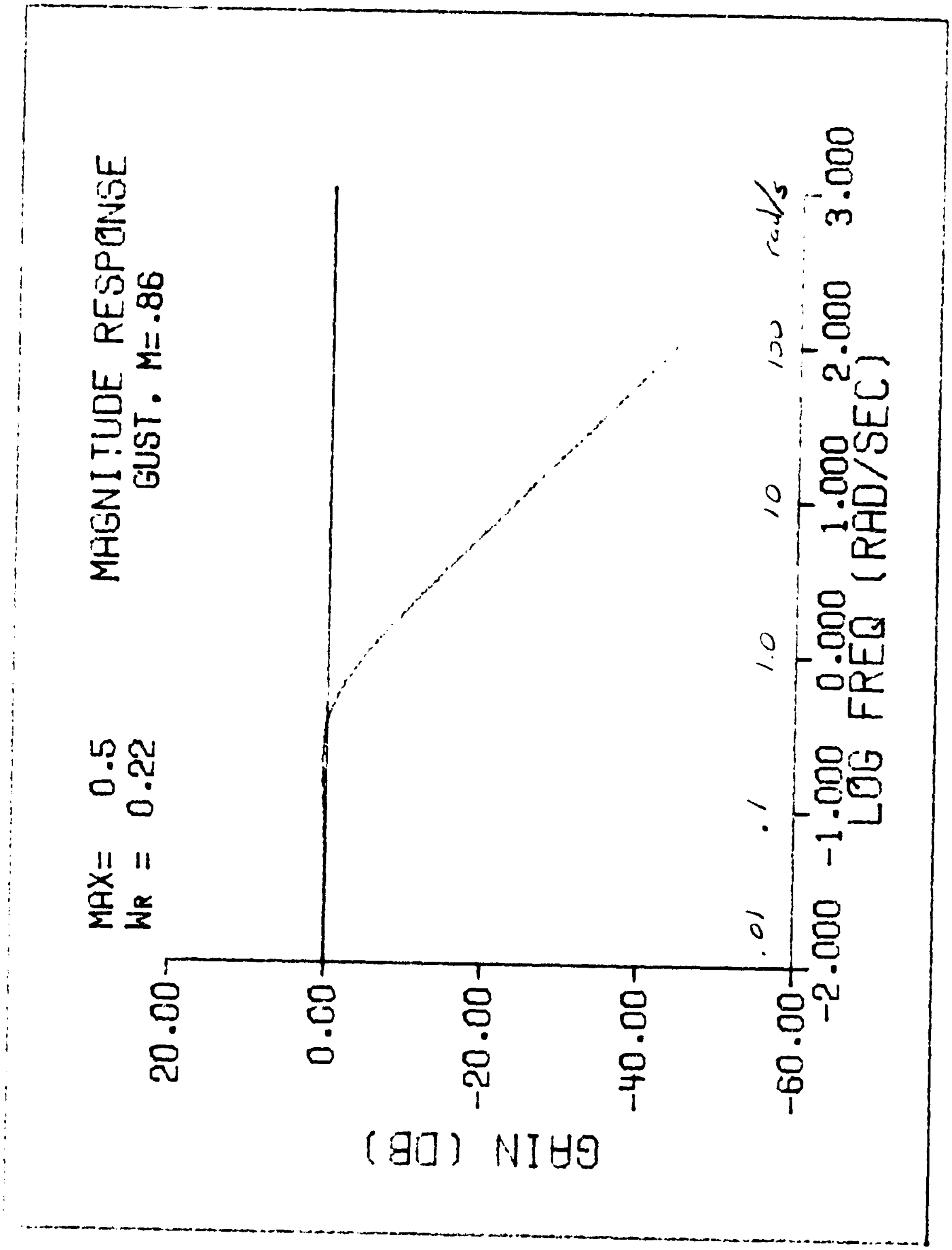

Fig 1

ORIGINAL PAGE IS
OF POOR QUALITY

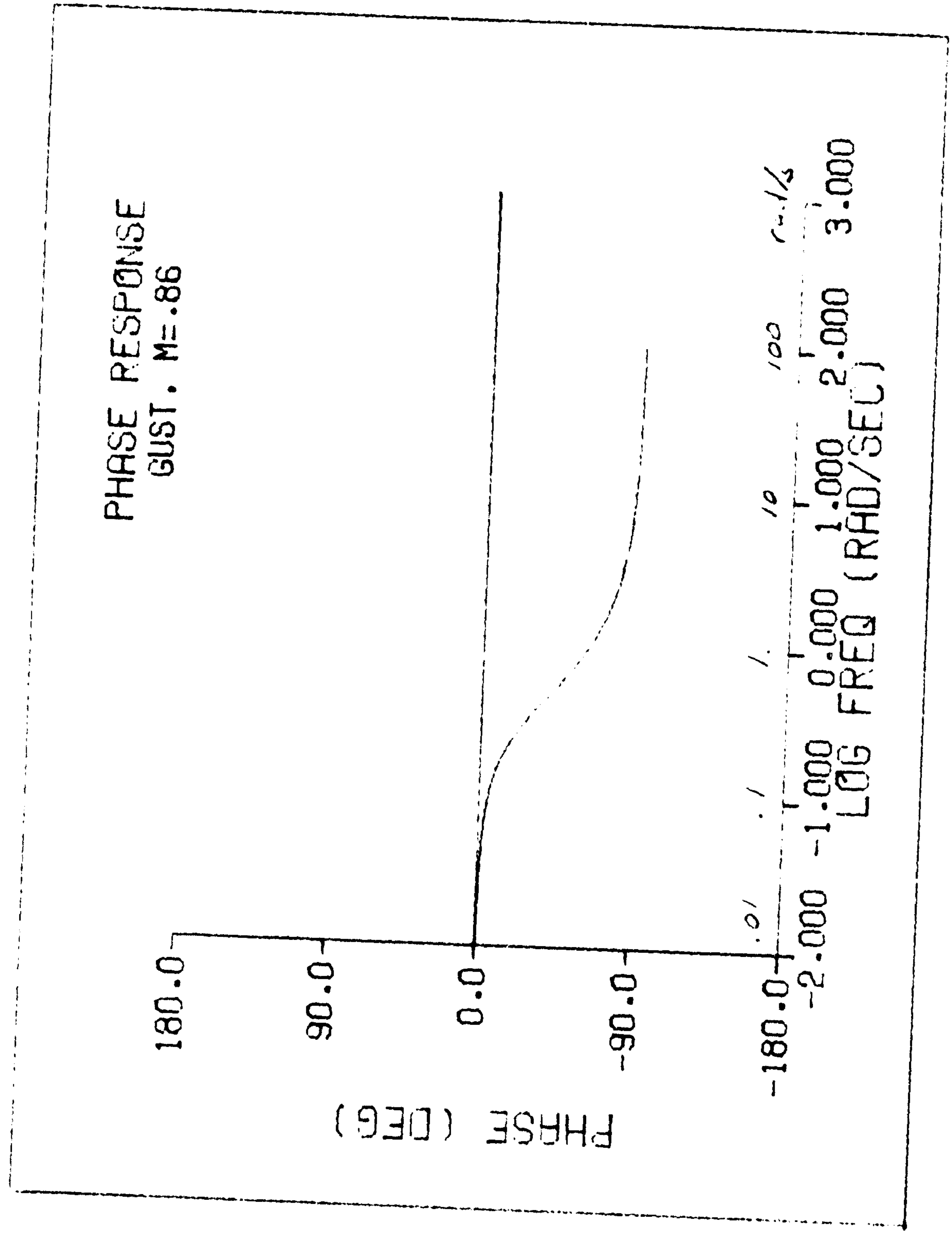

Fig 2

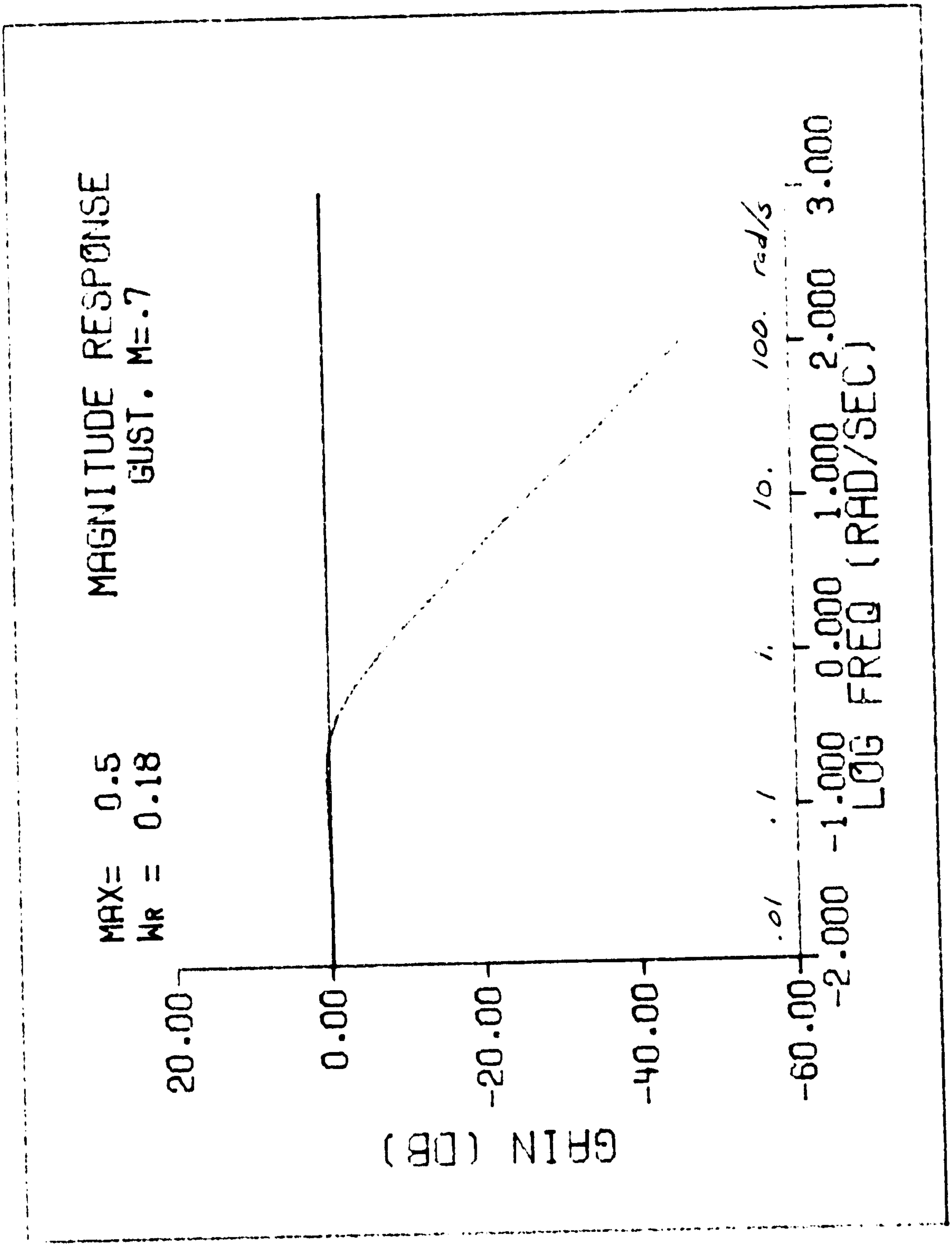
MAGNITUDE RESPONSE
GUST. M=.7
MAX= 0.5
WR = 0.18
GAIN (DB)
20.00
0.00
-20.00
-40.00
-60.00
-2.000
-1.000
0.000
1.000
2.000
3.000
LOG FREQ (RAD/SEC)
.01
.1
1.
10.
100. rad/s

Fig 3

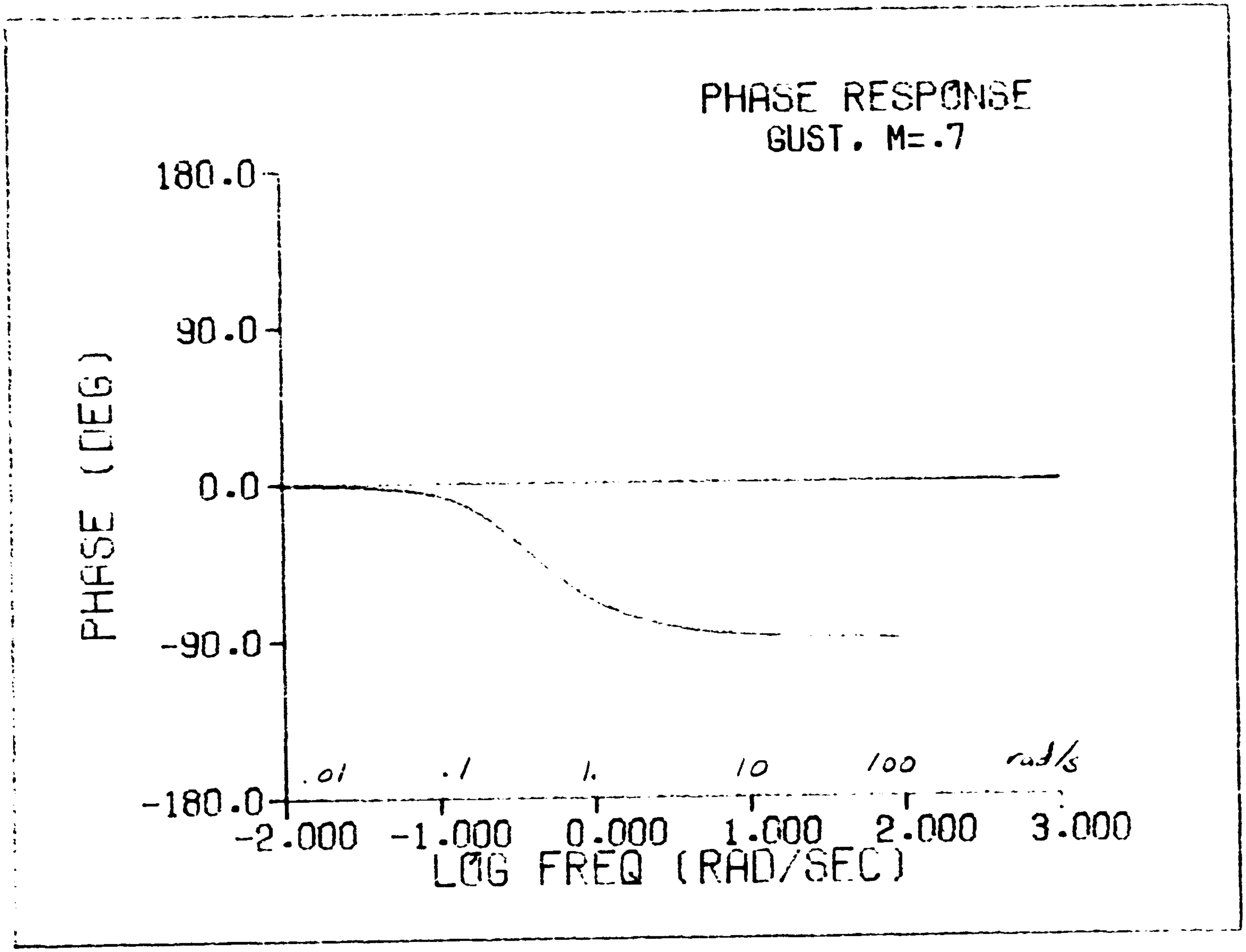
PHASE RESPONSE
GUST. M=.7
PHASE (DEG)
180.0
90.0
0.0
-90.0
-180.0
-2.000
-1.000
0.000
1.000
2.000
3.000
LOG FREQ (RAD/SEC)
.01
.1
1.
10
100
rad/s

Fig 4

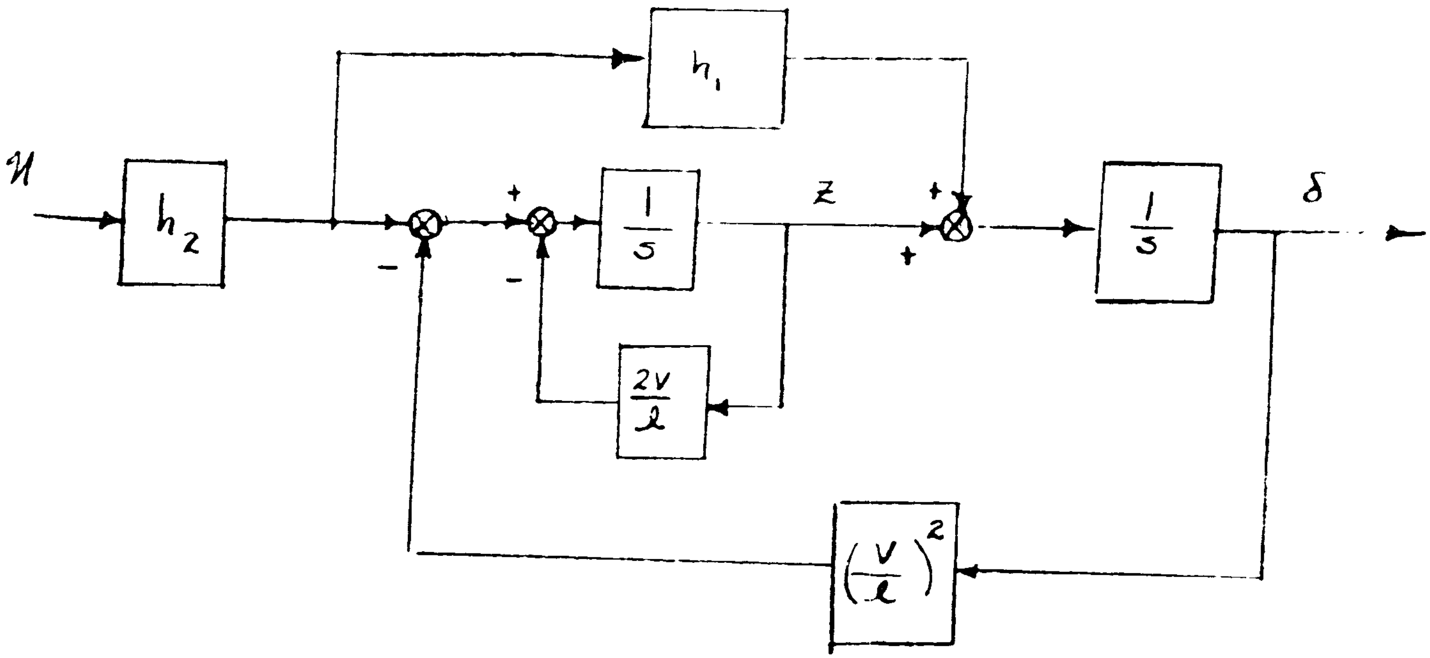

Fig 5

Working Paper No. 3

State Space Models for Flutter Control Study

Working Paper No. 3

State Space Models for Flutter Control Study

B. S. Liebst

Department of Aerospace Engineering and Mechanics

University of Minnesota

Introduction

The structural, aerodynamic, and actuator models proposed for use in the analysis of the DAST-2 vehicle have earlier been presented in the frequency domain (see working papers No. 1 and No. 2). This paper gives the corresponding state space representation of these models for use in the modal control system design.

Second Order State Equation

The following is the proposed second order form of the state equations of motion relating vertical gusts and control surface deflections to the structural response of the vehicle.

$\bar{x}$ = modal coordinates and rigid body modes

$\hat{u}$ = control surface deflections

δ = vertical gust velocity

V = forward velocity

$\bar{q}$ = $\frac{1}{2}\rho V^2$

$\bar{c}$ = mean aerodynamic chord

$$\left[M_{xx} + \bar{q} A_2^x \left(\frac{\bar{c}}{2V}\right)^2\right] \ddot{\bar{x}} + \left[C_s + \bar{q} A_1^x \left(\frac{\bar{c}}{2V}\right)\right] \dot{\bar{x}}$$

$$+ \left[K_s + \bar{q} A_0^x\right] \bar{x} + \sum_{i=1}^{L} y_i$$

$$+ \left[M_{xu} + \bar{q} A_2^u \left(\frac{\bar{c}}{2V}\right)^2\right] \ddot{\hat{u}} + \bar{q} A_1^u \left(\frac{\bar{c}}{2V}\right) \dot{\hat{u}}$$

$$+ \bar{q} A_0^u \hat{u} + \bar{q} A_2^\delta \left(\frac{\bar{c}}{2V}\right)^2 \ddot{\delta}$$

$$+ \bar{q} A_1^\delta \dot{\delta} + \bar{q} A_0^\delta \delta = 0$$

and

$$\dot{y}_i = -I\left(\frac{2V}{\bar{c}}\right) K_i y_i + D_i^x \dot{\bar{x}} + D_i^u \dot{\hat{u}} + D_i^\delta \dot{\delta}$$

or

$$M \ddot{\bar{x}} + C \dot{\bar{x}} + K \bar{x} + \sum_{i=1}^{L} y_i +$$

$$P \ddot{\hat{u}} + Q \dot{\hat{u}} + R \hat{u} +$$

$$S \ddot{\delta} + T \dot{\delta} + U \delta = 0$$

and

$$\dot{y}_i = -I\left(\frac{2V}{\bar{c}}\right) K_i y_i + D_i \dot{\bar{x}} + E_i \dot{\hat{u}} + F_i \dot{\delta}$$

where

$M = M_{xx} + \bar{q}\, A_2^x \left(\frac{\bar{c}}{2V}\right)^2$

$C = C_s + \bar{q}\, A_1^x \left(\frac{\bar{c}}{2V}\right)$

$K = K_s + \bar{q}\, A_0^x$

$P = M_{xu} + \bar{q}\, A_2^u \left(\frac{\bar{c}}{2V}\right)^2$

$Q = \bar{q}\, A_1^u \left(\frac{\bar{c}}{2V}\right)$

$R = \bar{q}\, A_0^u$

$S = \bar{q}\, A_2^\delta \left(\frac{\bar{c}}{2V}\right)^2$

$T = \bar{q}\, A_1^{\delta}$

$U = \bar{q}\, A_0^{\delta}$

$Di = D_i^{x}$

$Ei = D_i^{u}$

$Fi = D_i^{\delta}$

Actuator Model

The following is proposed frequency and corresponding state space models for the three actuators of the vehicle. See working paper No. 1 for details of the transfer function representations.

I. Elevator

$$\frac{\bar{u}_e(s)}{u_e(s)} = \frac{20}{s+20}$$

therefore,

$$\dot{\bar{u}}_e + 20\,\bar{u}_e = 20\,u_e$$

II. Inboard Aileron

$$\frac{\bar{u}_i(s)}{u_i(s)} = \frac{1.614 \times 10^{11}}{(s+335.5 \pm j\,339.8)(s+161 \pm j\,825.8)}$$

therefore,

$$\overset{....}{\bar{u}}_i + 993.0\,\dddot{\bar{u}}_i + 1.152 \times 10^{6}\,\ddot{\bar{u}}_i + 5.484 \times 10^{8}\,\dot{\bar{u}}_i + 1.614 \times 10^{11}\,\bar{u}_i = 1.614 \times 10^{11}\,u_i$$

III. Outboard Aileron

$$\frac{\bar{u}_o(s)}{u_o(s)} = \frac{1.774 \times 10^7}{(s+180)\,(s+125.5 \pm j\,287.8)}$$

therefore,

$$\dddot{\bar{u}}_o + 431.0\,\ddot{\bar{u}}_o + 1.438\times 10^5\,\dot{\bar{u}}_o + 1.774\times 10^7\,\bar{u}_o = 1.774\times 10^7\,u_o$$

Define

$$\bar{u} = \begin{Bmatrix} \bar{u}_e \\ \bar{u}_o \\ \dot{\bar{u}}_o \\ \ddot{\bar{u}}_o \\ \bar{u}_i \\ \dot{\bar{u}}_i \\ \ddot{\bar{u}}_i \\ \dddot{\bar{u}}_i \end{Bmatrix} \qquad u = \begin{Bmatrix} u_e \\ u_o \\ u_i \end{Bmatrix} = \text{commanded control inputs}$$

$$\hat{u} = \begin{Bmatrix} \bar{u}_e \\ \bar{u}_o \\ \bar{u}_i \end{Bmatrix} = \underbrace{\begin{bmatrix} 1.0 & 0 & 0 & 0 & 0 & 0 & 0 & 0 \\ 0 & 1.0 & 0 & 0 & 0 & 0 & 0 & 0 \\ 0 & 0 & 0 & 0 & 1.0 & 0 & 0 & 0 \end{bmatrix}}_{J} \bar{u}$$

= control surface deflections

$$\dot{\hat{u}} = J\dot{\bar{u}} = JG\bar{u} + JHu$$

then

$$\dot{\bar{u}} = \underbrace{\begin{bmatrix} -20.0 & 0 & 0 & 0 & 0 & 0 & 0 & 0 \\ 0 & 0 & 1.0 & 0 & 0 & 0 & 0 & 0 \\ 0 & 0 & 0 & 1.0 & 0 & 0 & 0 & 0 \\ 0 & -1.774\times10^7 & -1.438\times10^5 & -431.0 & 0 & 0 & 0 & 0 \\ 0 & 0 & 0 & 0 & 0 & 1.0 & 0 & 0 \\ 0 & 0 & 0 & 0 & 0 & 0 & 1.0 & 0 \\ 0 & 0 & 0 & 0 & 0 & 0 & 0 & 1.0 \\ 0 & 0 & 0 & 0 & -1.614\times10^{11} & -5.484\times10^8 & -1.152\times10^6 & -933.0 \end{bmatrix}}_{G} \bar{u} + \underbrace{\begin{bmatrix} 20.0 & 0 & 0 \\ 0 & 0 & 0 \\ 0 & 0 & 0 \\ 0 & 1.774\times10^7 & 0 \\ 0 & 0 & 0 \\ 0 & 0 & 0 \\ 0 & 0 & 0 \\ 0 & 0 & 1.614\times10^{11} \end{bmatrix}}_{H} u$$

Gust Model

The following is the white noise model for the vertical gust state. See working paper No. 2 for details of this derivation.

$$\dot{z} = -\left(\frac{V}{\ell}\right)^2 \delta - 2\left(\frac{V}{\ell}\right) z - .406\left(\frac{V}{\ell}\right)^2 \eta$$

$$\dot{\delta} = z + .285\left(\frac{V}{\ell}\right) \eta$$

where

δ = vertical gust velocity

z = intermediate gust state

η = zero mean white gaussian noise

$$\overline{\eta(t_1)\,\eta(t_2)} = \left(\frac{\ell}{V}\right)\sigma^2 = \Lambda$$

ℓ = characteristic gust length

σ^2 = rms value of the gust

First Order State Equation

Now that the structural, actuator, and gust models have been developed in the state space, they can all be adjoined to form one first order state equation. Neglecting the $S\ddot{\delta}$ and $P\ddot{\hat{u}}$ terms of the second order equations of motion the resulting first order state equation is

$$\dot{x} = Ax + Bu + w$$

where

$$x = \begin{Bmatrix} \bar{x} \\ \dot{\bar{x}} \\ y_1 \\ y_2 \\ \vdots \\ y_L \\ \bar{u} \\ \delta \\ z \end{Bmatrix} \qquad W \equiv w = \begin{Bmatrix} 0 \\ -M^{-1}T(.285)\left(\frac{V}{\ell}\right) \\ F1(.285)\left(\frac{V}{\ell}\right) \\ F2(.285)\left(\frac{V}{\ell}\right) \\ \vdots \\ FL(.285)\left(\frac{V}{\ell}\right) \\ 0 \\ (.285)\left(\frac{V}{\ell}\right) \\ (-.406)\left(\frac{V}{\ell}\right)^2 \end{Bmatrix} \eta$$

ORIGINAL PAGE IS
OF POOR QUALITY

and

$$\overline{w(t_1)\, w^T(t_2)} = W W^T \mathcal{L} = N$$

and

$$A = \begin{bmatrix}
0 & I & 0 & 0 & \cdots & 0 & 0 & 0 & 0 \\
-M^{-1}K & -M^{-1}C & -M^{-1} & -M^{-1} & \cdots & -M^{-1} & -M^{-1}(RJ+QJG) & -M^{-1}U & -M^{-1}T \\
0 & D1 & -I\frac{2V}{c}K_1 & 0 & \cdots & 0 & E1(JG) & 0 & F1 \\
0 & D2 & 0 & -I\frac{2V}{c}K_2 & \cdots & 0 & E2(JG) & 0 & F2 \\
\vdots & \vdots & & & \ddots & & \vdots & \vdots & \vdots \\
0 & DL & 0 & 0 & \cdots & -I\frac{2V}{c}K_L & EL(JG) & 0 & FL \\
0 & 0 & 0 & 0 & \cdots & 0 & G & 0 & 0 \\
0 & 0 & 0 & 0 & \cdots & 0 & 0 & 0 & 1.0 \\
0 & 0 & 0 & 0 & \cdots & 0 & 0 & -\left(\frac{V}{\ell}\right)^2 & -2\left(\frac{V}{\ell}\right)
\end{bmatrix}$$

$$B = \begin{Bmatrix} 0 \\ -M^{-1}QJH \\ E1(JH) \\ E2(JH) \\ \vdots \\ EL(JH) \\ H \\ 0 \\ 0 \end{Bmatrix}$$

Working Paper 4

Unsteady Aerodynamic Model and Rigid Body Analysis

S. J. Garg

TABLE OF CONTENTS

NOMENCLATURE:

$\tilde{M}$:	Generalized mass matrix
k:	Generalized stiffness matrix
C:	Generalized damping matrix
$\underline{x}$:	Vector of generalized coordinates for rigid and elastic modes and control surface deflections
$\underline{x}_G$:	Vector of generalized coordinates for gust inputs
Q(s):	Unsteady aerodynamic influence coefficient matrix
ω:	frequency in radians per second
c:	reference chord length
v:	velocity of the vehicle
$\bar{q}$:	dynamic pressure
ρ:	density of air
M:	Mach number
H:	Altitude
s:	laplace operator
$\bar{\sigma}[A]$:	maximum singular value of matrix A

INTRODUCTION

For the design of active control systems for the suppression of aerodynamic flutter, it is necessary to first obtain the state-space representation of the equations of motion for the flexible vehicle. This is so because at present all modern control design techniques are based on the availability of a state-space model.

In the study of flexible vehicles, the unsteady aerodynamic forces and moments are evaluated at various reduced frequencies by the use of some type of finite element computational procedure. Our objective is to obtain a model of the unsteady aerodynamic forces and moments in a form which can be incorporated into the structural equations of motion for the aircraft so as to get a suitable state-space representation of the vehicle dynamics.

This paper discusses the procedure for obtaining such a model. The following discussion presents an approximation of the unsteady aerodynamics by a rational polynomial and is based on the approximation first suggested by R.T. Jones [1]. The details of obtaining such an approximation using a least squares fit over the range of frequencies available is then presented.

A model for the unsteady aerodynamics of the DAST ARW-2 aircraft, the data for which was provided by NASA, was developed using the procedure discussed herein. Using this model, the rigid body motion of the aircraft was studied and the results compared with those obtained by NASA.

The programs developed to obtain the least squares approximation and do the rigid body analysis are appended for thoroughness.

MODEL FOR UNSTEADY AERODYNAMICS:

The general equations of motion for a flexible vehicle at a given Mach number are [2]:

$$\left[\tilde{M}s^2 + Cs + K\right]x + \bar{q}\, Q(s)\begin{bmatrix} x \\ x_G \end{bmatrix} = 0 \qquad (1)$$

If a simple harmonic motion is assumed, the matrix of aerodynamic influence coefficients $Q(s = j\frac{2v}{c}k)$, where k is the reduced frequency given by $k = \frac{\omega c}{2v}$, is calculated using finite difference procedures at a finite number of reduced frequencies k_i, $i = 1, 2 \ldots n$. This complex matrix can be approximated by a polynomial in s as:

$$Q(s) = A_0 + A_1\left(\frac{cs}{2V}\right) + A_2\left(\frac{cs}{2V}\right)^2 + \sum_{m=1}^{\ell} \frac{D_m s}{\left(s + \frac{2V}{c}\hat{k}_m\right)} \qquad (2)$$

This form of approximating Q was first suggested by R.T. Jones [1] for the case of two-dimensional flow. The matrix A_0 can be looked upon as representing aerodynamic stiffness while A_1 represents aerodynamic damping and A_2 represents added mass due to the aerodynamics. The term $\frac{D_m s}{s + \frac{2V}{c}\hat{k}_m}$ is an approximation for the time delays inherent in the unsteady aerodynamics and the values of $\hat{k}_m$ are chosen from the range of reduced frequencies for which Q(k) has been computed so as to minimize the error in this approximation.

Define the error matrix $E(s)$ as:

$$E(s) = Q(s) - \left\{A_0 + A_1\left(\frac{cs}{2V}\right) + A_2\left(\frac{cs}{2V}\right)^2 + \sum_{m=1}^{\ell} \frac{D_m s}{\left(s + \frac{2V}{c}\hat{k}_m\right)}\right\} \qquad (2(a))$$

Then the matrices A_0, A_1, A_2; D_m, $m = 1, \ldots \ell$ are computed so as to minimize the spectral norm of $E(s)$ ($\|E(s)\|_2$). The spectral norm of a matrix equals its maximum singular value [6]; i.e., $\|E(s)\|_2 = \bar{\sigma}[E(s)]$. Therefore the maximum singular value of $E(s)$ is a measure of the size of the error in our approximation of $Q(s)$ and we must choose the values of $\hat{k}_m$ such that the corresponding $\bar{\sigma}[E(s)]$ is the smallest possible.

The matrices A_0, A_1, A_2, and D_m, $m = 1, \ldots \ell$ are real and are computed by a least square fit of the aerodynamic data. This is carried out as follows [3]:

Consider the (p,q) element of the matrices, then for this element we can write (2) as:

$$\left[1 \quad \frac{cs}{2V} \quad \left(\frac{cs}{2V}\right)^2 \quad \frac{s}{(s+\frac{2V}{c}\hat{k}_1)} \quad \cdots\cdots \quad \frac{s}{(s+\frac{2V}{c}\hat{k}_\ell)}\right] \begin{bmatrix} A_{0\,p,q} \\ A_{1\,p,q} \\ A_{2\,p,q} \\ D_{1\,p,q} \\ \vdots \\ D_{\ell\,p,q} \end{bmatrix} = Q_{p,q}(s) \qquad (3)$$

Substituting for $s = jk_i$ where $j = \sqrt{-1}$ we get:

$$\left[1 \quad jk_i \quad -k_i^2 \quad \frac{jk_i}{jk_i+\hat{k}_1} \quad \cdots\cdots \quad \frac{jk_i}{jk_i+\hat{k}_\ell}\right] \begin{bmatrix} A_{0\,p,q} \\ A_{1\,p,q} \\ A_{2\,p,q} \\ D_{1\,p,q} \\ \vdots \\ D_{\ell\,p,q} \end{bmatrix} = Q_{p,q}(k_i) \qquad (4)$$

Writing out equations like (4) for every k_i, $i = 1,\ldots n$ and then combining in a matrix form we get:

$$\begin{bmatrix} 1 & jk_1 & -k_1^2 & \frac{jk_1}{jk_1+\hat{k}_1} & \cdots\cdots & \frac{jk_1}{jk_1+\hat{k}_\ell} \\ 1 & jk_2 & -k_2^2 & \frac{jk_2}{jk_2+\hat{k}_1} & \cdots\cdots & \frac{jk_2}{jk_2+\hat{k}_\ell} \\ \vdots & & & & & \\ 1 & jk_n & -k_n^2 & \frac{jk_n}{jk_n+\hat{k}_1} & \cdots\cdots & \frac{jk_n}{jk_n+\hat{k}_\ell} \end{bmatrix} \begin{bmatrix} A_{0\,p,q} \\ A_{1\,p,q} \\ A_{2\,p,q} \\ D_{1\,p,q} \\ \vdots \\ D_{\ell\,p,q} \end{bmatrix} = \begin{bmatrix} Q_{p,q}(k_1) \\ Q_{p,q}(k_2) \\ \vdots \\ Q_{p,q}(k_n) \end{bmatrix} \qquad (5)$$

Since we want the least square solution to (5) to be real valued we can write (5) as:

$$\begin{bmatrix} A_R \\ A_I \end{bmatrix} \underset{\sim}{x} = \begin{bmatrix} y_R \\ y_I \end{bmatrix} \qquad (6)$$

where:

$$A_R = \begin{bmatrix} 1 & 0 & -k_1^2 & \frac{k_1^2}{k_1^2+\hat{k}_1^2} & \cdots & \frac{k_1^2}{k_1^2+\hat{k}_\ell^2} \\ 1 & 0 & -k_2^2 & \frac{k_2^2}{k_2^2+\hat{k}_1^2} & \cdots & \frac{k_2^2}{k_2^2+\hat{k}_\ell^2} \\ \vdots & & & & & \\ 1 & 0 & -k_n^2 & \frac{k_n^2}{k_n^2+\hat{k}_1^2} & \cdots & \frac{k_n^2}{k_n^2+\hat{k}_\ell^2} \end{bmatrix}$$

$$A_g = \begin{bmatrix} 0 & k_1 & 0 & \frac{k_1\hat{k}_1}{k_1^2+\hat{k}_1^2} & \cdots & \frac{k_1\hat{k}_\ell}{k_1^2+\hat{k}_\ell^2} \\ 0 & k_2 & 0 & \frac{k_2\hat{k}_1}{k_2^2+\hat{k}_1^2} & \cdots & \frac{k_2\hat{k}_\ell}{k_2^2+\hat{k}_\ell^2} \\ \vdots & & & & & \\ 0 & k_n & 0 & \frac{k_n\hat{k}_1}{k_n^2+\hat{k}_1^2} & \cdots & \frac{k_n\hat{k}_\ell}{k_n^2+\hat{k}_\ell^2} \end{bmatrix}$$

$$\underline{\xi} = \begin{bmatrix} A_{0\,p,q} \\ A_{1\,p,q} \\ A_{2\,p,q} \\ D_{1\,p,q} \\ \vdots \\ D_{\ell\,p,q} \end{bmatrix} ; \quad y_R = \text{Real} \begin{bmatrix} Q_{p,q}(k_1) \\ Q_{p,q}(k_2) \\ \vdots \\ Q_{p,q}(k_n) \end{bmatrix} ; \quad y_g = \text{Imag.} \begin{bmatrix} Q_{p,q}(k_1) \\ Q_{p,q}(k_2) \\ \vdots \\ Q_{p,q}(k_n) \end{bmatrix}$$

The least squares solution to (6) can be obtained using any one of the many standard techniques. The program used for the purposes of this report is SNVDEC, developed by NASA [5] which uses singular value decomposition to get the least squares solution. An explanation of this procedure for solving the least squares problem can be found in [6]. Once we have computed A_0, A_1, A_2, D_m, $m = 1, \ldots \ell$ as the solution to (6), substituting for $Q(s)$ from (2) in (1) we get the equations of motion to be:

$$\left[Ms^2 + Cs + K\right]\underline{x} + \bar{q}\left[A_0 + A_1\left(\frac{cs}{2V}\right) + A_2\left(\frac{cs}{2V}\right)^2 + \sum_{m=1}^{\ell} \frac{D_m s}{s + \frac{2V}{c}\hat{k}_m}\right]\begin{bmatrix}\underline{x} \\ \underline{x}_G\end{bmatrix} = 0 \qquad (7)$$

From this we can now obtain a state-space model using any of the minimal realization techniques as

$$\dot{\underline{x}} = A\underline{x} + B\underline{u} + \Gamma\underline{\eta}$$

where $\underline{x}$ = state vector

$\underline{u}$ = control vector

$\underline{\eta}$ = gust vector

ORIGINAL PAGE IS
OF POOR QUALITY

MODIFICATION FOR RIGID BODY ANALYSIS:

Since the frequencies for the rigid body motion of the vehicle are small compared to that of the flexure modes, it is important to get a good fit for $Q(s)$ at low frequencies in order to analyze the rigid body motion.

One modification in the above procedure, which would achieve this, is to set $A_0 = Q_R(0)$ so that we now need to obtain a best least squares fit for only A_1, A_2, D_m, $m = 1, \ldots \ell$.

Using this approximation for A_0, equation (6) is modified as:

$$\begin{bmatrix} A_R' \\ A_g' \end{bmatrix} \underline{\xi}' = \begin{bmatrix} y_R' \\ y_g' \end{bmatrix} \qquad (7)$$

where $k_1 = 0$ which implies that $Q_g(0) = 0$

$$A_R' = \begin{bmatrix} 0 & -k_2^2 & \frac{k_2^2}{k_2^2+\hat{k}_1^2} & \cdots & \frac{k_2^2}{k_2^2+\hat{k}_\ell^2} \\ 0 & -k_3^2 & \frac{k_3^2}{k_3^2+\hat{k}_1^2} & \cdots & \frac{k_3^2}{k_3^2+\hat{k}_\ell^2} \\ \vdots & & & & \\ 0 & -k_n^2 & \frac{k_n^2}{k_n^2+\hat{k}_1^2} & \cdots & \frac{k_n^2}{k_n^2+\hat{k}_\ell^2} \end{bmatrix}$$

$$A_g' = \begin{bmatrix} k_2 & 0 & \frac{k_2\hat{k}_1}{k_2^2+\hat{k}_1^2} & \cdots & \frac{k_2\hat{k}_\ell}{k_2^2+\hat{k}_\ell^2} \\ k_3 & 0 & \frac{k_3\hat{k}_1}{k_3^2+\hat{k}_1^2} & \cdots & \frac{k_3\hat{k}_\ell}{k_3^2+\hat{k}_\ell^2} \\ k_n & 0 & \frac{k_n\hat{k}_1}{k_n^2+\hat{k}_1^2} & \cdots & \frac{k_n\hat{k}_\ell}{k_n^2+\hat{k}_\ell^2} \end{bmatrix}$$

$$\underline{\xi}' = \begin{bmatrix} A_{1\,p,q} \\ A_{2\,p,q} \\ D_{1\,p,q} \\ \vdots \\ D_{\ell\,p,q} \end{bmatrix}$$

$$y_R' = \mathrm{REAL}\begin{bmatrix} Q_{i,j}(k_2) - Q_{i,j}(k_1) \\ Q_{i,j}(k_3) - Q_{i,j}(k_1) \\ \vdots \\ \vdots \\ Q_{i,j}(k_n) - Q_{i,j}(k_1) \end{bmatrix} \quad ; \quad y_I = \mathrm{IMAG.}\begin{bmatrix} Q_{i,j}(k_1) \\ Q_{i,j}(k_2) \\ \vdots \\ \vdots \\ Q_{i,j}(k_n) \end{bmatrix}$$

The fit for A_1, A_2, D_m, $m = 1,\ldots \ell$ thus obtained will give a good approximation for the rigid body dynamics of the aircraft.

<u>MODEL FOR DAST ARW-2:</u>

The DAST (Drones for Aerodynamic and Structural Testing) ARW-2 (Aeroelastic Research Wing - Number 2) has a high aspect ratio (10.3) supercritical wing with a 25 degree sweep at midchord mounted on a Firebee drone fuselage.

The unsteady aerodynamic influence coefficient matrix for DAST ARW-2 at a flight condition of $M = 0.86$, $H = 15000$ ft was provided by NASA - the model consisted of two rigid body modes (plunge and pitch), 10 symmetric elastic modes, three control surfaces (stabilizer, outboard aileron, inboard aileron) and one gust state.

The aerodynamic forces were computed using an aerodynamic/structural interface and a doublet lattice aerodynamics code, contained in the ISAC program, for twelve reduced frequencies (0.0, 0.05, 0.1, 0.2, 0.3, 0.4, 0.5, 0.6, 0.7, 0.8, 1.0, and 1.2).

The elements of the aerodynamic coefficient matrix were plotted on polar plots with the magnitude in decibels versus the phase. Several of these plots which are typical of the first column of $Q(s)$ (the force due to plunge) are attached in Fig. 1. Plots typical of forces due to the other modes and the control surface deflections are shown in Fig. 2.

From the plots in Fig. 1 it was seen that the forces due to plunge are very small at low frequencies compared to the forces at higher frequencies. Therefore the fit for the first column of $Q(s)$ was obtained using the rigid body modifications described in the earlier section, i.e., the first column of A_0 (see Eq. (2)) was forced to be equal to the first column of $Q(s)$ at $k = 0$.

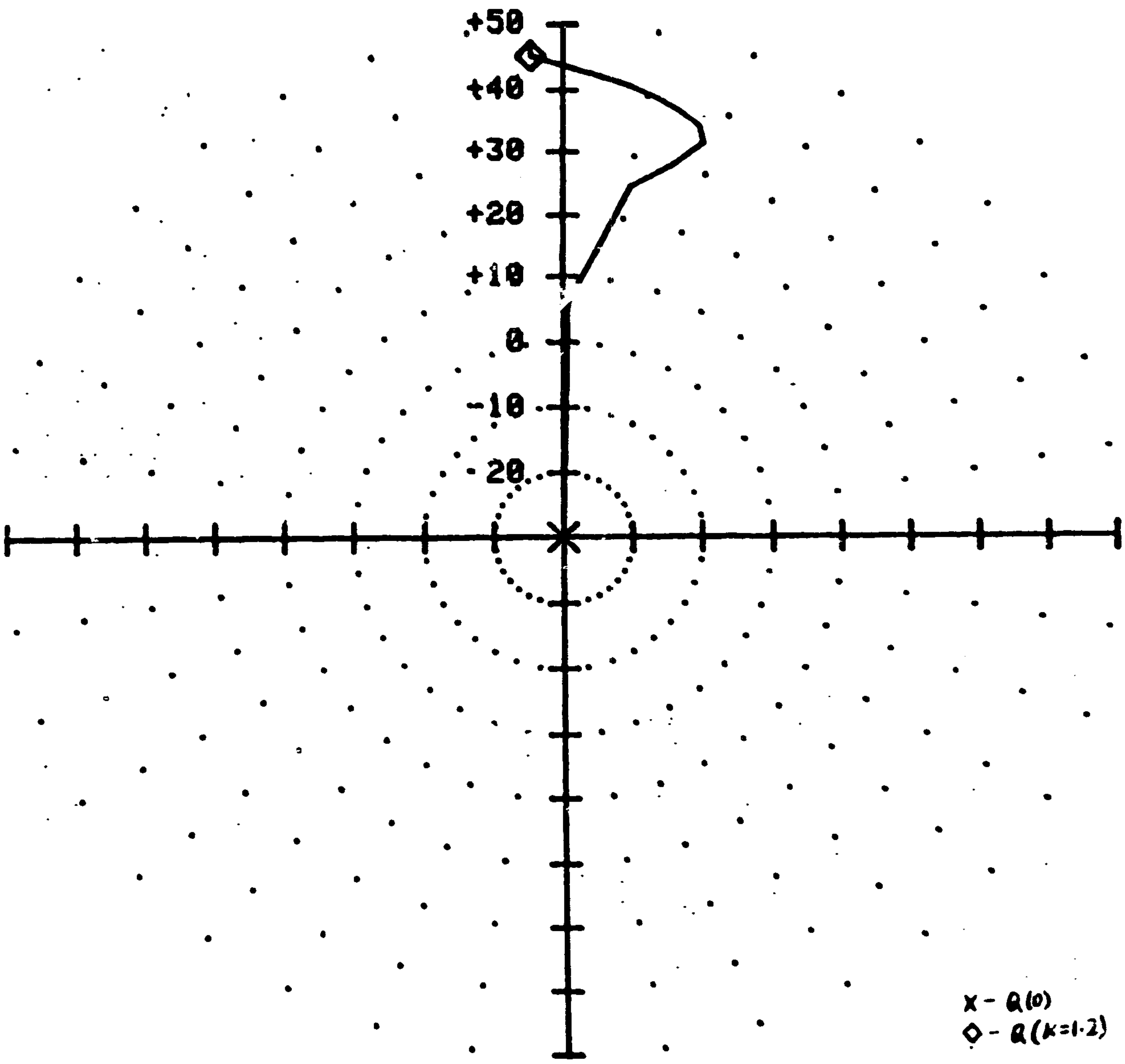

FIG. 1 : 1ST COLUMN OF Q(δ) (a) ELEMENT (3,1)

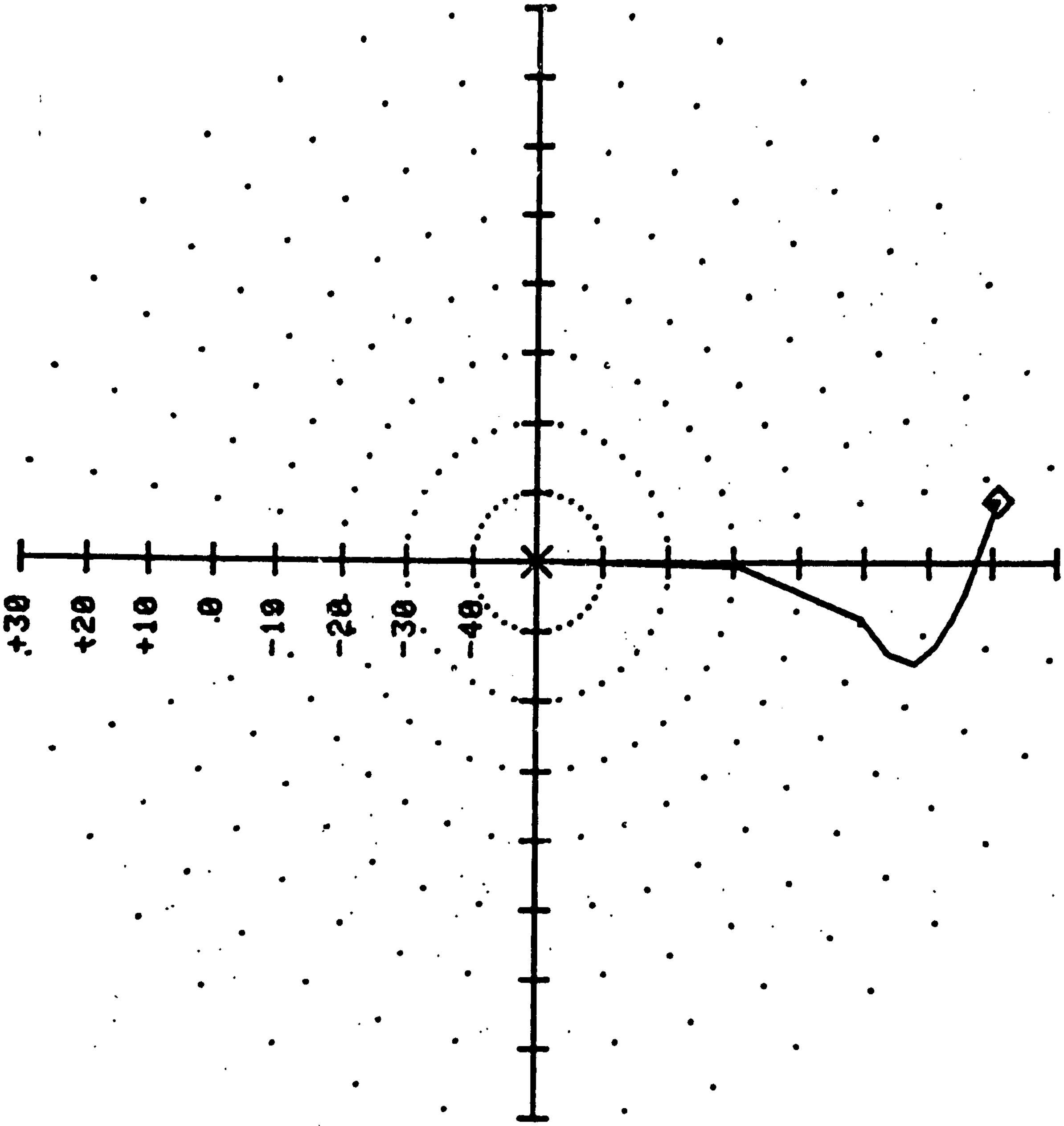

(b) ELEMENT (5,1)

FIG. 1 CONTINUED

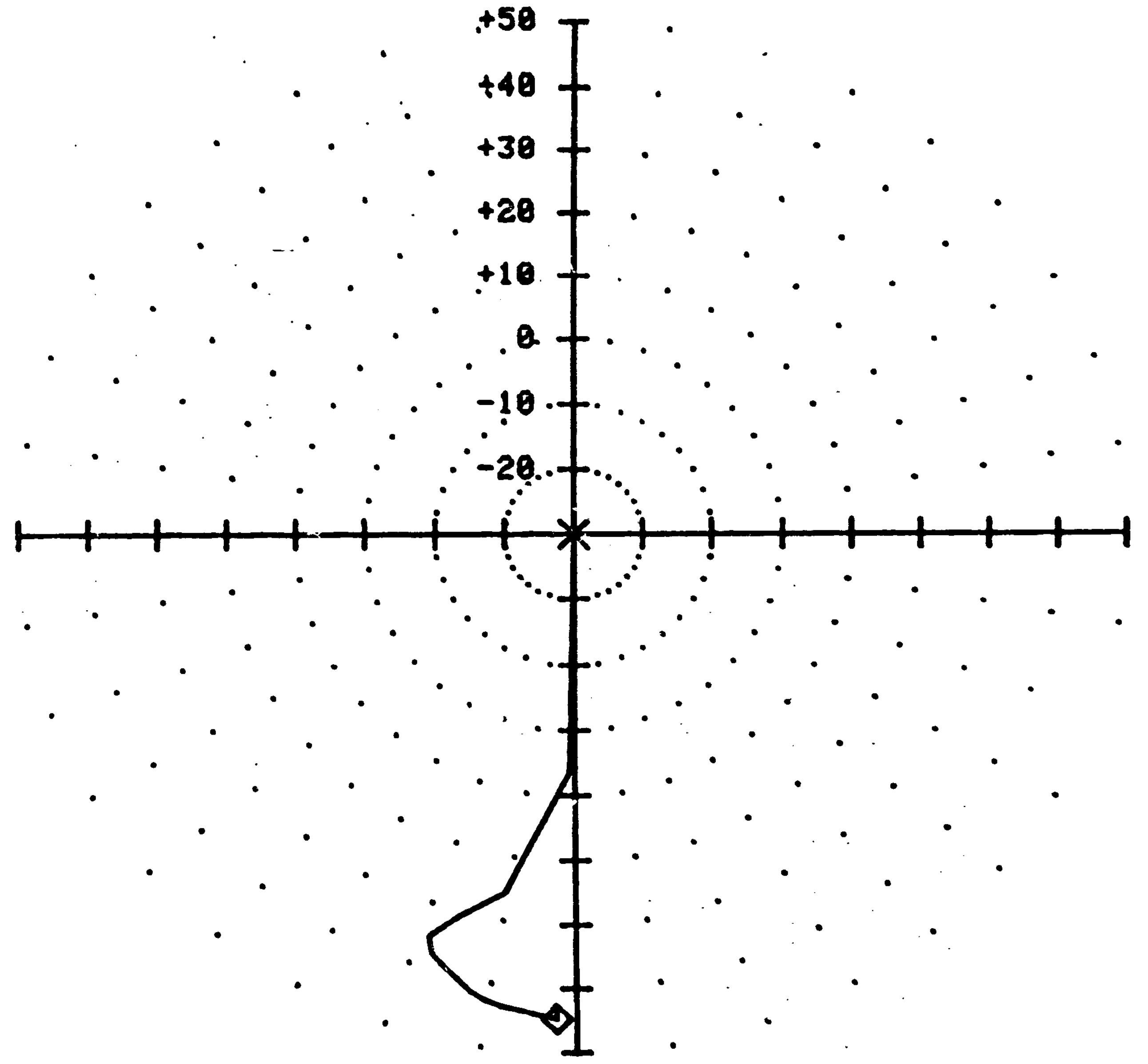

(c) ELEMENT (6,1)

FIG. 1 CONTINUED

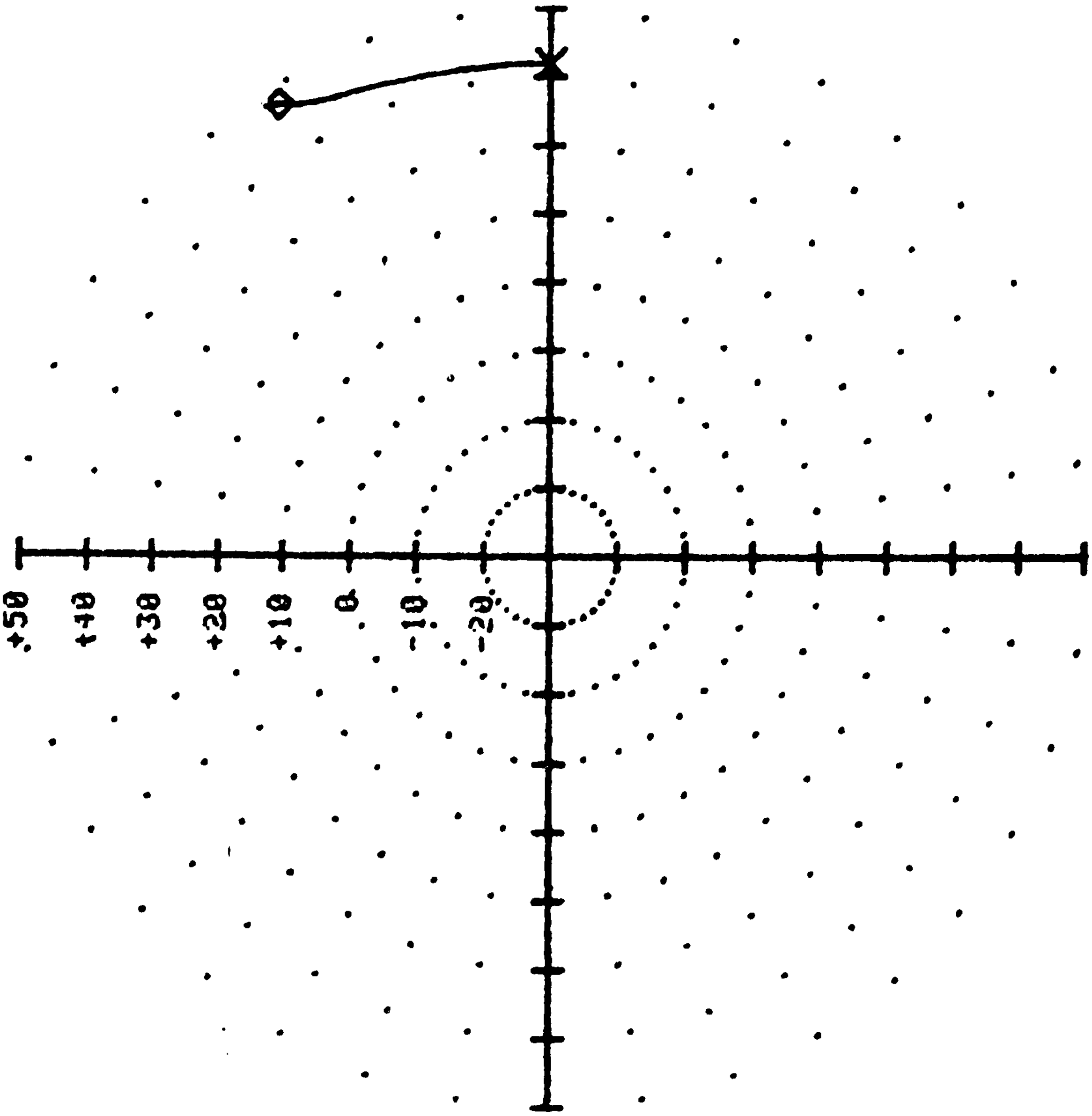

(a) ELEMENT (1,2)

FIG. 2 : TYPICAL ELEMENTS OF $Q(\lambda)$

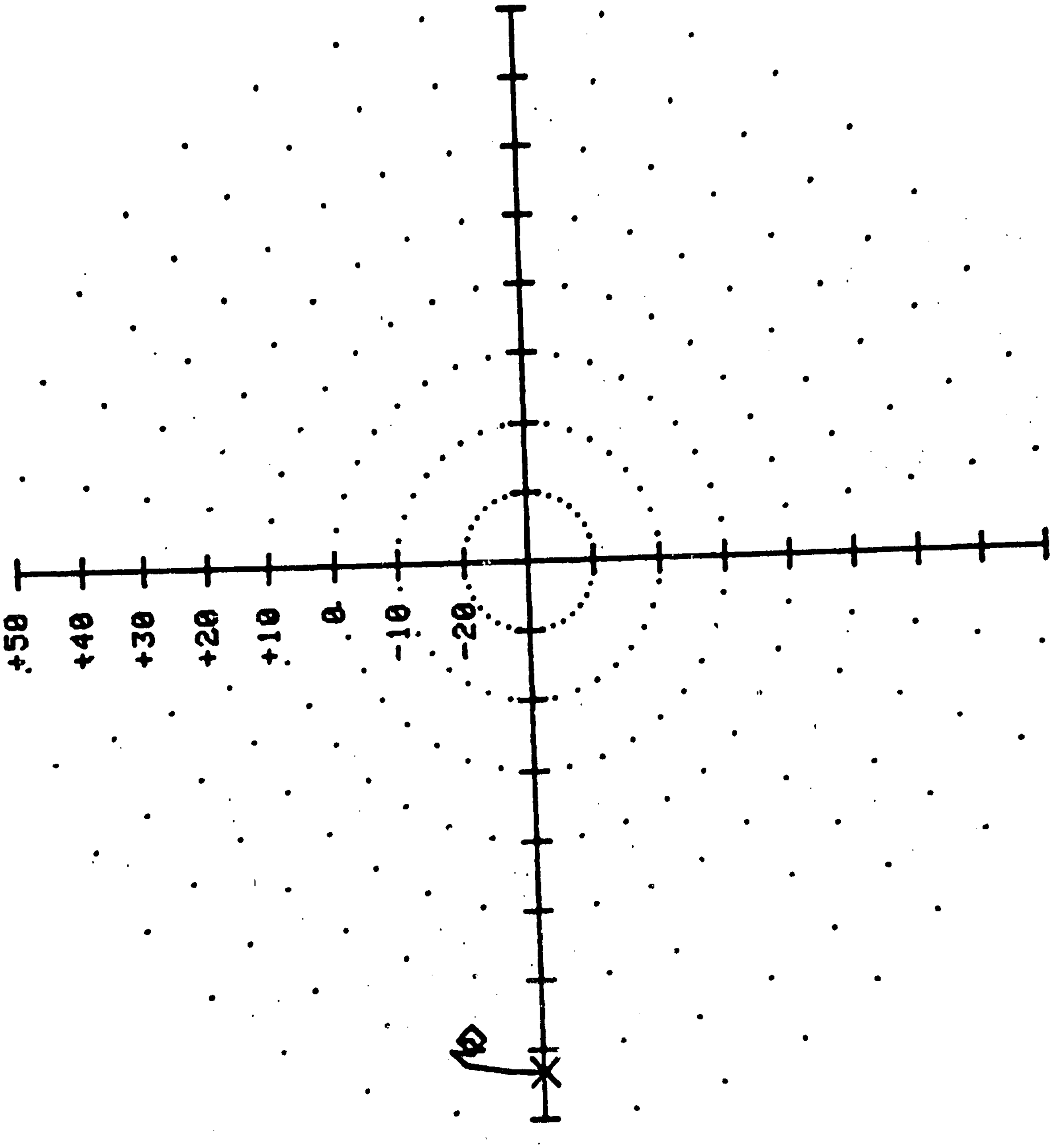

(d) ELEMENT (2,13)
FIG. 2 CONTINUED

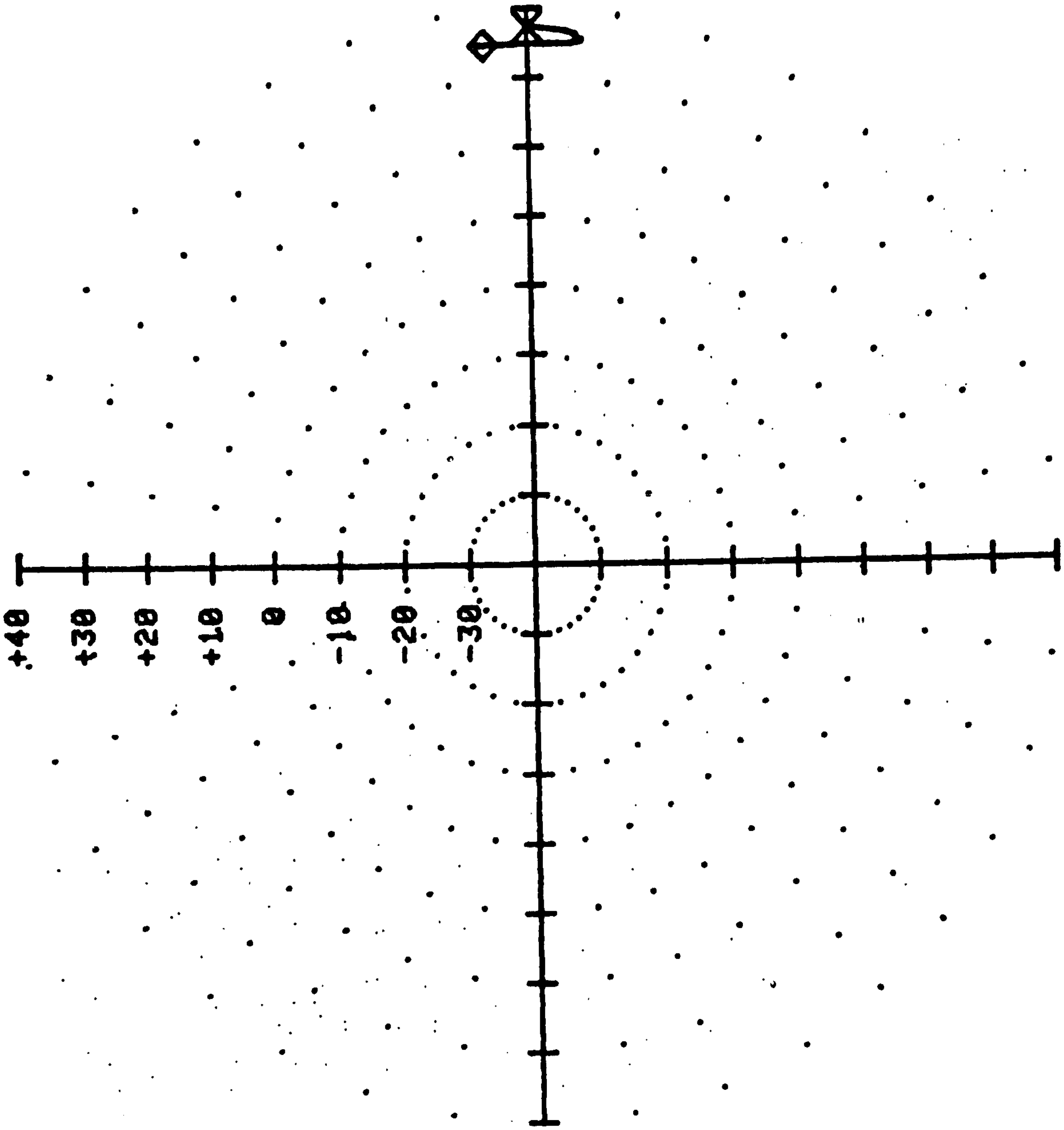

(c) ELEMENT (3,6)

FIG. 2 CONTINUED

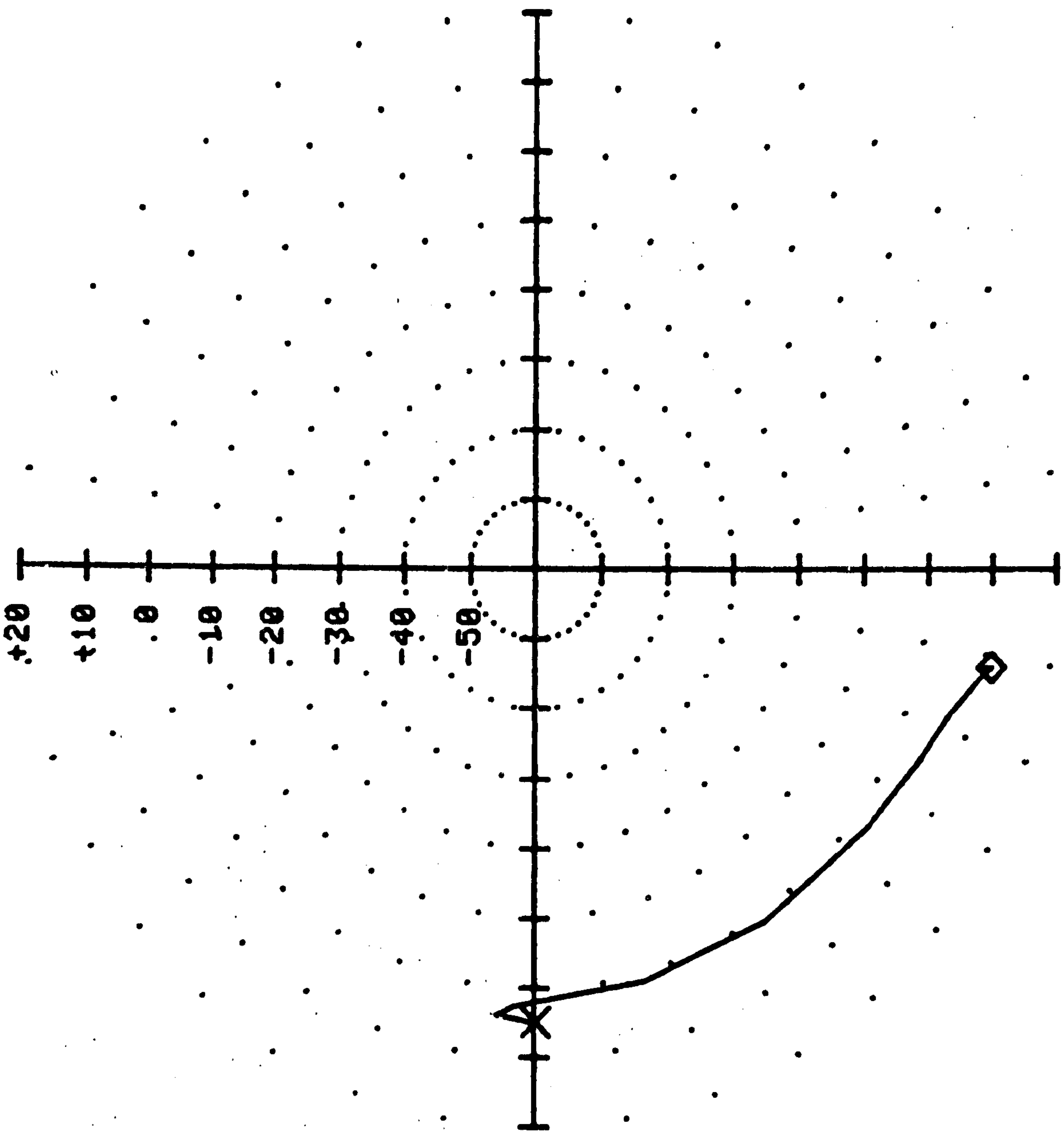

(d) ELEMENT (5,6)

FIG. 2 CONTINUED

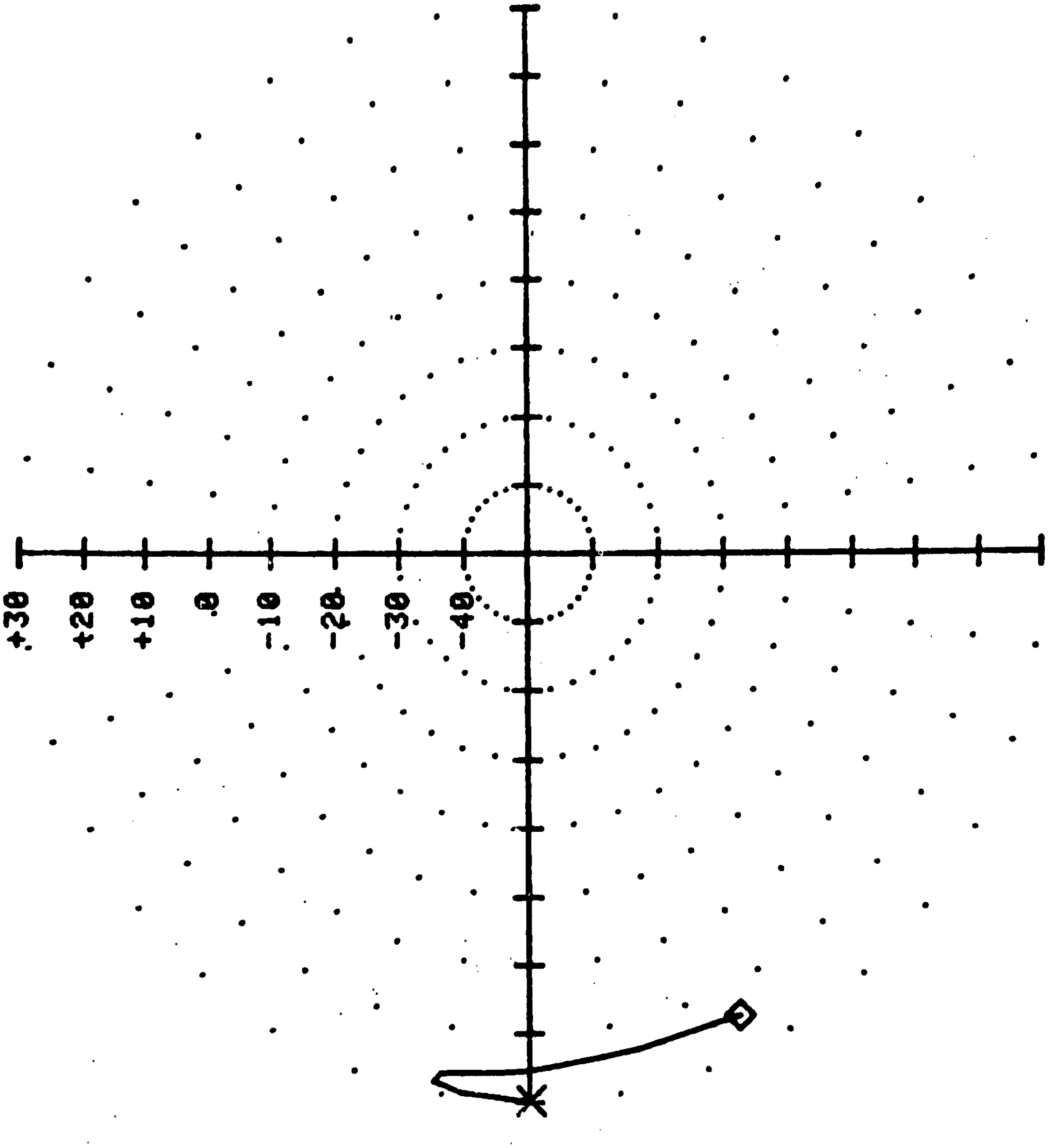

(e) ELEMENT (6,2)

FIG. 2 CONTINUED

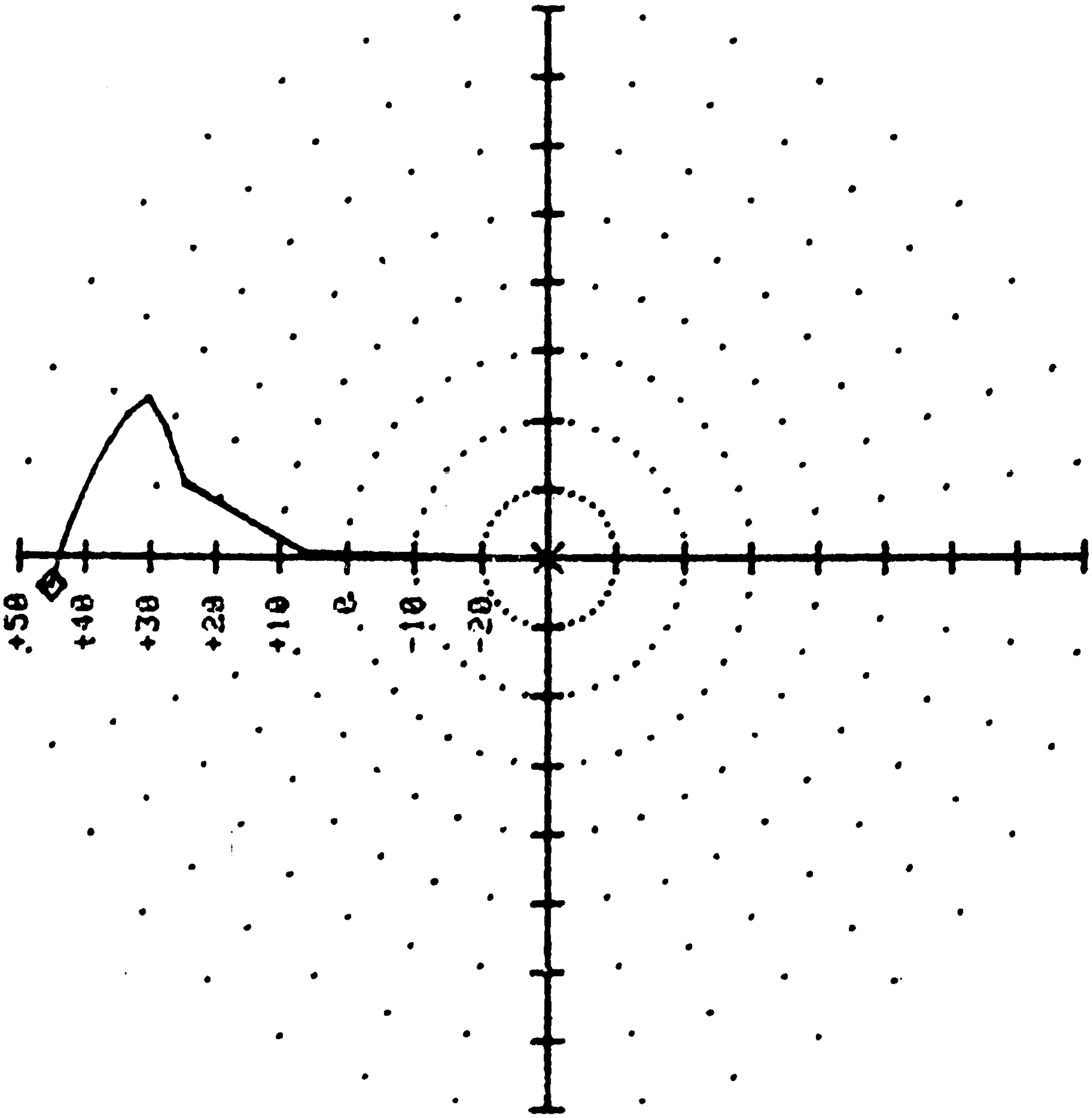

(a) ELEMENT (3,1)

FIG 3 : APPROXIMATION FOR 1ST COLUMN OF $Q(\lambda)$

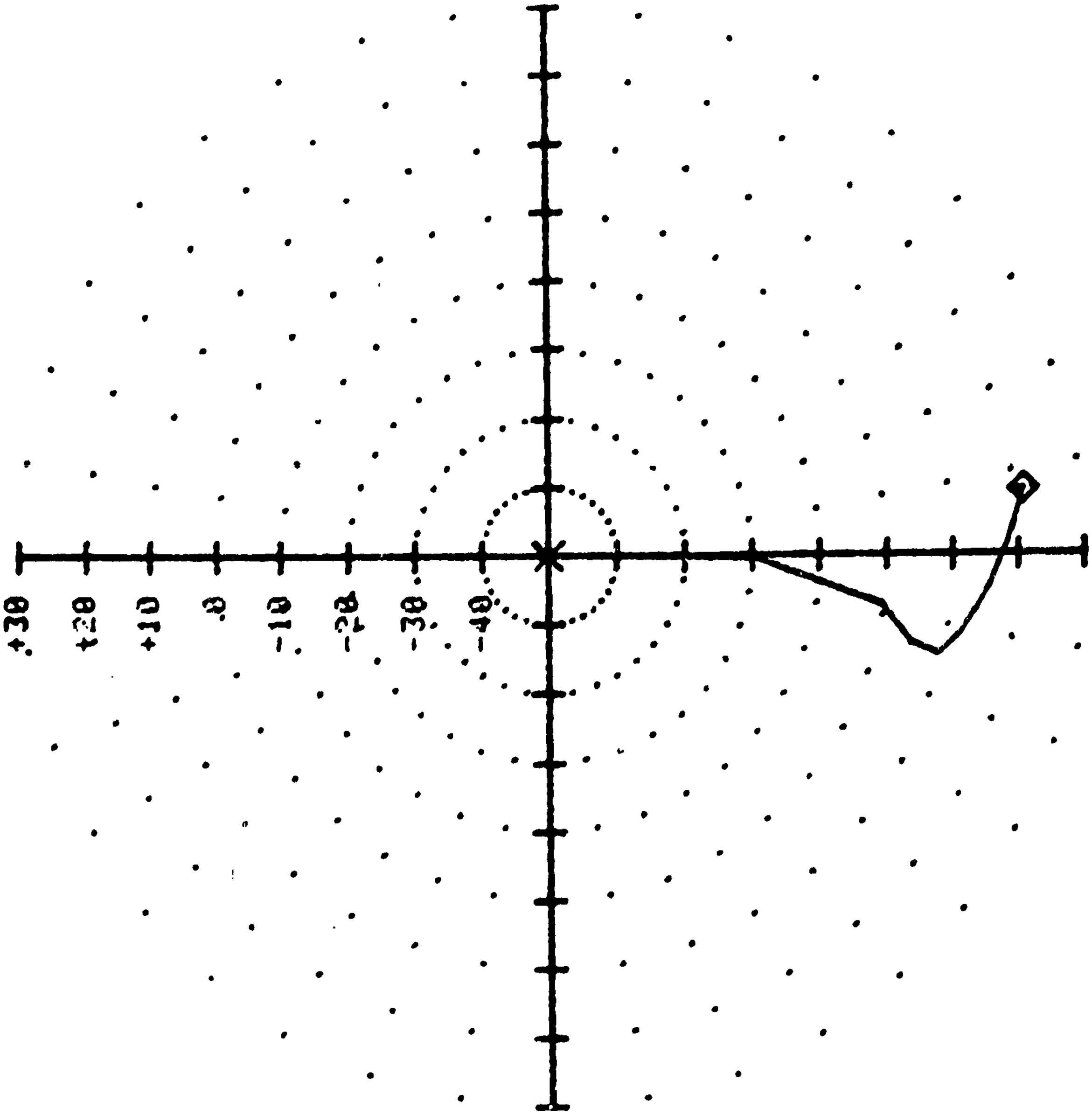

(b) ELEMENT (5,1)

FIG. 3 CONTINUED

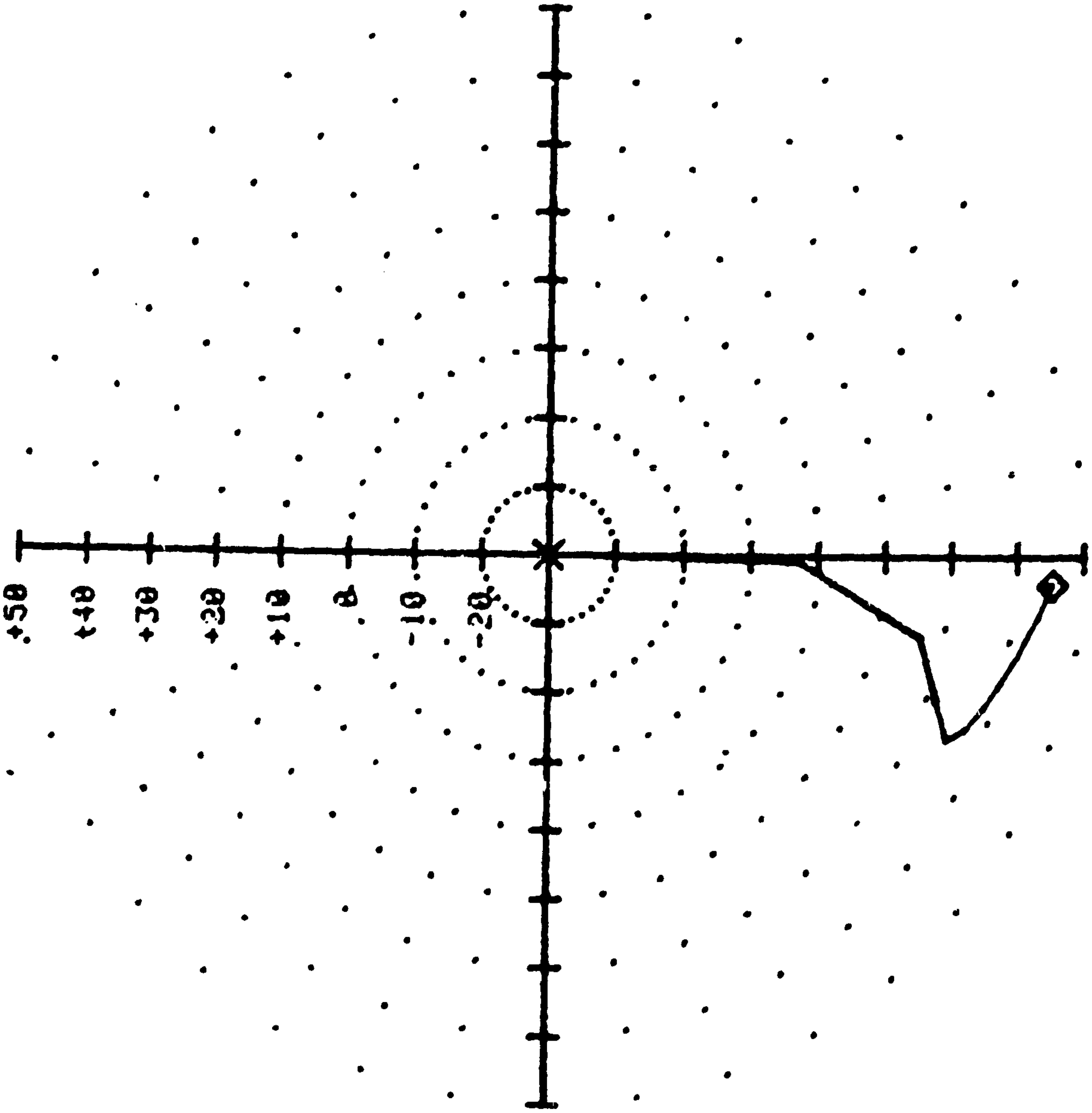

(c) ELEMENT (b,1)
FIG. 3 CONTINUED

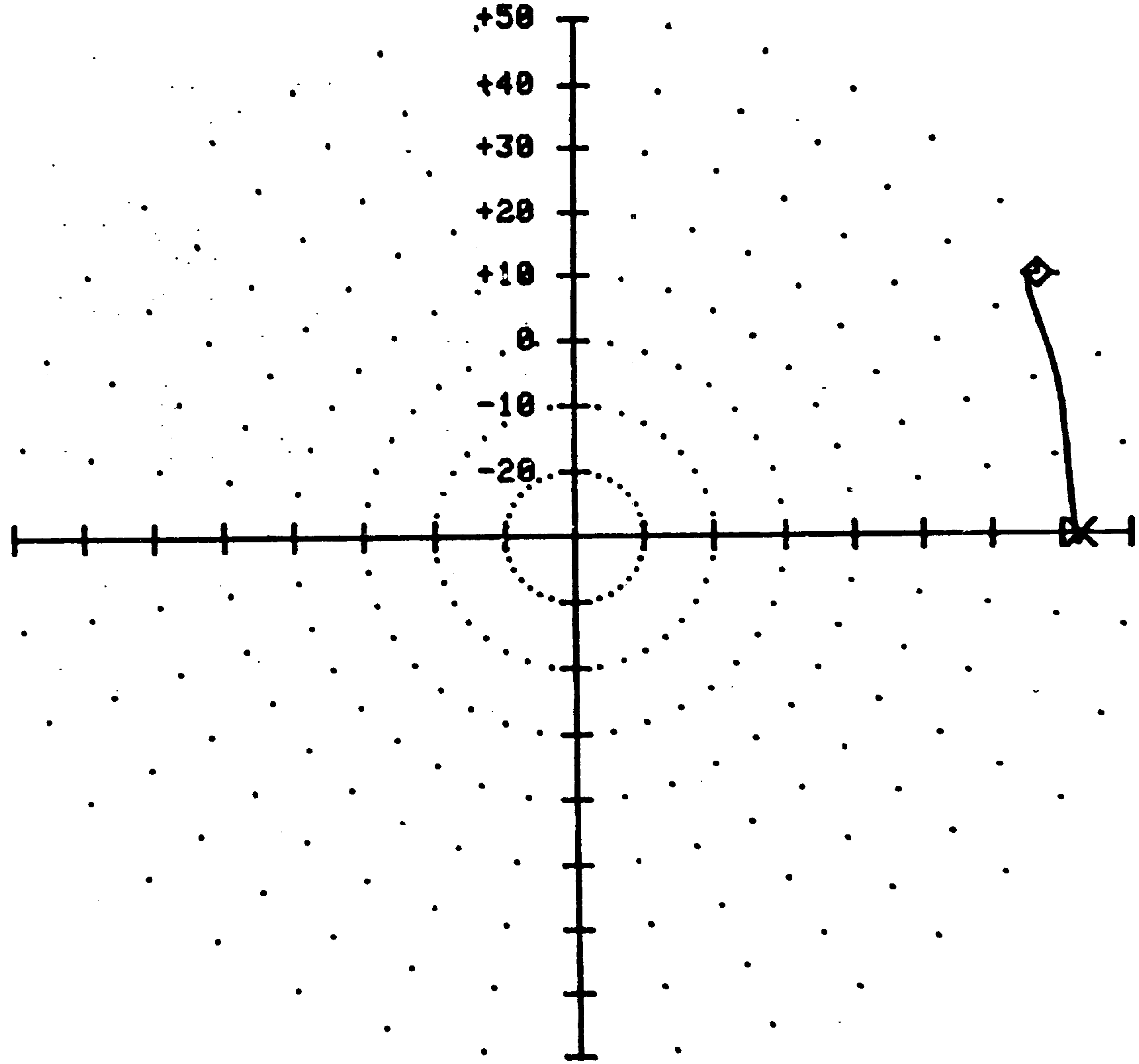

(a) ELEMENT (1,2)

Fig. 4 : Approximation For $Q(s)$

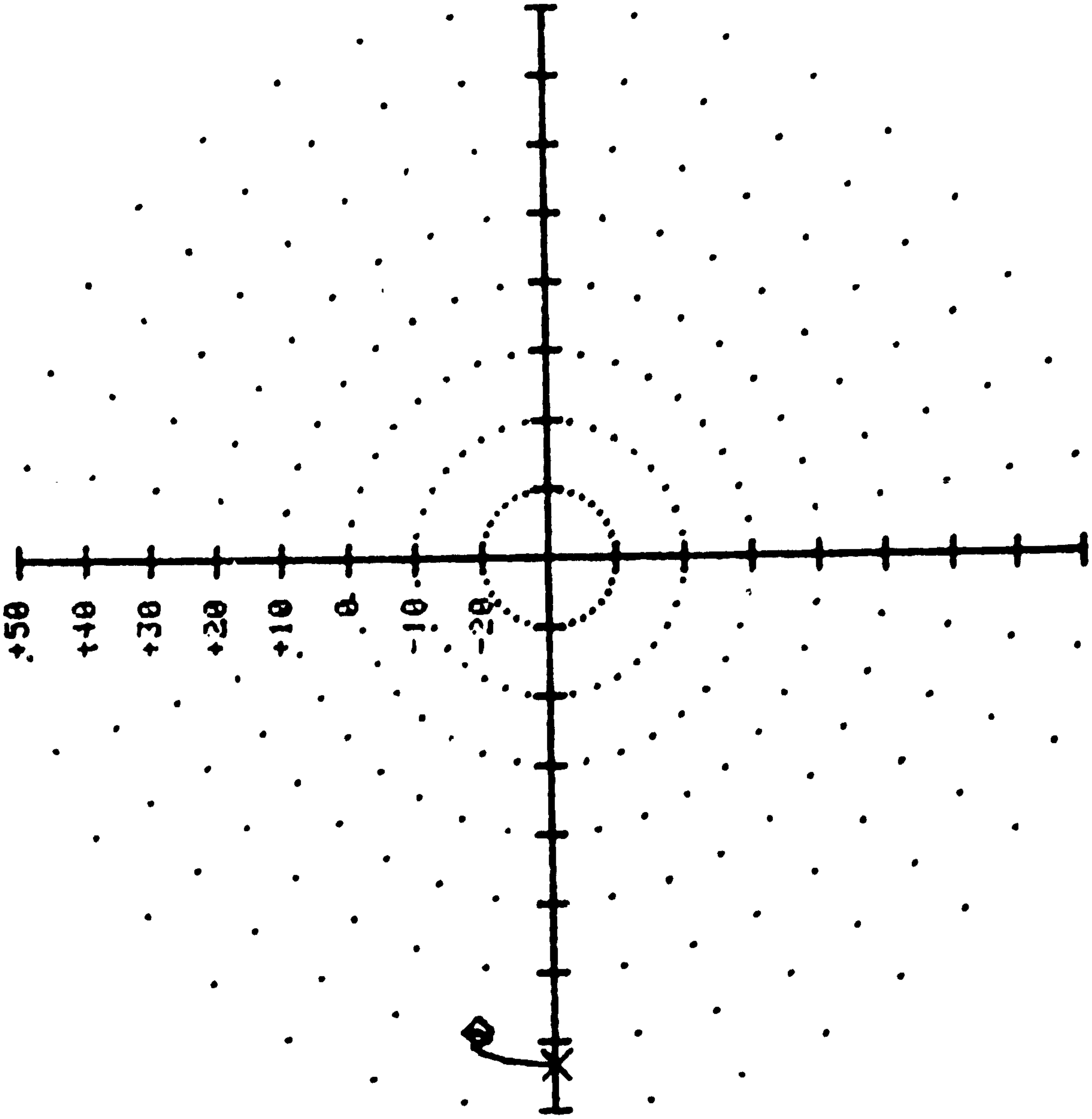

(ℓ) ELEMENT (2,13)

FIG. 4 CONTINUED

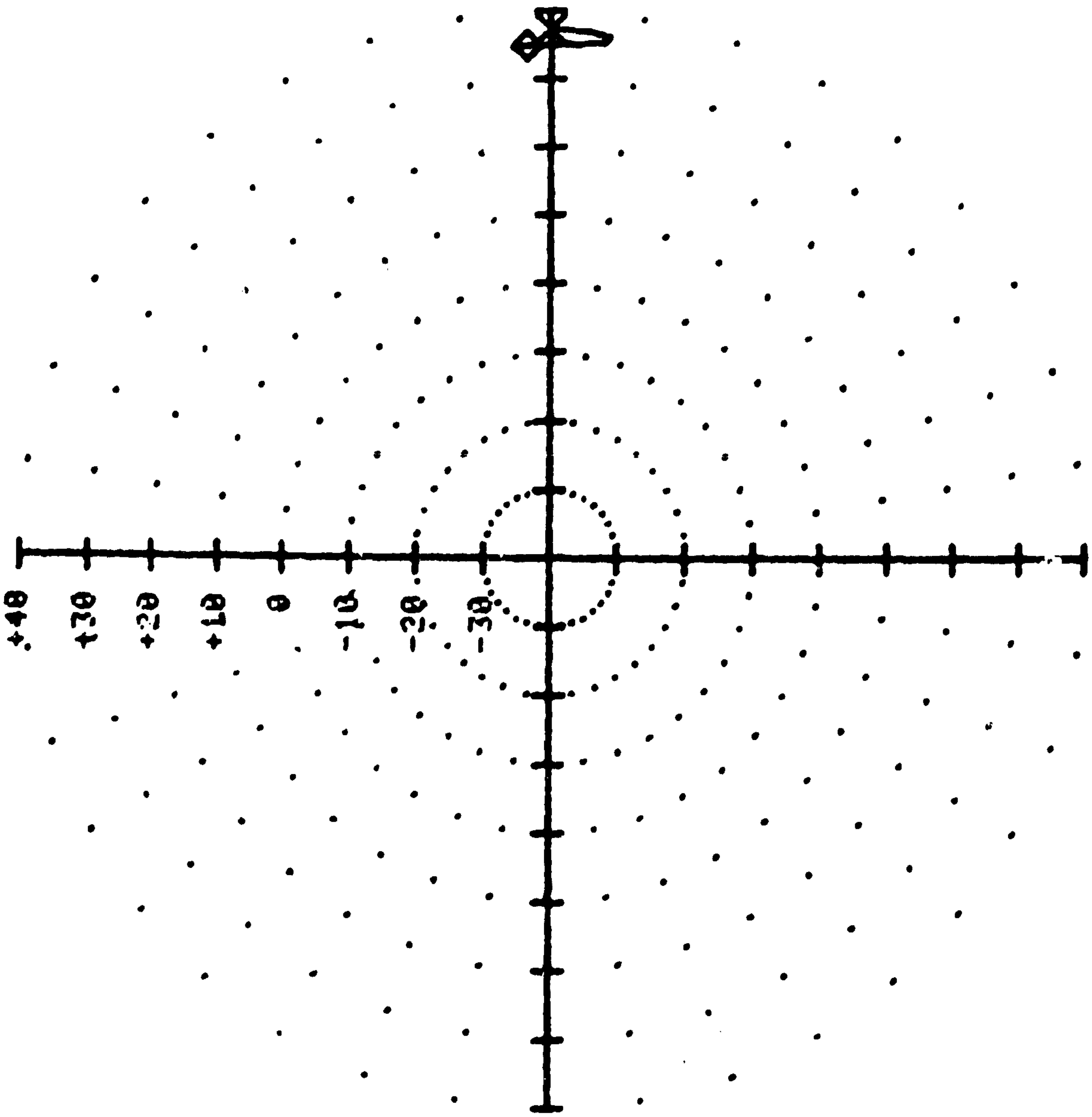

(c) ELEMENT (3,6)

FIG. 4 CONTINUED

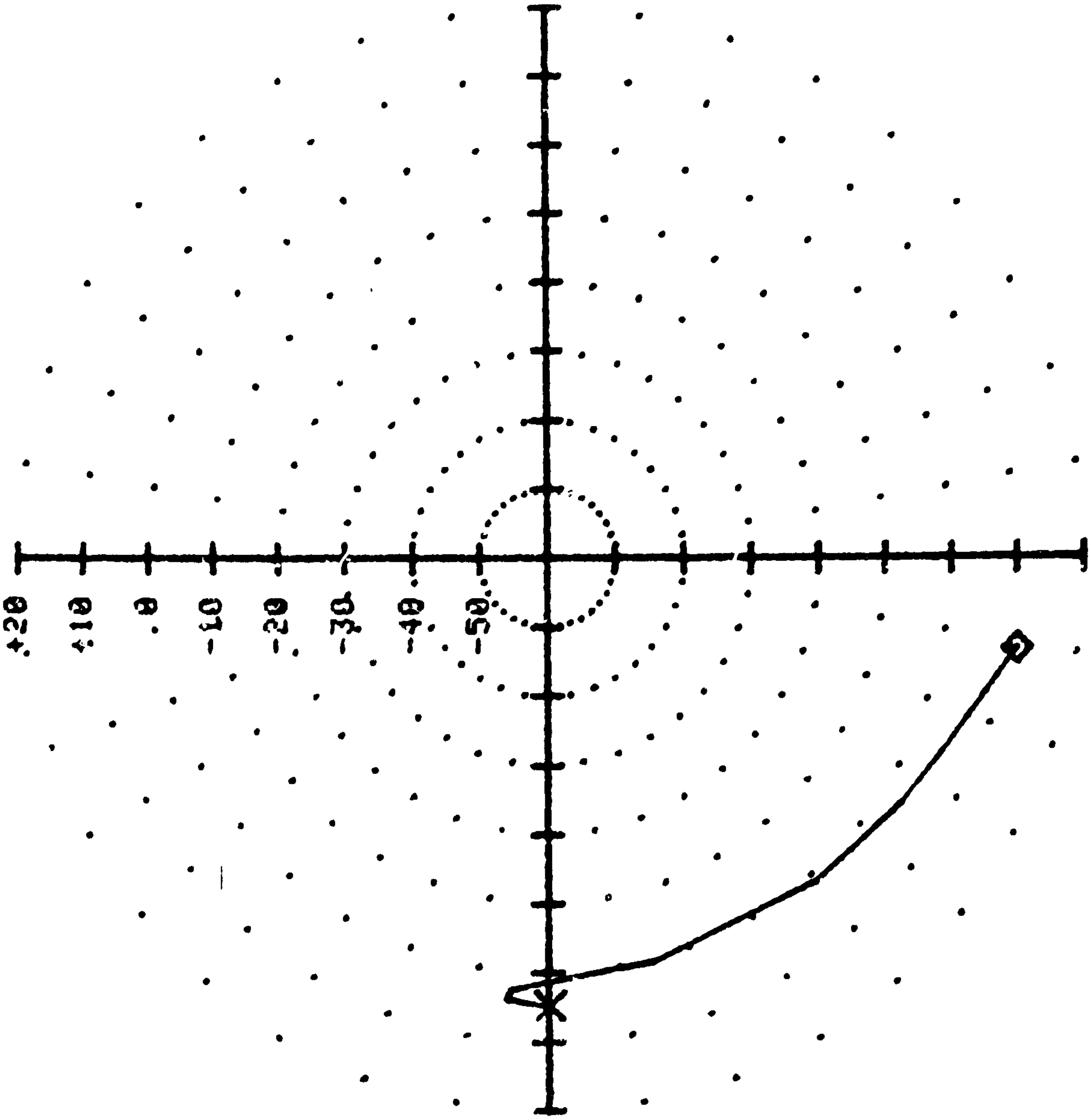

(d) ELEMENT (5,6)

FIG. 4 CONTINUED

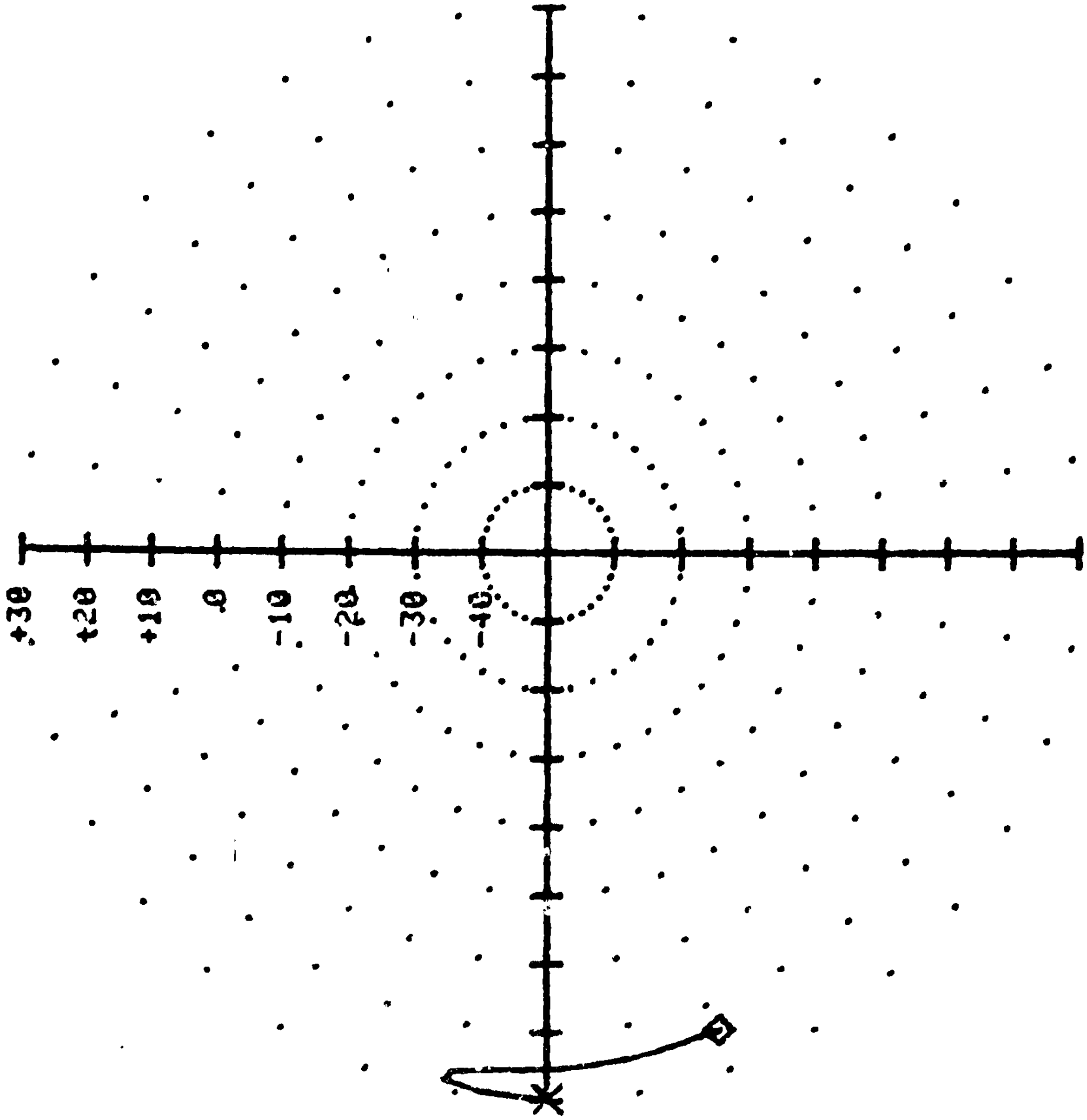

(e) ELEMENT (6,2)

FIG. 4 CONTINUED

The fits for $Q(s)$ were obtained for different values of $\hat{k}_m$ and a comparison of the maximum singular values of the difference between the actual values of $Q(s)$ and the approximations for different $\hat{k}_m$ showed that using $\hat{k} = 0.13$ gives the best approximation. The following table lists the values of the maximum singular value at zero reduced frequency for some values of $\hat{k}$.

S.N.	$\hat{k}$	$\bar{\sigma}[E(0)]$
1	0.1	214.4
2	0.125	138.2
3	0.13	137.0
4	0.135	147.0
5	0.15	162.8

The approximations of the aerodynamic forces using this value of $\hat{k}$ for the elements plotted in Figs. 1 and 2 are shown in Figs. 3 and 4 respectively. These plots show that the approximated values follow the actual values very closely. Also from these plots we notice that it is not worthwhile to use more than one value of $\hat{k}$ as that would not improve the fit much and would only lead to an increase in the number of states in the state space realization of the model.

A listing of the program written to obtain the desired fit is attached in the appendix. The matrices A_0, A_1, A_2, and D_1 corresponding to this fit are also listed. Finally an explanation of the parameters of the subroutine SNVDEC which was used to obtain these fits is listed.

RIGID BODY ANALYSIS FOR DAST ARW-2

At low frequencies the forces due to the flexure of the aircraft are small and the equations for the rigid body motion (with the controls fixed) can be written as:

$$\left[\frac{\hat{m}}{q} s^2 + A_0 + A_1\left(\frac{cs}{2V}\right) + A_2\left(\frac{cs}{2V}\right)^2 + D_1 \frac{s}{s + \frac{2V}{c}\hat{k}_1} \right] \underline{x} = 0 \qquad (8)$$

where $\tilde{M}$, A_0, A_1, A_2, D_1 are 2x2 matrices corresponding to the rigid body modes x_1 and x_2 (plunge and pitch).

Defining lag state $\underline{y}$ as $\underline{y}(s) = \dfrac{s}{s + \frac{2v}{c}k_1}\,\underline{x}(s)$

we have $$\dot{\underline{y}} = -\frac{2V}{c}\hat{k}_1\,\underline{y} + \dot{\underline{x}}$$

Let $$P = \frac{\tilde{M}}{\bar{q}} + A_2\left(\frac{c}{2V}\right)^2$$

Then a state space representation of (8) is given as:

$$\begin{bmatrix} \ddot{\underline{x}} \\ \dot{\underline{x}} \\ \dot{\underline{y}} \end{bmatrix} = \begin{bmatrix} -P^{-1}A_1 \cdot \frac{c}{2V} & -P^{-1}A_0 & -P^{-1}D_1 \\ I_{2\times 2} & 0 & 0 \\ I_{2\times 2} & 0 & -\frac{2V}{c}\hat{k}_1 I_{2\times 2} \end{bmatrix} \begin{bmatrix} \dot{\underline{x}} \\ \underline{x} \\ \underline{y} \end{bmatrix} \qquad (9)$$

For the DAST ARW-2 at a flight condition of M = 0.86, H = 15000 ft we have

$c = 23.47$ in

$\bar{q} = 4.29$ psi

$v = 908.79$ ft/sec

From the data provided by NASA and the fits obtained, the matrices $\tilde{M}$, A_0, A_1, A_2, and D_1 for $k_1 = 0.13$ are as follows:

$$\tilde{M} = \begin{bmatrix} 3.044099 & 0 \\ 0 & 0.509142 \end{bmatrix} \; ; \qquad A_0 = \begin{bmatrix} 0.3760334\times 10^{-6} & 0.13225\times 10^{3} \\ -0.18475\times 10^{-7} & 1.53134 \end{bmatrix}$$

$$A_1 = \begin{bmatrix} 0.107557\times 10^{4} & 0.130911\times 10^{3} \\ 0.12736\times 10^{2} & 0.69416\times 10^{2} \end{bmatrix} \; ; \qquad A_2 = \begin{bmatrix} 0.780027\times 10^{3} & -0.8879\times 10^{2} \\ -0.131119\times 10^{2} & 0.84112\times 10^{2} \end{bmatrix}$$

$$D_1 = \begin{bmatrix} 0.145607\times 10^{3} & -0.14302\times 10^{2} \\ 0.404408\times 10^{2} & 0.47338\times 10^{1} \end{bmatrix}$$

Using these values, a state space realization as in (9) was obtained for the DAST ARW-2.

The roots of the system for this realization were found to be 6.1146, 1.828×10^{-7}, $-5.1767 \pm j7.5443$, $-1.1977 \times 10^{2} \pm j0.17228$.

The last two roots correspond to the lag terms and the other complex pair to the short period motion of the aircraft.

Neglecting the lag terms, i.e., taking only the top left 4x4 part of the matrix in (9), the roots of the system were found to be 3.391×10^{-2}, 7.5875×10^{-5}, $-1.1188 \pm j3.5572$.

A possible explanation for the discrepancy between the roots for the rigid body motion with and without the lag terms is that the lag terms become important only at high frequencies and at those frequencies the flexure of the aircraft is large and we cannot neglect the forces due to the flexure modes.

CONCLUSION

A procedure for modelling unsteady aerodynamics of a flexible vehicle for control system design was developed. Using this procedure a model for DAST-ARW-2 was obtained and this model was found to approximate the actual unsteady aerodynamic forces very closely.

Using this model the eigenvalues for the rigid body motion of the aircraft were calculated and these were found to have good correspondence with those calculated by NASA.

This model can now be used for designing active flutter suppression control systems for the DAST ARW-2.

REFERENCES

1. Jones, R.T., "The Unsteady Lift of a Wing of Finite Aspect Ratio", NACA Report 681, 1940.

2. Sevart, F.D., "Development of Active Flutter Suppression Wind Tunnel Testing Technology", AFFDL-TR-74-126, 1975.

3. J.K. Mahesh, C.R. Stone, W.L. Garrard, and P.D. Hausman, "Active Flutter Control for Flexible Vehicles", NASA CR-159160, Nov. 1979.

4. Adams, William M., Jr. and Tiffany, Sherwood H., "An Updated Comparison of NASA/Boeing Predictions of the Open Loop, Symmetric Flutter Characteristics of the DAST ARW-2", Technical Memorandum to files, ACPO TM 81-1, Jan. 1981, Active Controls Project Office, NASA Langley Research Center.

5. NASA, LRC, Analysis and Computation Division Subprogram Library with modifications by E.S. Armstrong.

6. Ben Noble, James W. Daniel, "Applied Linear Algebra", 2nd edition, Prentice Hall Inc., 1977, (sec. 9.6, 11.6).

ORIGINAL PAGE IS
OF POOR QUALITY

APPENDIX I

```
 PROGRAM NEUFIT(INPUT,OUTPUT,TAPE1)
C***
C***      THIS PROGRAM COMPUTES THE LEAST SQUARE FIT FOR THE UNSTEADY AERODYNAMIC
C         COEFFICIENT MATRIX FOR DAST ARW-2 AT M=.86,H=15000FT
C***
 DIMENSION QR(15,16,12),QI(15,16,12),A(24,4),B(24,16),AO(15,16),
+ A1(15,16),A2(15,16),D1(15,16),D2(15,16),RK(12),V(24,4),Q(4),
+ APLUS(24,24),ADUM(24,4),DUM1(12),DUM2(12)
 REAL KHAT(2)
 DATA(RK(I),I=1,12) / 0.0,.005,.05,.1,.2,.3,.4,.5,.6,.7,.8,1.0 /
 CALL GETPF(5HTAPE1,5HDAT15,0,0)
 DO 2 K=1,12
 DO 2 J=1,16
 DO 2 I=1,15
 READ(1,100) QR(I,J,K),QI(I,J,K)
2CONTINUE
 DO 101 I=1,12
 AO(I,1)=QR(I,1,1)
101CONTINUE
100 FORMAT(2E16.8)
 KHAT(1)=.13
 DO 10 I=1,12
 J=I+12
 A(I,1)=0
 A(J,1)=RK(I)
 A(I,2)=-RK(I)*RK(I)
 A(J,2)=0
 DUM1(I)=RK(I)*RK(I)+KHAT(1)*KHAT(1)
 A(I,3)=RK(I)*RK(I)/DUM1(I)
 A(J,3)=KHAT(1)*RK(I)/DUM1(I)
10 CONTINUE
 IOP=3
 MD=24
 ND=24
 M=24
 N=3
 NOS=1
 IAC=10
 DO 20 I=1,12
 DO 30 K=1,12
 B(K,1)=QR(I,1,K)-AO(I,1)
 KPLUS=K+12
 B(KPLUS,1)=QI(I,1,K)
30CONTINUE
 DO 40 J=1,24
 DO 40 K=1,3
 ADUM(J,K)=A(J,K)
40CONTINUE
 CALL SNVDEC(IOP,MD,ND,M,N,ADUM,NOS,B,IAC,ZTEST,Q,V,IRANK,APLUS,IERR)
C
```

```
C
C
      PRINT,IERR
      A1(I,1)=B(1,1)
      A2(I,1)=B(2,1)
      D1(I,1)=B(3,1)
   20 CONTINUE
      DO 102 I=1,24
      A(I,4)=A(I,3)
      A(I,3)=A(I,2)
      A(I,2)=A(I,1)
      IF (I.GT.12) GO TO 103
      A(I,1)=1
      GO TO 102
  103 A(I,1)=0
  102 CONTINUE
      N=4
      NOS=15
      DO 104 I=1,12
      DO 105 J=2,16
      JJ=J-1
      DO 105 K=1,12
      B(K,JJ)=OR(I,J,K)
      KPLUS=K+12
      B(KPLUS,JJ)=OI(I,J,K)
  105 CONTINUE
      DO 106 J=1,24
      DO 106 K=1,4
      ADUM(J,K)=A(J,K)
  106 CONTINUE
      CALL SNVDEC(IOP,MD,ND,M,N,ADUM,NOS,3,IAC,ZTEST,Q,V,IRANK,APLUS,IERR)
      PRINT,IERR
      DO 104 J=2,16
      JJ=J-1
      A0(I,J)=B(1,JJ)
      A1(I,J)=B(2,JJ)
      A2(I,J)=B(3,JJ)
      D1(I,J)=B(4,JJ)
  104 CONTINUE
      REWIND 1
      DO 50 J=1,16
      DO 50 I=1,12
      WRITE(1,200) A0(I,J),A1(I,J),A2(I,J),D1(I,J)
   50 CONTINUE
  200 FORMAT(4E16.8)
      CALL REPLACE(5HTAPE1,6HONEFLAG,0,0)
      STOP
      END
C****
C***     THE SUBROUTINE SNVDEC SHOULD BE ATTACHED AT THIS POINT    *********
C****
```

ORIGINAL PAGE IS
OF POOR QUALITY

FIT FOR G(S) DAST ARW-2 AT M=0.86 , H=15000 FT

THE MATRICES A0,A1,A2,B1 ARE WRITTEN COLUMNWISE

1ST COLUMN

A0	A1	A2	B1
.37603340E-06	.10737462E+04	.78002766E+03	.14560723E+03
-.18475110E-07	.12736737E+02	-.13111972E+02	.40440853E+02
.96467900E-07	.18504167E+03	.40504833E+02	.30102076E+02
-.30699260E-07	-.75823772E+02	.47563358E+01	.91573321E+01
-.50542910E-08	-.11717877E+02	-.27789210E+01	-.11910643E+01
-.97841290E-07	-.18181098E+03	-.23706107E+02	-.34526697E+02
.11805980E-07	-.14245807E+02	-.18748114E+00	-.18259528E+02
.25987840E-06	.50658007E+02	-.27785720E+03	.19215422E+03
-.54181130E-08	.18795377E+02	.42889036E+02	.12194857E+02
-.66935820E-09	.53028117E+02	-.31890206E+02	-.83022992E+01
.20949430E-07	.67556730E+02	.19904798E+02	.93032076E+00
.31524370E-06	.41467740E+02	-.17386298E+03	.24897784E+03

2ND COLUMN

A0	A1	A2	B1
.13225484E+03	.13091121E+03	-.88794862E+02	-.14301898E+02
.15313462E+01	.63416047E+02	.84112276E+02	.47338357E+01
.28868841E+02	.31591959E+02	.27670570E+01	-.12680094E+02
-.90996486E+01	.11096861E+02	.62059510E+01	.48961975E+01
-.15911085E+01	-.11238764E+01	-.77819454E+00	.63988320E+00
-.30549514E+02	-.70957214E+01	-.36902840E+01	.12244909E+02
.15231603E+00	-.24554730E+02	-.37993927E+02	-.41788734E+01
.77573963E+02	-.20366603E+02	-.14333518E+02	-.43152991E+02
.13792468E+01	.17095509E+02	.74224375E+01	.24919249E+01
.19491097E+01	-.25213003E+00	.22242056E+02	.76436235E+00
.67076209E+01	-.59802550E+01	-.15779407E+01	.99377887E+00
.10414616E+03	-.65086695E+02	.58070410E+02	-.87819664E+02

3RD COLUMN

A0	A1	A2	B1
.50145298E+02	.20147569E+03	.37241762E+02	-.25384225E+01
.45088540E+01	.24100966E+02	.83733845E+01	-.87639639E+00
.17618642E+02	.10955126E+03	.19658645E+02	.28169529E+01
-.59063481E+00	.15275983E+02	.31106636E+01	.76300480E+00
-.68474697E+00	-.46239116E+01	-.20445811E+01	.32054130E+00
-.10628135E+02	-.21300543E+02	.35593508E+01	-.26178152E+01
-.94639767E+00	-.17015633[illegible]	-.39872221E+01	.84832407E+00
.41534056E+02	.13233116E+03	.13975330E+03	.47473009E+02
.31626343E+00	-.63327652E+00	.93712168E+00	-.54990329E+00
-.78163239E+00	-.10129090E+02	-.27446825E+01	.14747801E+00
.15337373E+00	-.11334580E+02	-.23511042E+00	-.11227332E+01
.18918474E+02	-.27917532E+02	.17784330E+02	-.10609228E+02

************ 4TH COLUMN ***************

*

.46774854E+02	-.81085770E+02	-.43481[illegible]E+02	-.46965243E+02
.16722178E+02	.50004150E+02	-.13068678E+02	-.566[illegible]129E+01
.10708837E+02	.19496020E+02	.13500[illegible]E+01	-.51875809E+01
.25132622E+01	.53426721E+02	.153506[illegible]E+02	-.[illegible]686539E+01
-.30882524E+00	-.25285400E+00	-.37222221E+00	.52138326E+00
-.42563659E+01	.38524037E+02	.11726811E+02	.73673141E+01
-.52094281E+01	-.22286433E+02	.33492704E+01	.22909958E+01
.34048268E+02	.63506302E+02	-.61802395E+01	-.21483460E+02
.45767989E+01	.11963679E+02	-.29589119E+01	-.35655361E+01
-.64880535E+00	-.12628113E+02	-.13168552E+02	.28950853E+01
-.82414013E+00	-.21429574E+02	-.14799135E+01	-.23766525E+01
.43876296E+01	-.26089819E+02	.37607648E+02	-.68715534E+02

*

************ 5TH COLUMN *******************

*

-.53773186E+01	-.12101467E+02	-.42761725E+01	-.12396789E+01
-.14271761E+01	-.13110156E+01	-.90935130E+00	-.17082499E-02
-.59555552E+01	-.67333046E+01	-.12981327E+01	.12145281E+00
-.24611257E+01	-.12052686E+01	-.13746128E+00	.14724615E+00
.17040921E+00	.14019724E+01	.24658315E+00	-.33047369E-01
-.26725373E+01	-.41849697E+01	.25317641E-01	-.45620283E+00
-.87263999E+00	-.16098149E+01	.30934953E+00	-.23300059E+00
-.18045067E+02	.71422044E+01	-.46051942E+00	-.63822558E+00
.55296736E-01	.70958641E-01	-.23382628E+00	-.68463414E-01
-.31100776E+00	-.55738538E+01	-.22099767E+01	.16332294E-01
.10064323E+01	-.66357812E+01	-.22131644E+01	.25323577E+00
.19465868E+02	-.14758503E+02	.86125680E+01	-.24642279E+01

*

*********** 6TH COLULN *****************

*

.12202583E+03	-.13454275E+03	-.69449634E+02	-.78288093E+02
.20227065E+02	.89648389E+01	-.16207627E+02	-.11915522E+02
.72806972E+02	.50041754E+01	.13739247E+01	-.16724347E+02
.17317503E+02	.48157454E+02	.76214005E+01	.71588227E+00
-.17452666E+01	-.37056286E+01	-.72887382E-01	.10257835E+01
-.11842483E+02	.12901256E+03	.21468949E+02	.16664829E+02
-.34736111E+00	.21380940E+02	.17769754E+02	.43363816E+01
.22833730E+03	-.85304059E+02	.16380999E+03	-.10496115E+03
.10887043E+01	.19572167E+01	-.62416885E+01	-.39862077E+01
-.54713902E+01	.13911486E+02	.17260668E+01	-.59539084E+01
-.11340863E+02	-.10063231E+01	.18369040E+01	-.74033502E+01
-.68680294E+02	-.14184551E+03	.88493571E+02	-.79574790E+02

*

*********** 7TH COLUMN *****************

*

-.17204305E+03	-.60578055E+02	.31245616E+02	.48949690E+02
.72519137E+01	-.37725126E+02	-.38703136E+02	-.10620930E+02
-.41671533E+02	-.13937709E+02	.38518340E+01	.18271935E+02
.23437322E+02	.69222584E+01	-.79331246E+01	-.83945716E+01
.21893965E+01	-.12045050E+00	-.30037370E+00	-.82394310E+00
.48089780E+02	.32603835E+02	.10262443E+02	-.19407371E+02
-.90824259E+01	.28254968E+02	.22973128E+02	.82539564E+01
-.10402285E+03	.13938738E+03	-.23970908E+02	.67769292E+02
.27803696E+01	-.75136072E+01	-.58964670E+01	-.32315176E+01
-.41111160E+01	.33929168E+00	-.49561563E+01	-.35518936E+01
-.95314637E+01	.85140380E+01	.51048178E+00	.67253968E+00
-.15164121E+03	.46859206E+02	-.27904483E+02	.10959333E+03

*

ORIGINAL PAGE IS
OF POOR QUALITY

********* 8TH COLUMN ***********

-.42091876E+04	-.11770107E+04	.51197304E+02	.17185136E+04
-.40790005E+03	-.18401376E+03	.22900872E+02	.13759957E+03
-.16863138E+04	-.48651484E+03	.45537564E+02	.33975823E+03
-.51976995E+02	-.28354533E+02	.28588871E+02	-.10640239E+03
.52364066E+02	.56583672E+02	-.20596652E+02	-.17896377E+02
.81482059E+03	-.10820058E+03	.17726136E+03	-.40708506E+03
.42216013E+02	.11538341E+03	-.30498458E+00	-.40199848E+02
-.47136664E+04	.51845309E+04	-.19845656E+04	.15637257E+04
-.13334993E+02	-.18397642E+02	.78252601E+00	.28654575E+02
.72853603E+02	.12700411E+03	-.45316515E+02	.46593182E+02
.76665898E+02	.41431220E+02	-.36726805E+01	.11488361E+03
-.38868544E+03	-.23729102E+02	.26877793E+03	.12842351E+04

************ 9TH COLUMN **************

.27692233E+02	.36680767E+02	.12278581E+02	-.64458731E+01
.13733536E+02	.21282309E+02	.52119802E+01	-.20025983E+01
.38550133E+01	.79327955E+00	-.36754966E+00	-.50863301E+00
.66545770E+01	.11616051E+02	.33521934E+01	-.35388171E+00
-.86428128E-01	-.14747249E+00	.89886945E-01	.29253174E-01
-.75826032E+00	.68790969E+00	-.43631539E+00	.71852124E+00
-.71768987E+01	-.11914258E+02	-.30145662E+01	.11351081E+01
.14685419E+02	-.71697799E+01	.62070872E+01	-.23061370E+01
.66418757E+01	.15450190E+02	.52085920E+01	-.71077099E+00
.17557146E+01	.75581170E+01	.31466753E+01	-.25341349E+00
-.10502884E+01	-.23743339E+01	-.90647967E+00	-.35721691E+00
-.47478079E+01	.63436616E+01	-.39561057E+01	-.23671686E+00

*********** 10TH COLUMN *************

-.38910153E+02	.28841946E+02	.33814467E+02	.74090333E+02
-.17995251E+02	-.11889935E+02	.39586917E+02	.25978897E+02
-.60790091E+02	-.36227792E+02	.44718792E+01	.25894374E+01
-.21239520E+02	-.41544933E+02	.80777876E+01	.60879348E+01
-.59960106E+00	-.41316257E+01	-.29864587E+01	-.19682938E+00
.12264141E+02	-.95017800E+00	.15226491E+02	-.61492002E+01
.75608829E+01	.16081519E+02	-.22781553E+02	-.14805945E+02
-.15107780E+03	.11477528E+03	-.30500976E+00	.70167006E+01
.33915139E+01	.52269312E+01	.18280378E+02	.11497292E+02
.24311046E+02	.10963953E+03	.42895604E+02	.42715811E+01
.29239743E+02	.89172207E+02	.20577595E+02	.27413953E+01
.12386324E+03	-.20783600E+03	.49586823E+02	.61779115E+01

************ 11TH COLUMN ***************

*

-.11612275E+03	.69640370E+01	.92124661E+02	.77931421E+02
-.27976115E+02	-.22163067E+02	.20220499E+02	.24939749E+02
-.51574377E+02	-.27789961E+02	.25796582E+01	.83367547E+01
-.13102100E+02	-.25516059E+02	.65025021E+01	.55267771E+01
-.55200030E+00	-.69963540E+01	-.22879518E+01	-.45502780E+00
.40335668E+02	.17468929E+01	.97961292E+01	-.73408613E+01
.17709030E+02	.15157118E+02	-.84201864E+01	-.13095167E+02
-.13048656E+03	.89873443E+02	-.18352327E+02	.40572982E+02
-.69212951E+01	-.75199442E+01	.10427959E+02	.10006550E+02
.23154270E+02	.84766624E+02	.23285854E+02	.47494069E+01
.21859073E+02	.96547568E+02	.24724367E+02	.20601090E+01
-.26987518E+02	-.77839782E+01	-.57638098E+02	.47739782E+02

*

*********** 12TH COLUMN ************

*

-.31357376E+04	-.67569187E+03	-.23712536E+03	.15165939E+04
.62486716E+02	-.70833899E+01	-.14188059E+03	-.91860543E+02
-.26266162E+03	.34020166E+02	.63265645E+01	.29315449E+03
.63528353E+03	.24700296E+03	-.10859816E+03	-.21915646E+03
.31843534E+02	-.30560110E+02	.15416682E+02	-.18893736E+02
.12056312E+04	.50606490E+03	-.17270217E+03	-.28561114E+03
.66866582E+02	.19609647E+03	.59593304E+01	.13556489E+03
-.50968863E+03	.15065603E+04	-.10077923E+04	.11777249E+04
.18597452E+02	.19033667E+02	-.73811618E+02	-.51308999E+02
-.11920018E+03	-.66238346E+02	-.12413786E+03	.71460562E+01
-.37906331E+03	.17965865E+02	-.11331880E+03	.96440807E+02
-.45543710E+04	.44929386E+04	-.15214266E+04	.18896105E+04

*

********** 13TH COLUMN ************

*

-.18845993E+04	-.10977619E+04	.17555697E+03	.34578743E+03
-.10842930E+04	-.70616891E+03	.82154747E+02	.17813149E+03
.29368883E+02	.20677163E+02	-.68302880E+00	.30544404E+01
-.44202105E+03	-.34624457E+03	.93395017E+01	.65747918E+02
-.28267991E+00	-.16790885E+00	.26752528E-01	-.32716014E+00
-.23088933E+02	-.10618451E+02	.33002307E+00	-.27295776E+01
.60982894E+03	.32610795E+03	-.28336319E+02	-.10662332E+03
-.22516553E+03	-.16199764E+03	-.12618812E+02	.51522570E+02
-.40330527E+03	-.38286761E+03	-.93898564E+02	.68729162E+02
.31141996E+02	-.14708760E+03	-.15267053E+03	-.92787777E+00
-.26931512E+02	.23459523E+02	.41464628E+02	.47591287E+01
-.14309772E+02	-.52486698E+01	.42630615E+01	.11258372E+02

*

************ 14TH COLUMN *************

*

-.30519860E+03	.70140330E+02	-.10291392E+03	.28247602E+03
-.14673790E+03	.10626484E+02	-.14478647E+02	.40556176E+02
-.53827414E+03	.82175819E+02	-.10588601E+03	.99070901E+02
-.15293520E+03	.28707500E+02	-.62219490E+02	.69511252E+01
.35746918E+02	-.30897333E+01	.12340567E+01	.14671328E+01
-.16742955E+03	.32056963E+02	-.25651467E+02	-.79749058E+02
-.16408230E+02	.18780049E+02	-.14734812E+02	-.17410964E+02
.77967507E+03	.36258590E+03	-.25543621E+03	.47847363E+03
-.75729487E+01	-.40492608E+01	.42284541E+01	.67998519E+01
.39987051E+02	.16470247E+02	.18011640E+02	-.16448380E+02
.98022359E+02	-.41114599E+01	.43931740E+02	-.22113728E+02
-.23173931E+03	-.32206011E+03	.32097025E+03	-.10171023E+03

*

************ 15TH COLUMN ****************

*

-.34263414E+04	.45707941E+01	-.77673169E+03	.22398753E+04
.42876289E+02	.14348737E+03	-.42511366E+03	-.28771905E+03
-.44766682E+03	-.81892384E+02	.66928514E+02	.47408712E+03
.71373299E+03	.48255247E+02	-.83442720E+02	-.51730802E+03
.43870832E+02	-.52737737E+00	.26125166E+01	-.30826033E+02
.88814450E+03	-.44541775E+01	.94630541E+02	-.63721607E+03
.80864417E+02	-.13372557E+03	.32579867E+03	.19923505E+03
.10703024E+04	-.83843600E+03	.12539709E+04	.10667708E+04
.12022881E+03	.66683395E+02	-.16041885E+03	-.19967166E+03
-.63676027E+03	.61074891E+02	-.16617811E+03	.44259015E+02
-.63554346E+03	.35825296E+02	-.96518896E+02	.20663066E+03
.21621952E+04	-.96695108E+03	.16156101E+04	.22539710E+04

*

*********** 16TH COLUMN *************

*

.22245548E+05	.29787903E+04	-.32096934E+03	-.26414652E+05
.44581880E+03	.80575622E+03	-.76644810E+03	-.11405029E+04
.49999777E+04	.22343841E+04	-.17753994E+04	-.72382524E+04
-.18118220E+04	.74285183E+03	-.13411859E+04	.12919606E+04
-.26538508E+03	-.26770333E+02	-.93317474E+00	.31171545E+03
-.51619089E+04	-.39317212E+03	-.98972738E+03	.59384235E+04
.10007252E+03	-.16093799E+03	-.39785667E+02	.61422816E+02
.12832804E+05	.74741606E+04	-.83088389E+04	-.20086965E+05
.16290237E+03	.50114671E+02	-.69180067E+02	-.21809537E+03
.43534588E+03	-.52978949E+03	.48303703E+03	-.43767597E+01
.11120970E+04	-.64786105E+03	.76824165E+03	-.70661854E+03
.15803302E+05	-.11823527E+04	.53172653E+04	-.16162349E+05

Subroutine SNVDEC

Description: The purpose of SNVDEC is to compute the singular-value decomposition (ref. 2) of a real $m \times n$ ($m \geq n$) matrix A by performing the factorization,

$$A = UQV'$$

where U is an $m \times n$ matrix whose columns are n orthonormalized eigenvectors associated with the n largest eigenvalues of AA', V is an $n \times n$ matrix whose columns are the orthonormalized eigenvectors associated with the n eigenvalues of A'A, and

$$Q = \text{diag}(\sigma_1, \sigma_2, \ldots, \sigma_n)$$

where σ_i ($i = 1,2,\ldots,n$) are the nonnegative square roots of the eigenvalues of A'A, called the singular values of A. Options are provided for the computation of rank A, singular values of A, an orthonormal basis for the null space of A, the pseudoinverse of A, and the least squares solution to

$$AX = B$$

Both A and B are stored as variable-dimensioned two-dimensional arrays. The computational procedure is described in reference 2 on pages 135-151. Basically, Householder transformations are applied to reduce A to bidiagonal form after which a QR algorithm is used to find the singular values of the reduced matrix. Combining results gives the required construction.

Source of software: LaRC Analysis and Computation Division subprogram library with modifications by Ernest S. Armstrong, LaRC

Calling sequence: CALL SNVDEC(IOP,MD,ND,M,N,A,NOS,B,IAC,ZTEST,Q,V,IRANK, APLUS,IERR)

Input arguments:

IOP Option code:

1 The rank and singular values of A will be returned.

2 The matrices U and V will be returned in addition to the information for IOP = 1.

3 In addition to the information for IOP = 2, the least squares solution to AX = B will be returned.

4 The pseudoinverse of A will be returned in addition to the information for IOP = 2.

5 The least squares solution will be returned in addition to the information for IOP = 4.

MD — The maximum first dimension of the array A as given in the DIMENSION statement of the calling program

ND — Maximum first dimension of the array V

M — The number of rows of A

N — The number of columns of A

A — Matrix stored as a variable-dimensioned two-dimensional array. Input A is destroyed.

NOS — The number of column vectors of the matrix B

B — Two-dimensional array that must have row dimension at least NOS in the calling program. B contains the right sides of the equation to be solved for IOP = 3 or IOP = 5. B need not be input for other options but must appear in the calling sequence.

IAC — The number of decimal digits of accuracy in the elements of the matrix A. This parameter is used in the test to determine zero singular values and thereby the rank of A.

<u>Output arguments</u>:

A — On normal return, A contains the orthogonal matrix U except when IOP = 1.

B — On normal return, B contains the least squares solution for IOP = 3 or IOP = 5.

ZTEST — The zero test computed as $\|A\| \times 10^{-(IAC)}$ using the matrix Euclidean norm except when N = 1. When N = 1,

$$ZTEST = 10^{-(IAC)}$$

Q — A one-dimensional array of dimension at least N which upon return contains the singular values in descending order

V — A two-dimensional array that must have first dimension ND and second dimension at least N. Upon normal return, this array contains the orthogonal matrix V except when IOP = 1. The last N - IRANK columns of V form a basis for the null space of A.

IRANK — Rank of the matrix A determined as the number of nonzero singular values using ZTEST

APLUS A two-dimensional array of first dimension ND and second dimension at least M. Upon normal return, this array contains the pseudo-inverse of the matrix A. If IOP does not equal 4 or 5, this array need not be dimensioned, but a dummy parameter must appear in the calling sequence.

IERR Error indicator:

IERR = 0	A normal return
IERR = K > 0	The Kth singular value has not been found after 30 iterations of the QR algorithm procedure.
IERR = -1	Using the given IAC, A is close to a matrix which is of lower rank and if the accuracy is reduced, the rank of the matrix may also be reduced.

COMMON blocks: None

Error messages: None. The user should examine IERR after return.

Field length: 2072 octal words (1082 decimal)

Subroutines employed by SNVDEC: None

Subroutines employing SNVDEC: FACTOR, CTROL, CSTAB, DSTAB, DISCREG

Comments: SNVDEC may be applied to matrices stored as one-dimensional arrays by setting MD = M and ND = N in the calling sequence.

The subroutine is internally restricted to N ≤ 150.

APPENDIX II : (THE FLEXURE MODES)

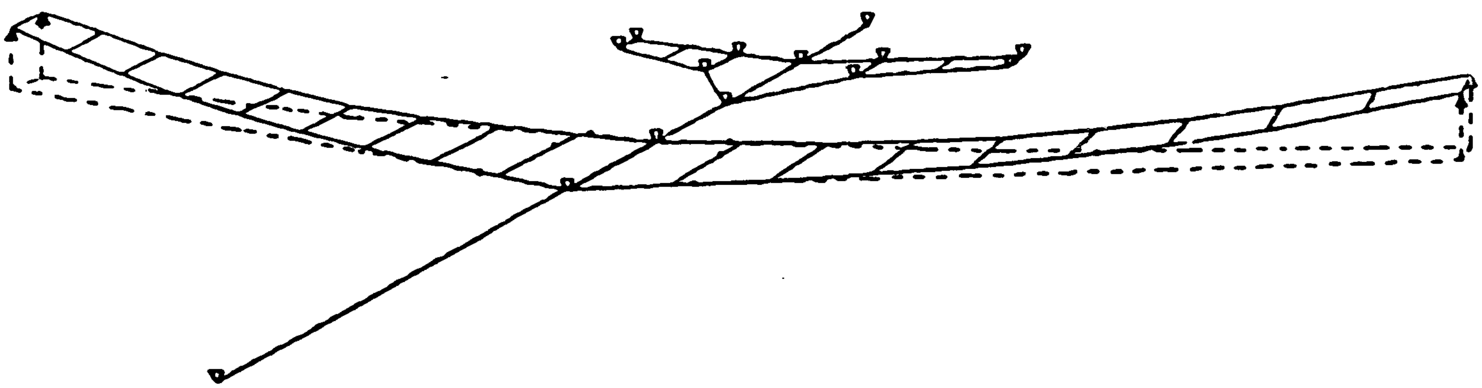

(a) mode 1, frequency = 8.44 hz, generalized mass = 0.0169 ib-sec^2/in

Figure 1.- Vertical component of elastic mode shapes.

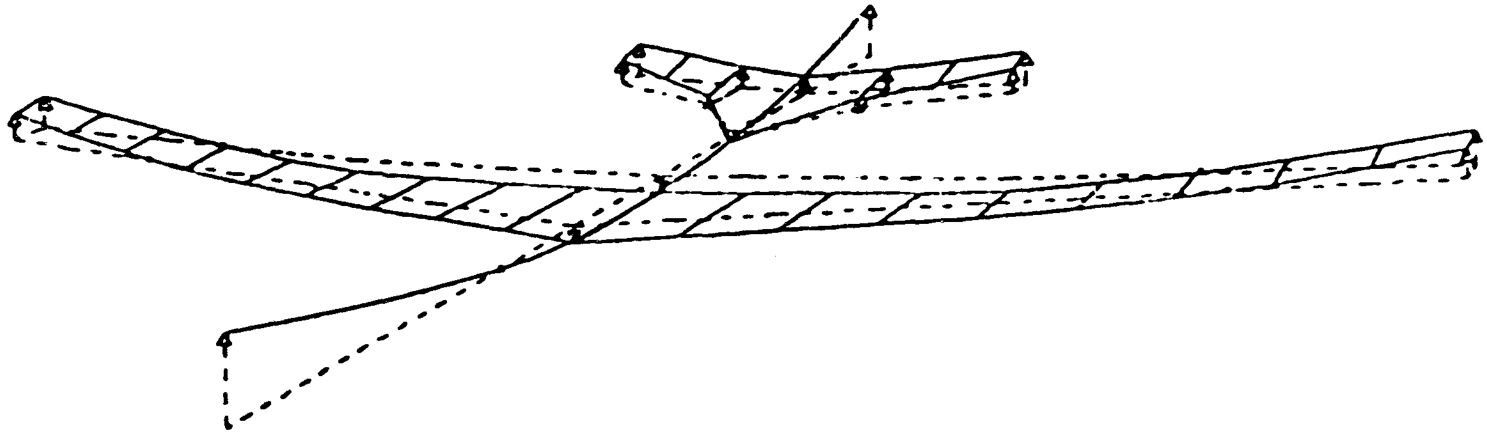

(b) mode 2, frequency = 15.7 hz, generalized mass = 0.326 lb-sec^2/in

Figure 1 - Continued.

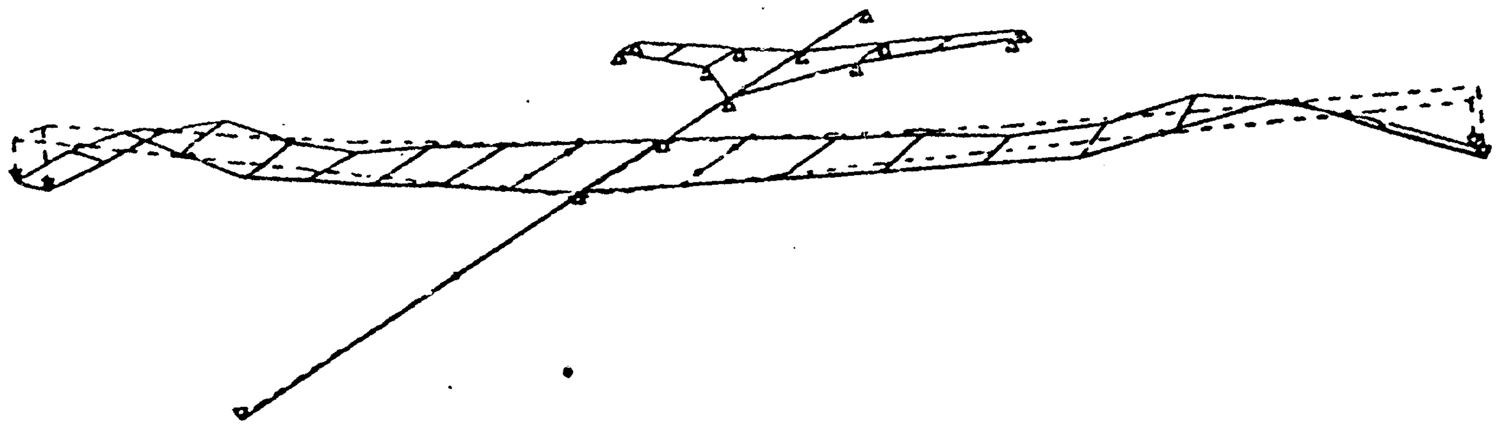

(c) mode 3, frequency = 23.7 hz, generalized mass = 0.0153 lb-sec^2/in

Figure 1.- Continued.

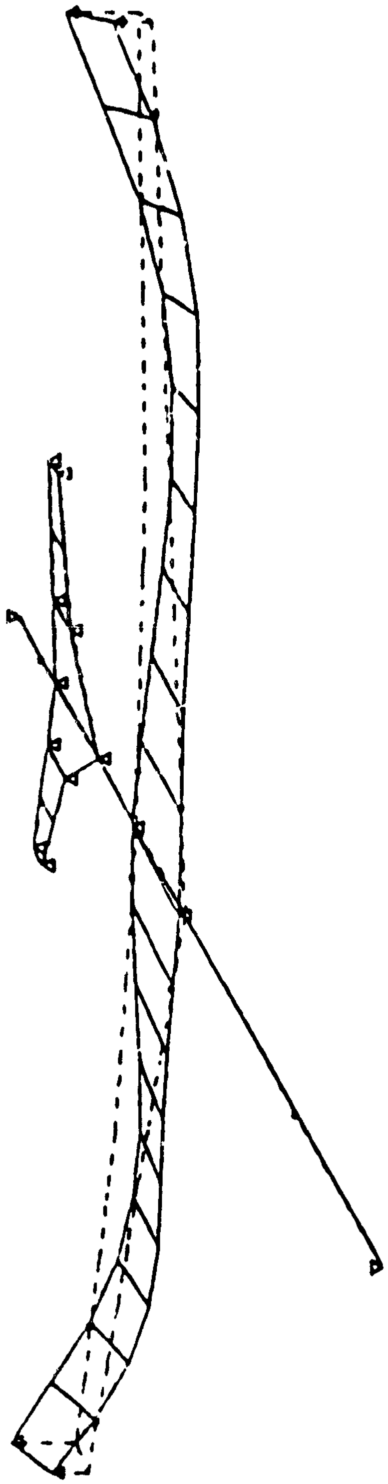

(d) mode 4, frequency = 31.7 hz, generalized mass = 0.0158 lb-sec^2/in

Figure 1.- Continued.

ORIGIN
OF POOR QU...

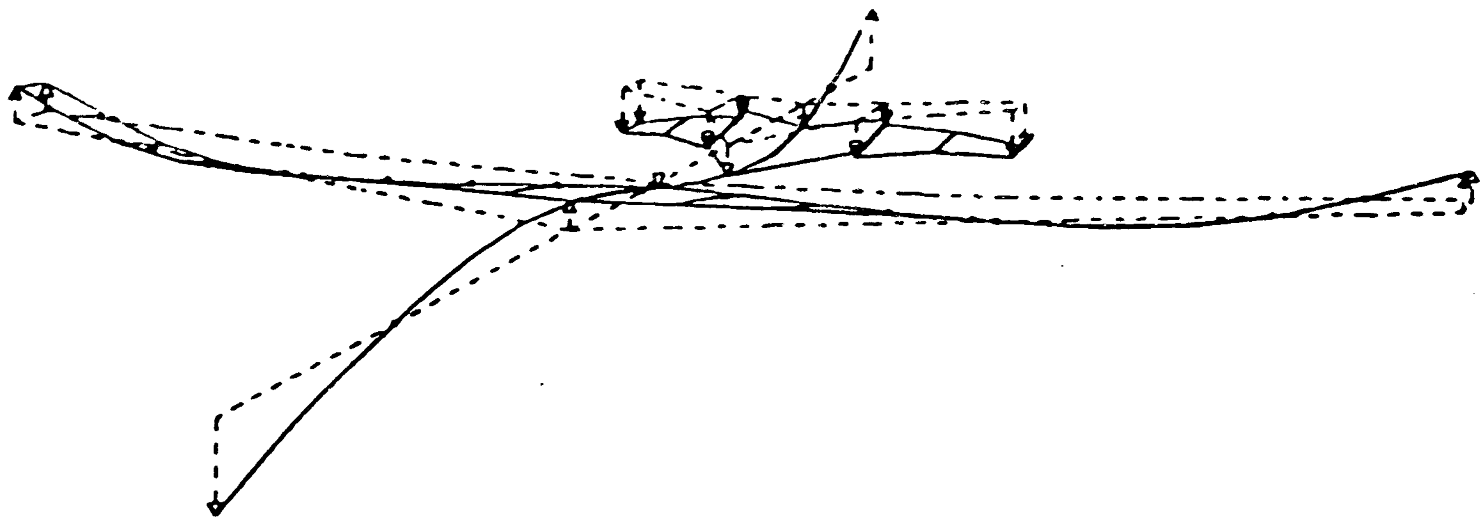

(e) mode 5, frequency = 39.3 hz, generalized mass = 0.178 lb-sec^2/in

Figure 1.- Continued.

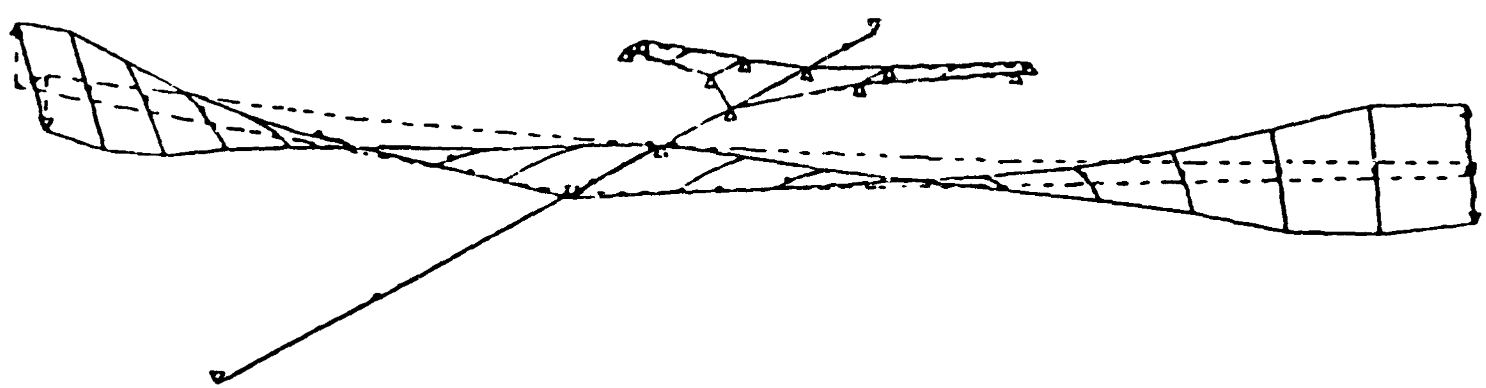

(f) mode 6, frequency = 44.8 hz, generalized mass = 0.593 lb-sec^2/in

Figure 1.- Continued.

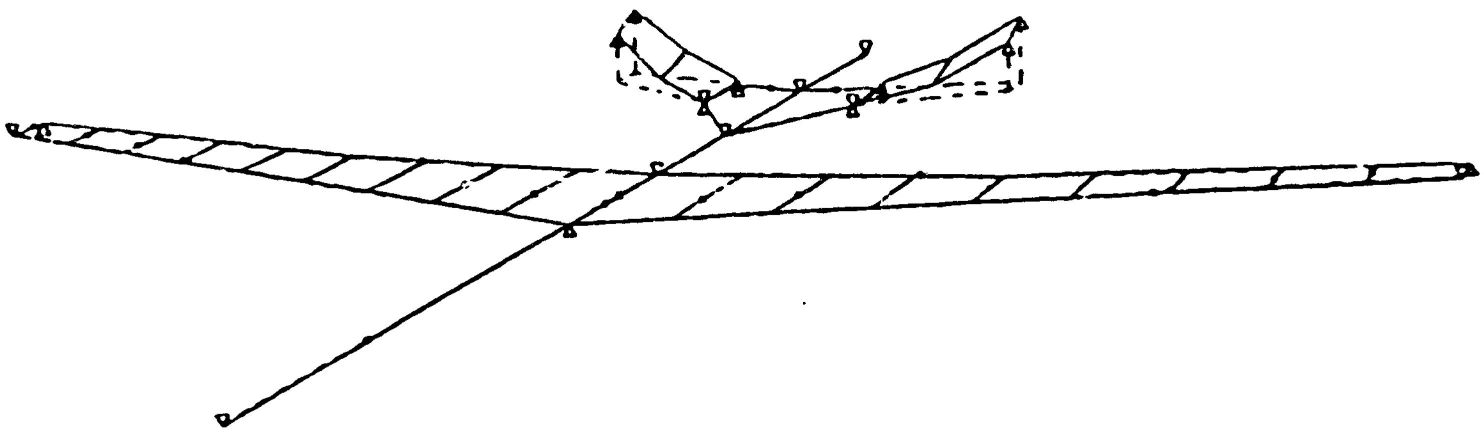

(g) mode 7, frequency = 47.3 hz, generalized mass = 0.00335 lb-sec^2/in

Figure 1.- Continued.

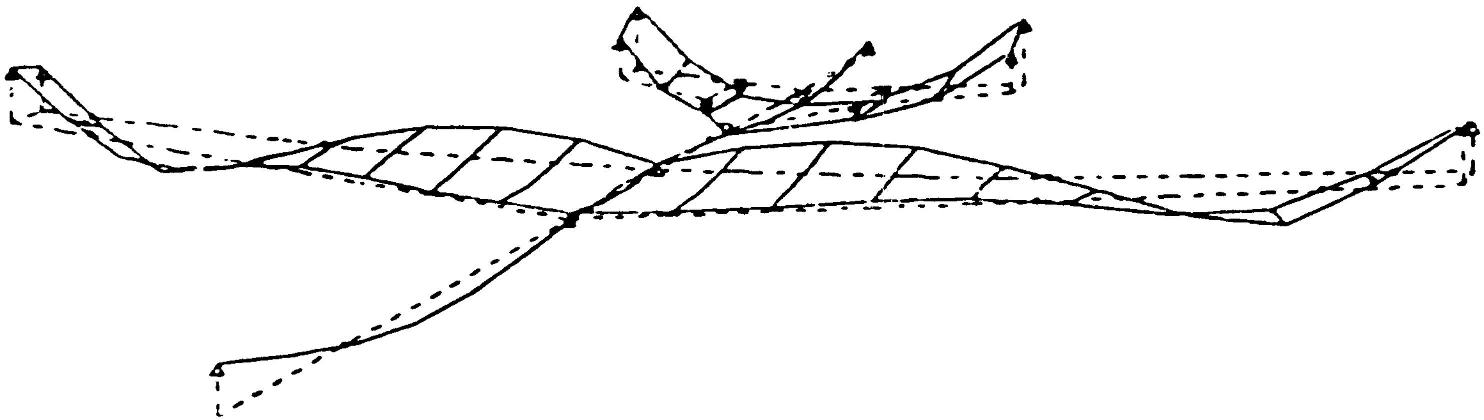

(h) mode 8, frequency = 66.6 hz, generalized mass = 0.0621 lb-sec^2/in

Figure 1.- Continued.

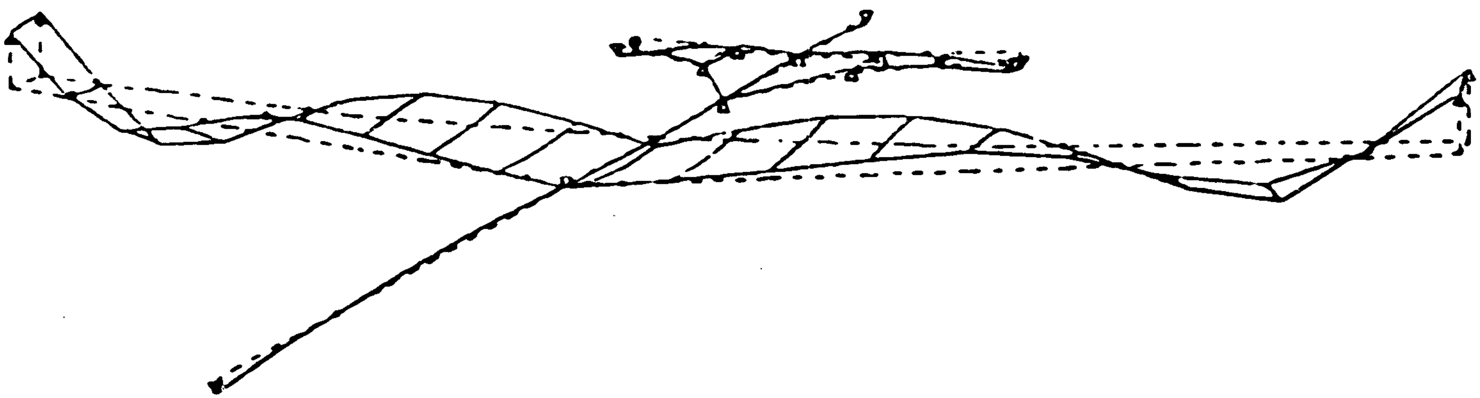

(i) mode 9, frequency = 71.2 hz, generalized mass = 0.0286 lb-sec^2/in

Figure 1.- Continued

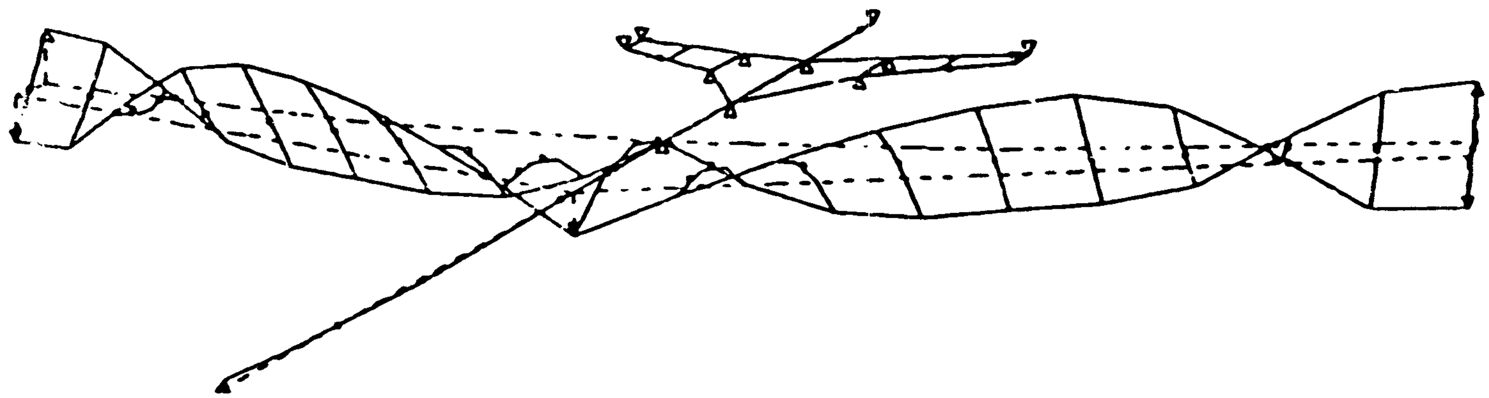

(j) mode 10, frequency = 80.3 hz, generalized mass = 0.696 lb-sec^2/in

Figure 1.- Concluded.

Working Paper No. 5
Modified Outboard Control Surface Transfer Function

W. L. Garrard
Department of Aerospace
Engineering and Mechanics
University of Minnesota
Minneapolis, Minnesota

This paper discusses the modified transfer function for the outboard aileron. The new transfer function is

$$\frac{\mu_o}{\mu_{o_c}} = \frac{4.046 \times 10^{12}\left(s^2 + 28.6s + (477.5)^2\right)}{(s+180)\left(s^2 + 251s + (8.14)^2\right)\left(s^2 + 229s + (477.5)^2\right)\left(s^2 + 286s + (477.5)^2\right)}$$

Note that the numerator term and two of the denominator terms have the same nondamped natural frequency, the damping factor of the numerator is 0.03 while the damping factors associated with the denominator terms of the same frequency are 0.23 and 0.3. Thus the numerator dynamics effectively cancels the phase shift resulting from the one of the denominator factors and except at near the natural frequency of 477.5 rad/sec the numerator dynamics also cancel the 40 db/decade roll-off resulting from one of the denominator factors. Bode plots for the response of the exact model of the outboard aileron are shown in Figs 1 and 2.

ORIGINAL PAGE IS
OF POOR QUALITY

The most obvious approximation is the cancellation of the numerator dynamics with the most lightly damped of the quadratic terms of the same frequency in the denominator. This results in the 5th order model below

$$\frac{\mu_o}{\mu_{o_c}} = \frac{4.046 \times 10^{12}}{(s+180)(s^2+251s+(314)^2)(s^2+286s+(477.5)^2)}$$

The Bode plots for this transfer function are given in Figs 3 and 4. Phase is almost the same as for the exact model and gain only differs near 477.5 rad/s. A 3rd order approximation results from neglecting the highest frequency term in the denominator. This results in the approximation

$$\frac{\mu_o}{\mu_{o_c}} = \frac{1.774 \times 10^{7}}{(s+180)(s^2+251s+(314)^2)}$$

Bode plots for this transfer function are shown in Figs 5 and 6. Up to approximately 300 rad/sec this gain and phase are the same as for the exact model. Since the 6th structural mode has a frequency of 225 rad/s at the flutter frequency it is felt that the 3rd order actuator model is adequate for initial control studies.

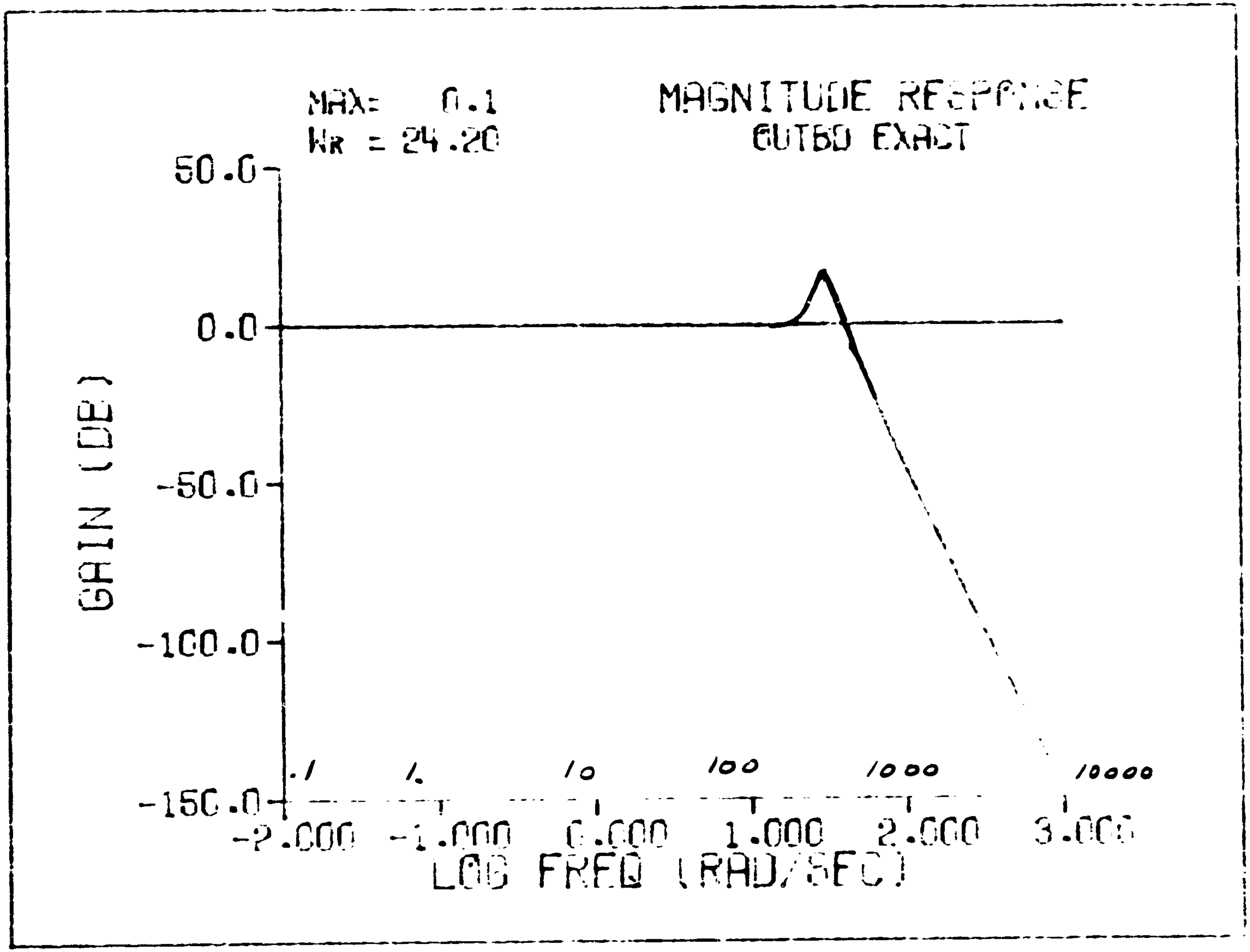
MAX= 0.1
WR = 24.20
MAGNITUDE RESPONSE
6UTBD EXACT
GAIN (DB)
50.0
0.0
-50.0
-100.0
-150.0
.1
1.
10
100
1000
10000
-2.000
-1.000
0.000
1.000
2.000
3.000
LOG FREQ (RAD/SEC)

Fig 1

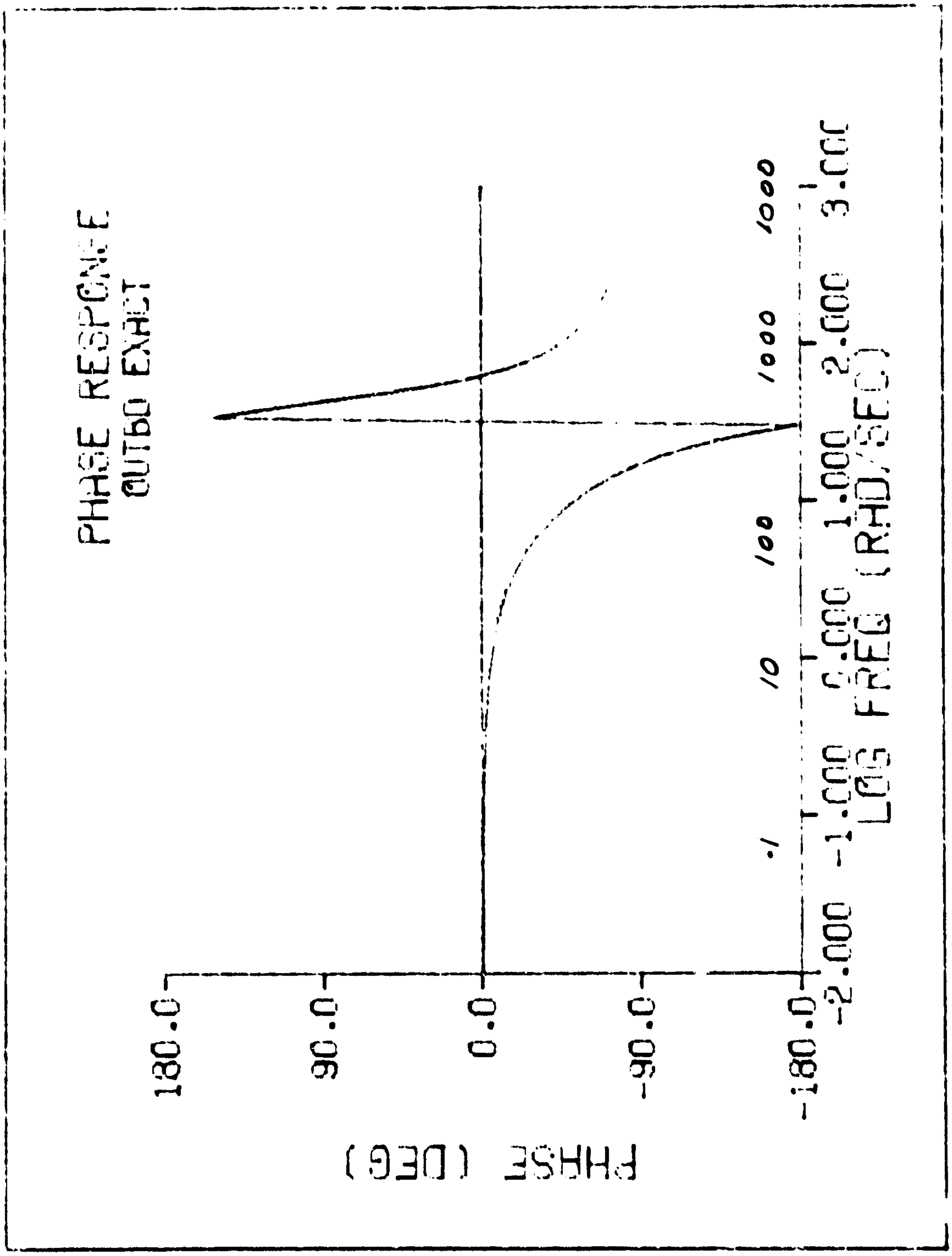
PHASE RESPONSE
PHASE (DEG)
180.0
90.0
0.0
-90.0
-180.0
-2.000
-1.000
0.000
1.000
2.000
3.000
LOG FREQ (RAD/SEC)
.1
10
100
1000
1000
1000

Fig 2

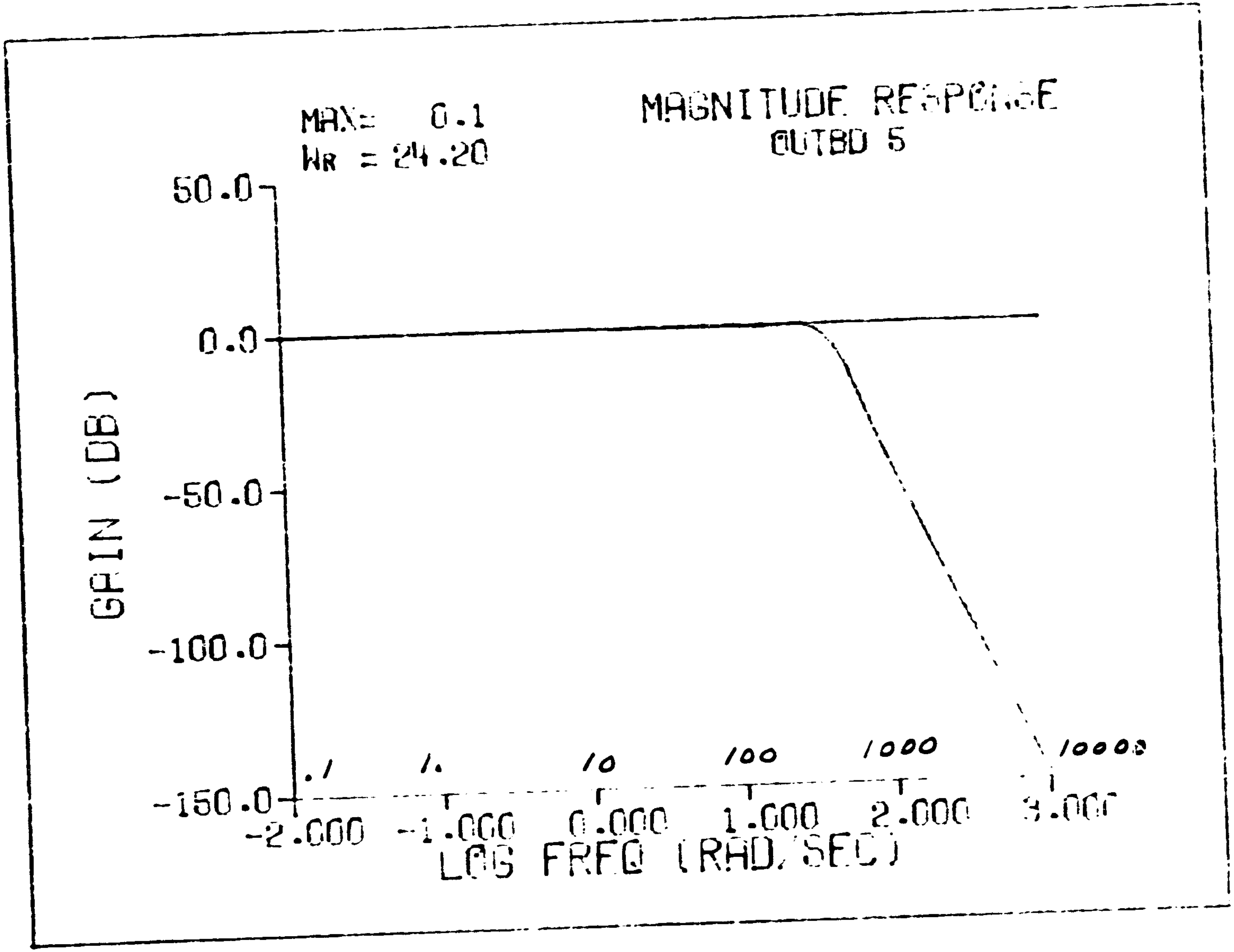
MAX= 0.1
WR = 24.20
MAGNITUDE RESPONSE
OUTBD 5
50.0
0.0
-50.0
-100.0
-150.0
GAIN (DB)
.1
1.
10
100
1000
10000
-2.000
-1.000
0.000
1.000
2.000
3.000
LOG FREQ (RAD/SEC)

Fig 3

ORIGINAL PAGE IS
OF POOR QUALITY

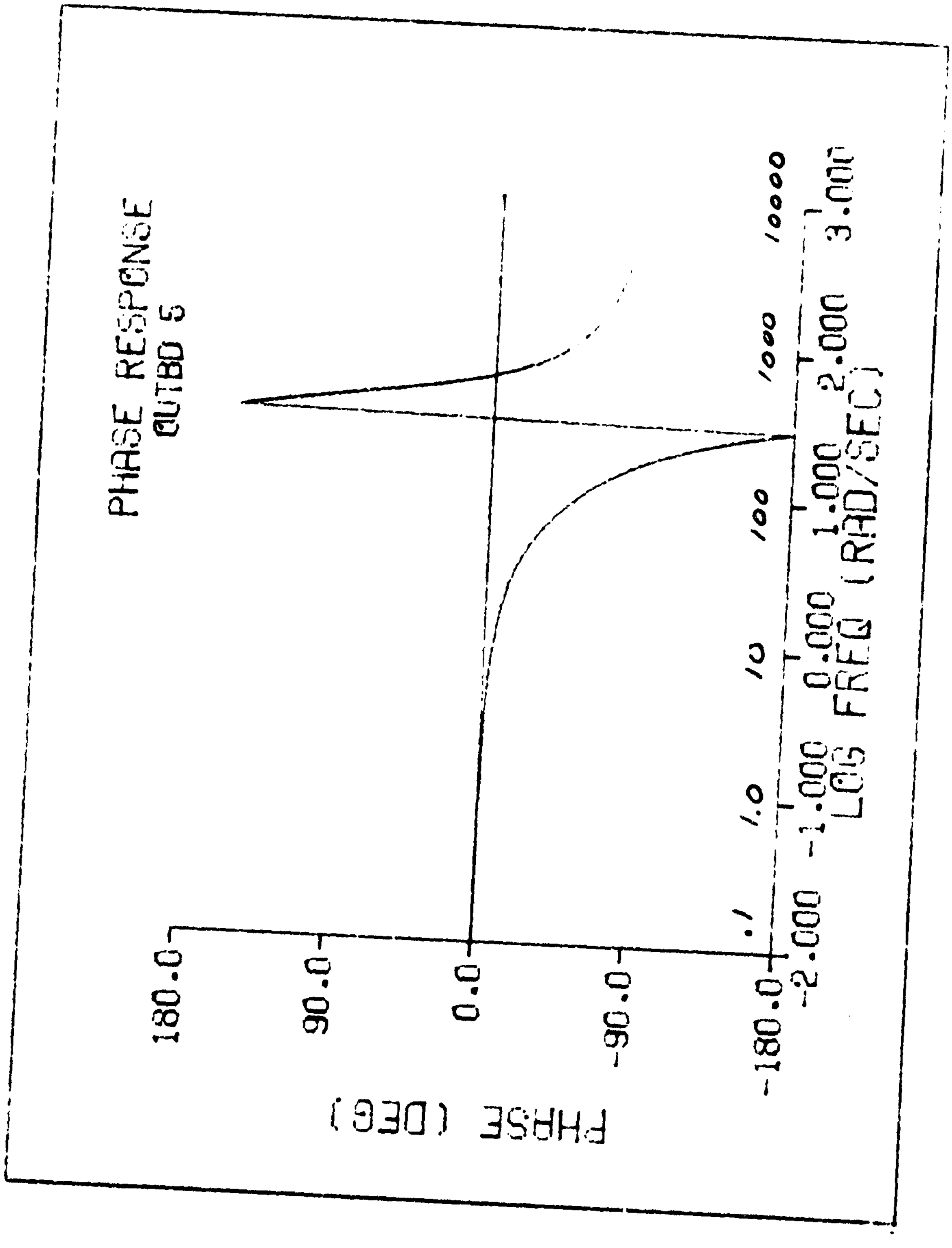

Fig 4

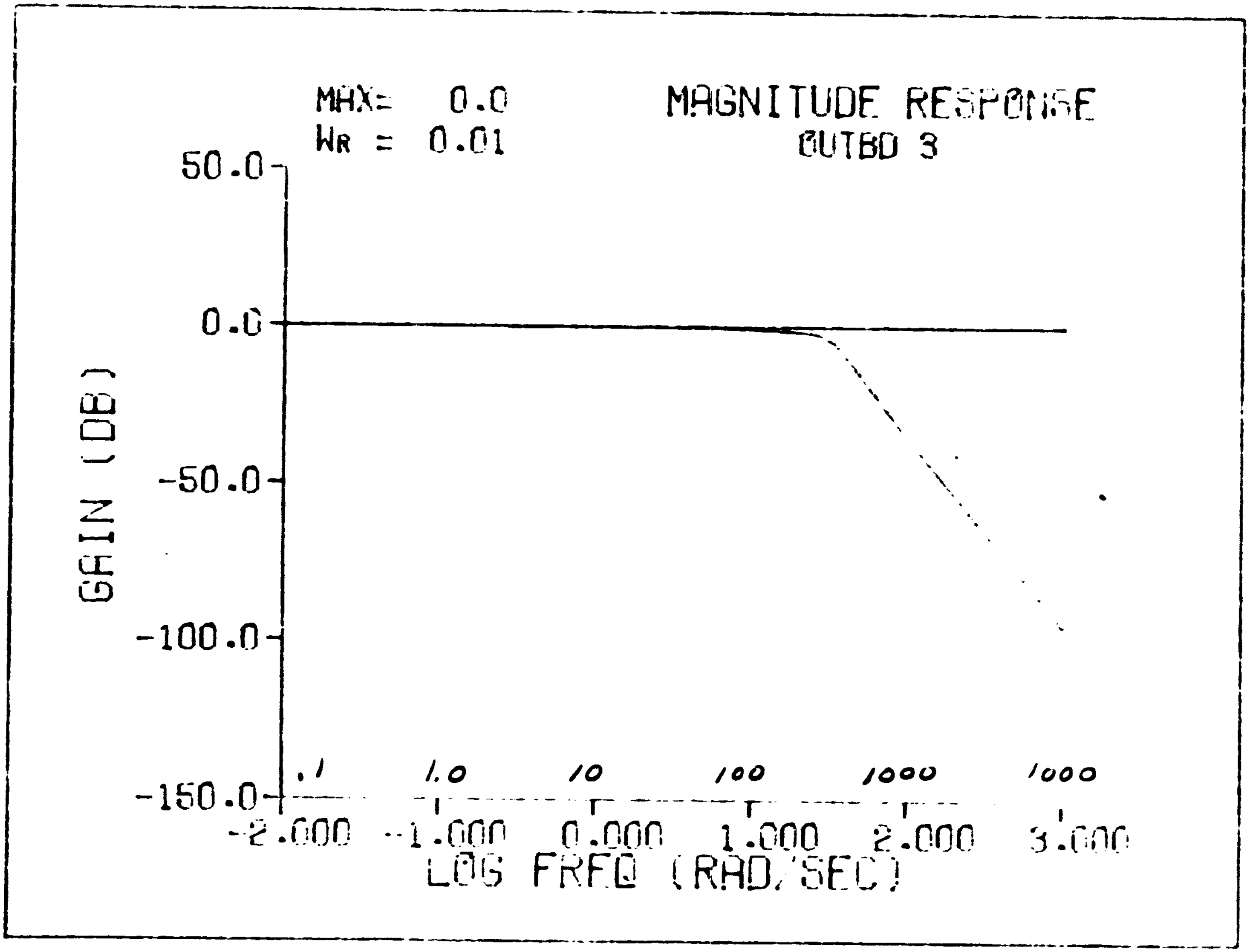
MAX= 0.0
WR = 0.01
MAGNITUDE RESPONSE
OUTBD 3
GAIN (DB)
50.0
0.0
-50.0
-100.0
-150.0
.1
1.0
10
100
1000
1000
-2.000
-1.000
0.000
1.000
2.000
3.000
LOG FREQ (RAD/SEC)

Fig 5

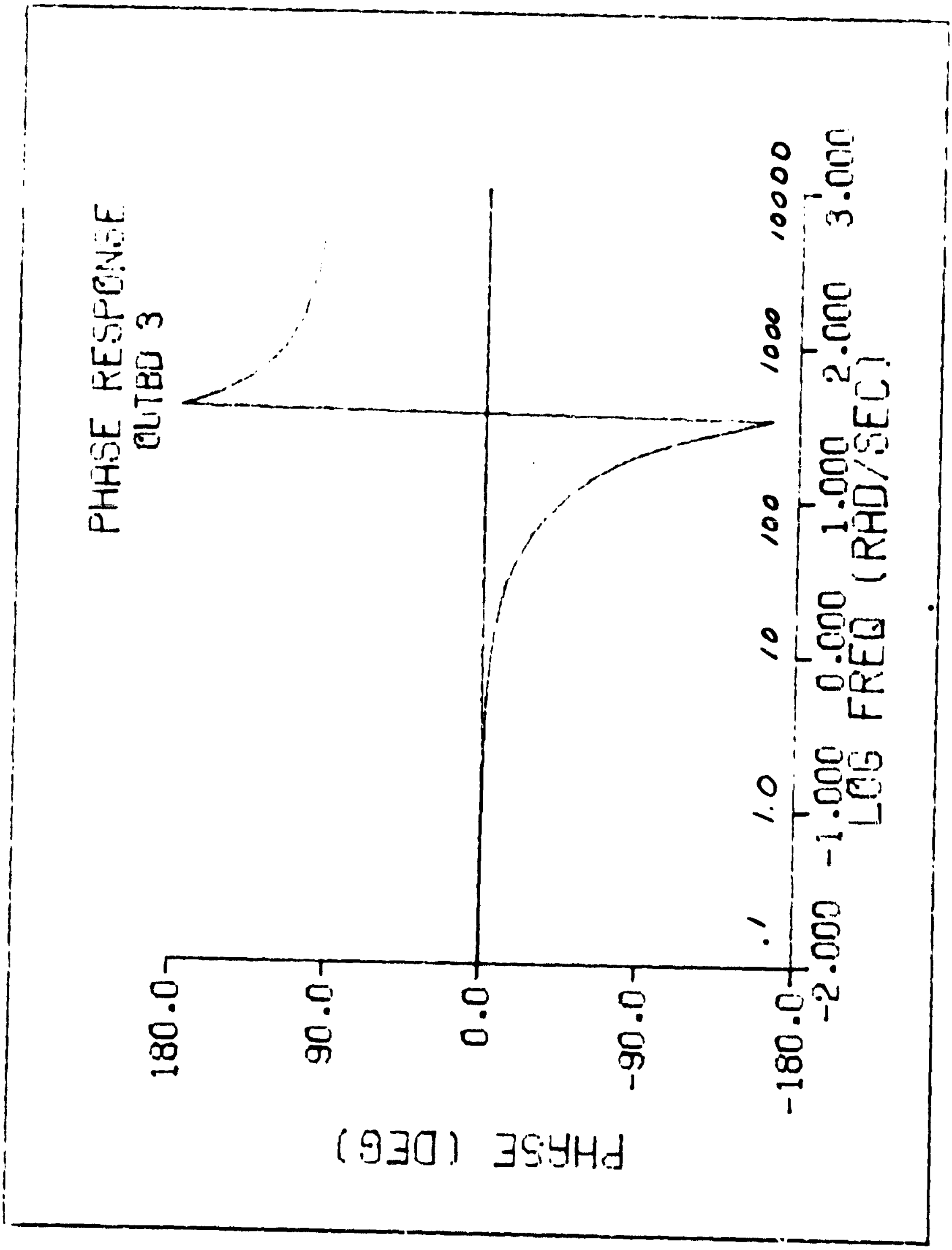
PHASE RESPONSE
OUTBD 3
180.0
90.0
0.0
-90.0
-180.0
PHASE (DEG)
-2.000
-1.000
0.000
1.000
2.000
3.000
LOG FREQ (RAD/SEC)
.1
1.0
10
100
1000
10000

Fig 6